CR 137568
AVAILABLE TO THE PUBLIC

PIONEER MARS SURFACE PENETRATOR MISSION
Mission Analysis and Orbiter Design

NASA Contract NAS 2-8424

AUGUST 1974

HUGHES

AUGUST 1974

PIONEER MARS SURFACE PENETRATOR MISSION

Mission Analysis and Orbiter Design

NASA Contract NAS 2-8424

HUGHES

CONTENTS

1. INTRODUCTION

The objective of the Mars Surface Penetrator Mission is to provide a capability for multiple and diverse subsurface science measurements at a low cost. Such a mission concept can be readily implemented by integrating appropriately instrumented subsurface probes — penetrators — with a low cost Mars orbiting spacecraft. The penetrators are a derivation of the Sandia terradynamic probes utilized successfully for Earth geological surveys and other applications. The Mars orbiting spacecraft — Pioneer Mars orbiter — will be derived from the Hughes Pioneer Venus program.

New equipment required to adapt the Pioneer Venus spacecraft for this mission can easily be developed by minor modifications to hardware used in current Hughes satellite and missile programs. Thus, a high level of confidence exists for achieving the Pioneer Mars orbiter flight hardware at a low cost and without schedule delays.

Analysis and design topics which are similar and/or identical to the Pioneer Venus program are not covered in depth in this report. Documentation of the Pioneer Venus spacecraft design and analysis is available in Reference 1; the penetrator science potential is discussed in Reference 2; and their science instrumentation and design is described in Reference 3.

2. SUMMARY

In the Pioneer Mars Surface Penetrator mission, the Pioneer Mars orbiter (PMO) serves as a bus for the penetrators during the interplanetary flight from Earth to Mars. At arrival, the PMO is inserted into a highly elliptical orbit about the planet. During the Mars orbital phase, the PMO serves as a launcher for the penetrators (launch times to be selected by the science experimenters) and as a communications relay between the deployed penetrators and the Earth tracking stations.

The penetrators, after deployment from the PMO, are on an impact trajectory to Mars. An atmospheric deceleration system allows the penetrators to arrive at the planet surface in an attitude and with a velocity to penetrate to a depth of 1 to 15 meters. After the penetrators are implanted in the Mars soil, their science payload may be activated and science measurements for one Mars year (about 686 days), or longer are feasible.

2.1 MISSION PROFILE

Conceptually the interplanetary transfer phase is quite similar to that for the Pioneer Venus (PV) mission. The PMO spin axis orientation is nominally maintained normal to the ecliptic throughout the mission.

The baseline PMO Mars orbits have a period which is synchronous with Mars rotation and permits the orbiter to pass repeatedly over the penetrator impact sites for the mission duration. The periapsis altitude of the orbit has been selected at 1000 km to avoid planetary quarantine requirements for the orbiter and to allow sufficient time for communications with the deployed penetrators. The lifetime of the PMO is a minimum of one Mars year and is limited primarily by the velocity and attitude control system fuel depletion. During the mission, up to six penetrators may be deployed, either singly or in pairs, with the penetrator deployment times to be selected during the mission by the science experimenters.

An evaluation of the PV orbiter science payload indicated that the 1000 km periapsis altitude exceeds the planned PV science instrument range and that the PMO look angles at periapsis differ significantly from those encountered during the PV mission at latitudes of interest. Thus, for the PMO mission no orbiter science has been included. New or modified orbiter science can be added subject to the constraints discussed in subsection 3.3.

PMO
APOAPSIS
VELOCITY

SOUTH POLAR ORBIT
(PERIAPSIS = 72°S)

PERIOD (MARS SYNCHRONOUS) = 24.6 hr
PERIAPSIS = 1000 km
INCLINATION = 90°
LIFETIME = 1 MARS YEAR

MARS

EQUATORIAL
PLANE

PMO
APOAPSIS
VELOCITY

NORTH POLAR ORBIT
(PERIAPSIS = 37°N)
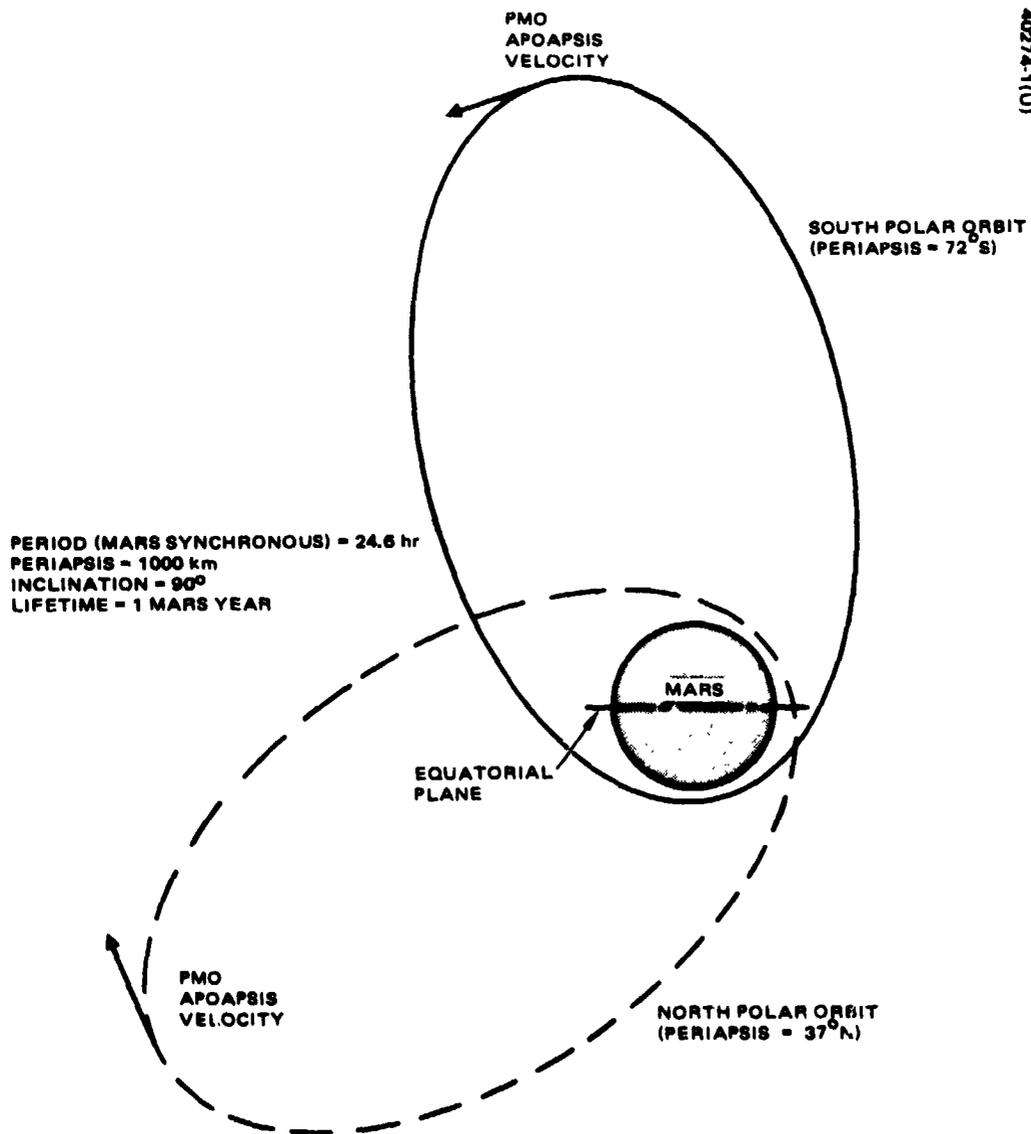
FIGURE 1. BASELINE PMO MARS ORBITS

2.2 PENETRATOR DEPLOYMENT OPTIONS

Two baseline PMO Mars orbits have been chosen (see Figure 1) to
illustrate the penetrator deployment options. Both of these orbits have
1000 km periapsis altitude and a nominal period of 24.6 hours. The inclina-
tion is 90° to the Mars equator. This inclination is chosen as illustration
only, and is not limited by any spacecraft considerations. The difference
between the orbits is the initial periapsis latitude which is 37°N ±6° for the
north polar orbit and 72°S ±6° for the south polar orbit.

4
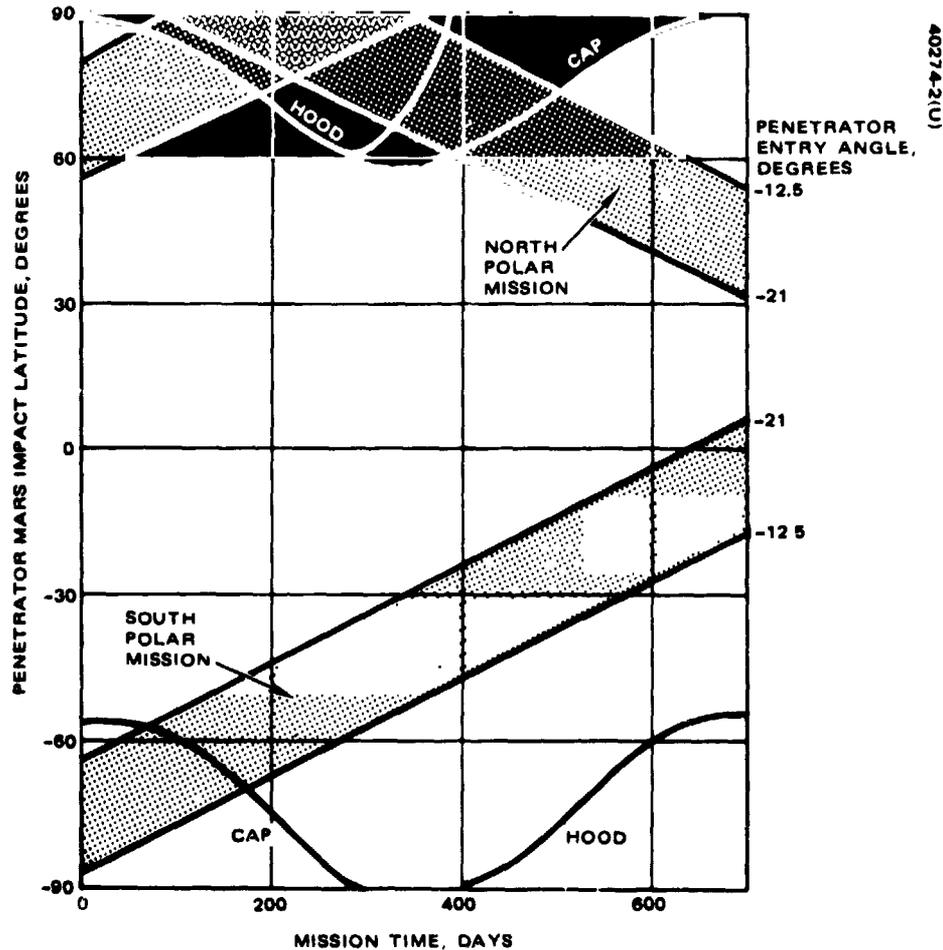
FIGURE 2. PENETRATOR DEPLOYMENT OPTIONS

For these orbits with a penetrator atmospheric entry angle between
-12.5° and -21.0°, the attainable penetrator targeting latitudes are shown
in Figure 2 as a function of mission time after the PMO Mars orbit insertion.
For both orbits the deployment occurs along a great circle. The south polar
orbit gives the opportunity for penetrator targeting near the south pole
at the beginning of the mission, and the attainable latitudes decrease with
time into mission. For the north polar orbit the initial latitudes that can be
attained are between 56° and 80°N and the north pole is attainable approxi-
mately 100 days after orbit insertion. All the penetrators deployed from these
orbits are within the acceptable communications region from the orbiter.
That is, a penetrator deployed on the first day of the mission will still be
able to relay its data via the PMO to an Earth station at the end of the mission
if the orbit period is controlled to maintain the periapsis at a constant Mars
latitude. For both baseline orbits, communications throught the entire
mission are possible with any penetrator up to 1500 km on either side of the
ground track of the nominal orbit.

5

A variety of PMO Mars orbits and penetrator deployments are possible if communications for shorter time periods are acceptable. Penetrator deployment around any desired meridian (longitude) can be attained simply by changing temporarily the orbital period to permit orbital precession and then deploying the penetrators from the new nominal orbit.

The penetrator deployment accuracy is primarily defined by the magnitude of the deboost velocity vector imparted at deployment near apoapsis. Current estimates of the deboost motor ΔV magnitude indicate a 1.5 percent (3σ) error which results in penetrator targeting errors of less than ± 100 km in plane. Out of plane errors can be held within ± 30 km.

The penetrator impact position with respect to the orbiter position can be determined by utilizing the PMO communications system in a doppler tracking mode. Along and normal to the orbital path the penetrator positions can be determined to an accuracy of about ± 23 meters (3σ) and ± 50 meters (3σ), respectively.

2.3 COMMUNICATIONS AND DATA HANDLING

The penetrator science data is read out to the Earth stations via the PMO which serves as a communications relay. Two distinct links can be identified; namely, the penetrator/PMO link, and the PMO/Earth link. The latter can be implemented with the planned PV equipment without any modifications. The only additional communications equipment required is that for the penetrator/PMO link. The additions required in the PMO are a receiver, a transmitter, and an antenna. These items can readily be developed from conventional communications satellite hardware.

A penetrator has a constant power transmitter. Communications with the PMO take place in the proximity of the periapsis and, depending on the antenna patterns and their respective pointing directions, different data rates can be used. A summary of typical data rates and the feasible total data readout of each penetrator is contained in Table 1. A nominal 200 bps data rate allows complete readout of the 50 kilobit penetrator memory each day.

TABLE 1. MAXIMUM PENETRATOR DATA READOUT PER ORBITER PASS

Rate, bps	Communications Time, min	Total Data, bits
12.5	21.0	15,750
25	19.6	29,400
50	16.1	48,300
100	11.7	70,200
200	6.4	76,800

2.4 PIONEER MARS ORBITER DESIGN

A Mars orbiting spacecraft experiences an environment significantly different from Venus. The salient differences are the increased distance from the Sun (which affects the spacecraft thermal control and lowers the solar panel output) and the increased communications distance to Earth. The thermal environment changes can be resolved by implementing a passive thermal control concept similar to that used for the operational Hughes synchronous satellites. A modest increase in the solar panel size achieved by covering the entire PV substrate with solar cells provides sufficient power to implement a PMO to Earth data transmission capability that exceeds the potential penetrator science data return.

Another unique feature of this mission is the integration of penetrators with the PMO. This results in a larger spacecraft launch mass, a requirement for penetrator deployment mechanisms, and some configuration and subsystem changes to accommodate the penetrator mass and volume. The combined mass of the PMO and penetrators is significantly larger than the PVO launch mass and requires the use of the Atlas/Centaur/TE 364-4 launch vehicle (a configuration used for the Pioneer 10 mission). The penetrator deployment mechanism is a derivation from the Hughes tube launched, optically sighted, wire guided (TOW) missile launcher program. The feasibility of implementing the deployment system has been demonstrated with close to 4000 TOW launches.

The required PV spacecraft changes are shown in Figure 3. The penetrator and the deployment mechanism are contained inside a launch tube, shown on the left of the figure. The launch tubes pass through the equipment shelf and are supported by a secondary structure just inside the solar panel. The additional changes indicated in Figure 3: addition of extra solar cells, alternate orbit insertion motor, alternate propellant tanks, and added communications equipment for the penetrator/PMO link are simple adaptations from various Hughes hardware programs and utilize proven technology.

The penetrator assembly: launch tube, penetrator, and deboost motor is shown in Figure 4. The penetrator and the deboost motor are connected with a simple mechanism which sustains the launch and penetrator deployment loads yet permits easy penetrator/motor separation after burnout. Prior to deployment the penetrator/deboost motor is held inside the launch tube by a restraint mechanism.

The planetary quarantine imposes a requirement that the penetrators be sterilized and that during the time period between the sterilization and their deployment the penetrators must not be recontaminated. To satisfy these requirements, heat compatible penetrator launch tube, deployment mechanism, and deboost motor designs have been selected; and the launch tube is hermetically sealed with appropriate end covers until the penetrator deployment.

7

SLEEVE DIPOLE ANTENNA

WIDEBEAM OMNI ANTENNA

UHF ANTENNA (NEW)

S BAND HIGH GAIN ANTENNA

BAPTA

BAPTA SUPPORT

ADDED SOLAR CELLS

SOLAR PANEL CYLINDER

PENETRATOR ASSEMBLY (TOW)

EQUIPMENT SHELF WITH PENETRATOR CUTOUTS

SECONDARY STRUCTURE (NEW)

SUPPORT STRUTS

PROPELLANT TANKS (MARISAT)

RADIAL THRUSTERS

THRUST TUBE

AXIAL THRUSTERS

ORBIT INSERTION MOTOR

AFT THERMAL BARRIER (INTELSAT IV, TELESAT)
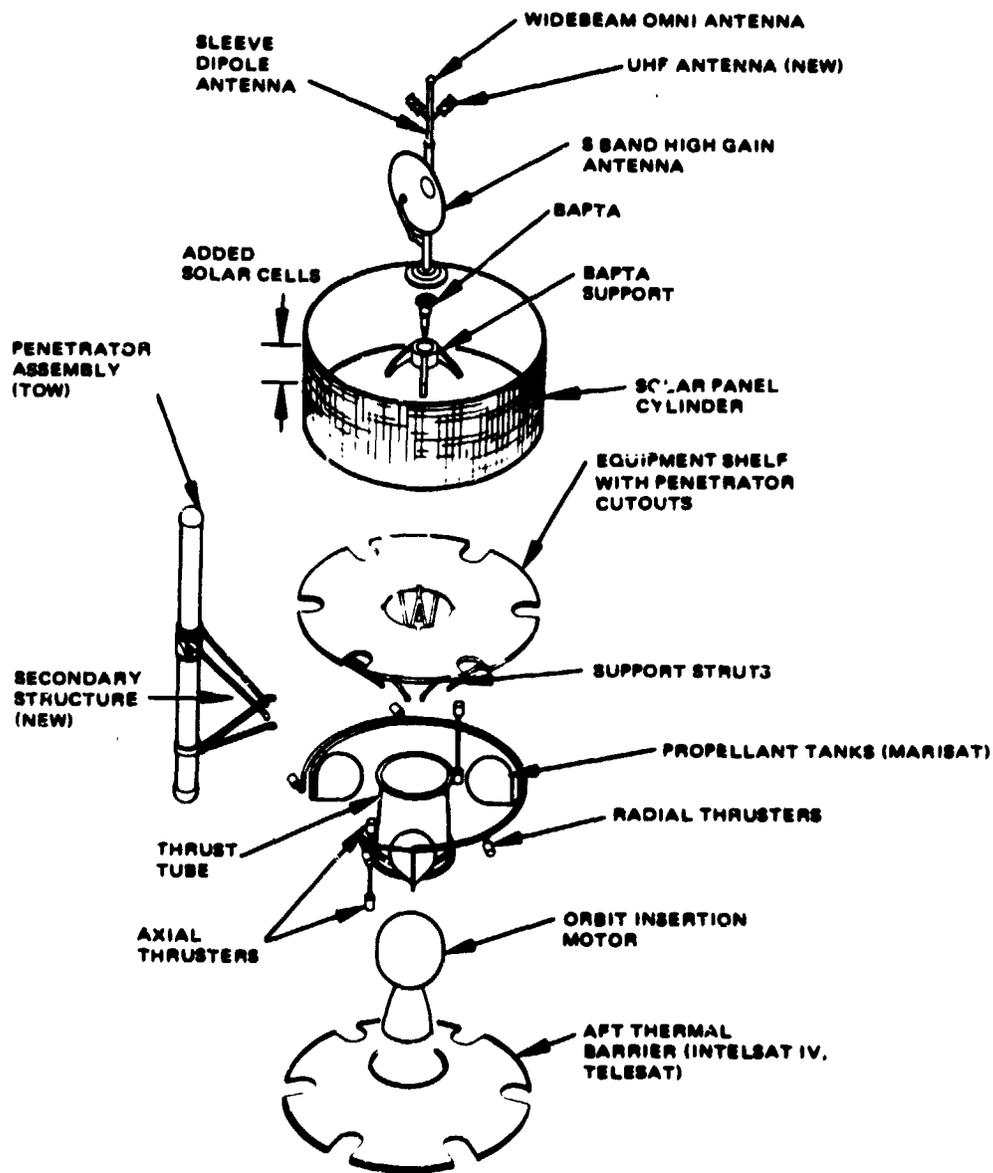
FIGURE 3. EXPLODED VIEW OF PMO WITH PENETRATORS

8
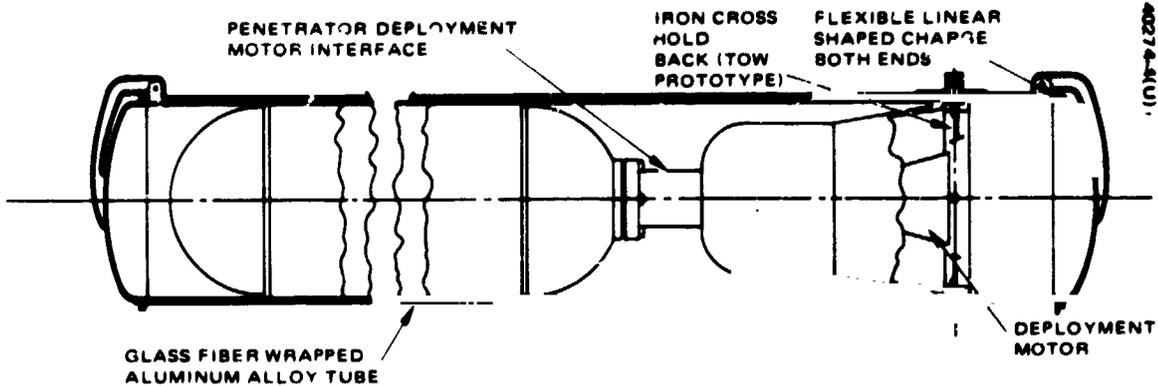
FIGURE 4. PENETRATOR ASSEMBLY

A summary of the PMO mass and a comparison of same with the PV is included in Table 2. The indicated contingency for the PMO is approximately twice as large as that for the PV.

TABLE 2. PIONEER SPACECRAFT MASS COMPARISON

Item/Subsystem	PV Orbiter, kg	PMO with Penetrators, kg
Subsystem and science totals	295.96	349.08
Contingency	21.77	40.10
Spacecraft total (dry)	317.73	389.18
Penetrators (6)	0	270.00
Launch mechanism (6)	0	42.18
Spacecraft dry (with penetrators)	—	701.36
Propellant (liquid)	18.50	71.02
Pressurant	0.05	0.23
Orbit insertion motor expendables	151.75	296.00
Spacecraft total	488.03	1068.61
Spacecraft attach fitting	34.97	22.40
Launch vehicle payload	523.00	1091.01

9

3. MISSION ANALYSIS

The key topics of mission analysis: flight mechanics, operations, orbiter science potential, penetrator deployment options, communications, and orbiter dynamics are discussed in this section. Topics for which extensive inheritance from other programs exists; e.g., launch and inter-planetary transit phase, are discussed only briefly. Concepts unique to this program are discussed in terms of the baseline solutions and pertinent results.

The flight mechanics aspects of this mission were initially derived in Reference 4. They have been modified for this program to limit the launch window to 10 days and to maintain a constant arrival velocity at Mars. The mission operations are identical for the most part with the Pioneer Venus (PV). The salient differences are in the orbit insertion and penetrator launch maneuvers. These are discussed in subsections 3.2.1 and 3.2.2. The science potential of the PV instrumentation is incompatible with this mission profile and, therefore, the PV science has been deleted from the orbiter. New orbiter science, if compatible with the available mass contingency, power, and data storage, as discussed in subsection 3.3., may be implemented.

The penetrator deployment options and the communications geometry are discussed in subsection 3.4. Essentially, data transmission from p'etrators for a full Mars year is feasible from polar orbits, which provide mid-latitude and polar penetrator targeting options. Low latitude penetrator targeting options are also feasible at the expense of reducing the duration of available communications. The penetrator data transmission, commands and tracking are briefly discussed in subsection 3.5.1. All of the require-ments can be met with state of the art hardware derived from Hughes com-munications satellite programs.

The orbiter dynamics analysis of subsection 3.6, has verified the PMO stability. It also shows that the transient dynamic responses during penetrator deployment are small and therefore do not interfere with mission operations.

3.1 PIONEER MARS ORBITER FLIGHT MECHANICS

The Pioneer Mars Surface Penetrator mission utilizes the Atlas/ Centaur/TE 364-4 launch vehicle. This launch vehicle and the launch profile are nearly identical to the Pioneer 10 mission.

TABLE 3. MARS 1979 TYPE II TRANSFER CHARACTERISTICS

	(JD 2440000)	Time of Flight, days	Launch Energy (C₃) km/sec²	Launch Asymptote Declination, deg	Asymptotic Mars Approach Velocity, km/sec
Arrival Date 2444460	4140	320	20.5	14.2	2 902
	4150	310	15 8	14.0	2.922
	4160	* 300	12.3	14 8	2 9° ¹
	4170	290	10.0	16.8	2 994
	4180	280	9 0	20 6	3.021
	419C	270	10.5	38.2	2.999
	4200	.	.	.	.
	4210	.	.	.	.
Arrival Date 2444490 (9 7/80)	4140	250	21 9	16 9	2 927
	4150	340	16 4	17 6	2 792
	4160	330	12.5	19 6	2.707
	4170	320	10 0	23.4	2.657
	4180	310	9 1	29 1	2 630
	4190	300	9.9	37 6	2 630
	4200	290	16 0	55.9	2 833
	4210	.	.	.	.
Arrival Date 2444520	4140	380	26 8	17 4	3.620
	4150	370	19 6	18 2	3 329
	4160	360	14 5	20 2	3 123
	4170	350	11 2	23 9	2 986
	4180	340	9 6	29 3	2.907
	4190	330	9 6	35 8	2 882
	4200	320	11 8	43 0	2 931
	4210	310	18 2	53 9	3 180

*Type I Transfers

The interplanetary trajectory parameters and Mars arrival conditions have been obtained from Reference 4. The referenced results have been modified to reflect a 10 day launch window (PV assumption) and a constant asymptotic Mars approach velocity.

Discussions of PMO launch and interplanetary transit phase, baseline interplanetary trajectory, PMO Mars arrival conditions, and PMO Mars orbit phase are contained in the subsections that follow.

3. 1. 1   Launch and Interplanetary Transit Phase

The PMO will be launched from the Eastern Test Range by an Atlas/ Centaur/TE 364-4 launch vehicle. As a result of range safety requirements, the maximum allowable launch azimuth is 108°. Type II trajectory (transit angle > 180°) has been selected in order to minimize the approach velocity at Mars and thus the retrovelocity requirements for orbit insertion. Table 3 summarizes the relevant trajectory data for Earth-Mars transfers launched during October-November 1979 and arriving August-October 1980.
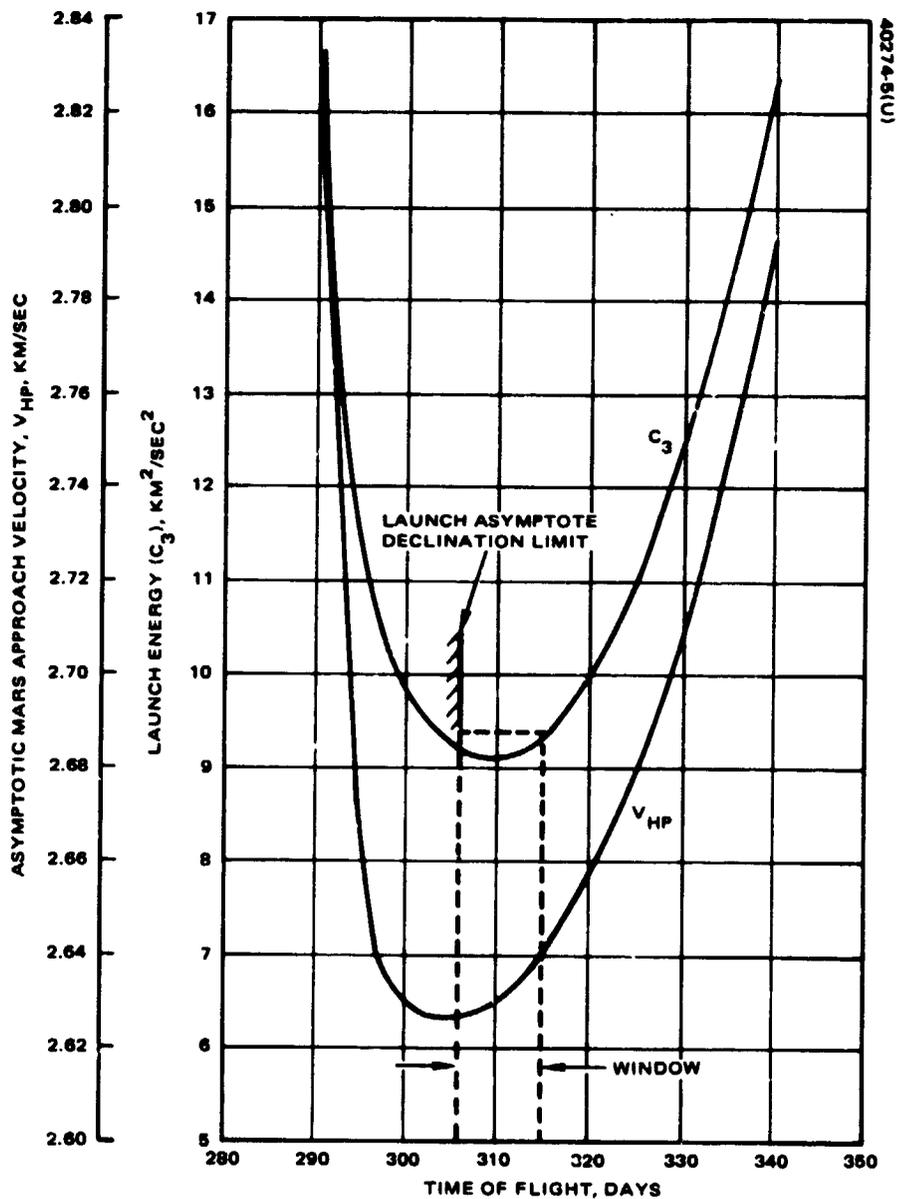
FIGURE 5. LAUNCH WINDOW FOR MARS ARRIVAL ON 7 SEPTEMBER 1980

In optimization of the interplanetary transit trajectory, maximum payload into Mars orbit is the primary objective. Thus, launch energy C_3, and Mars orbit insertion energy (equivalently, Mars approach velocity V_{hp}) must be minimized over the launch window. These parameters are shown in Figure 5. The baseline launch window is 10 days. Launch asymptote declination sets a lower limit on time of flight if no plane change in Earth orbit is allowed. Since the ΔV of the TEM-616 orbit insertion motor is fixed, minimal approach velocity variation is desired. These considerations can be satisfied with a constant Mars arrival date of 7 September 1980, with a 10 to 15 minute daily launch window for 10 consecutive days starting 28 October 1979 (see Figure 5). The nominal approach velocity is
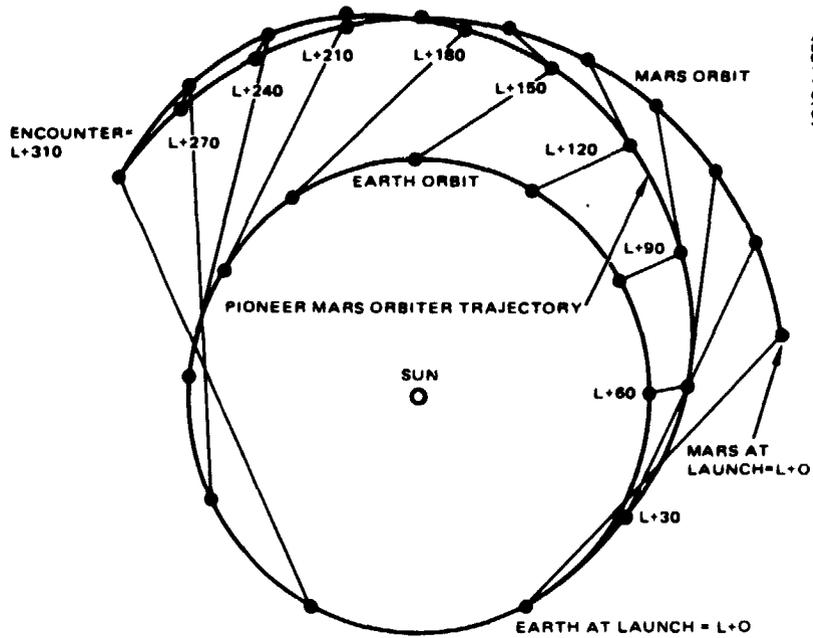
FIGURE 6. BASELINE PMO INTERPLANETARY TRAJECTORY
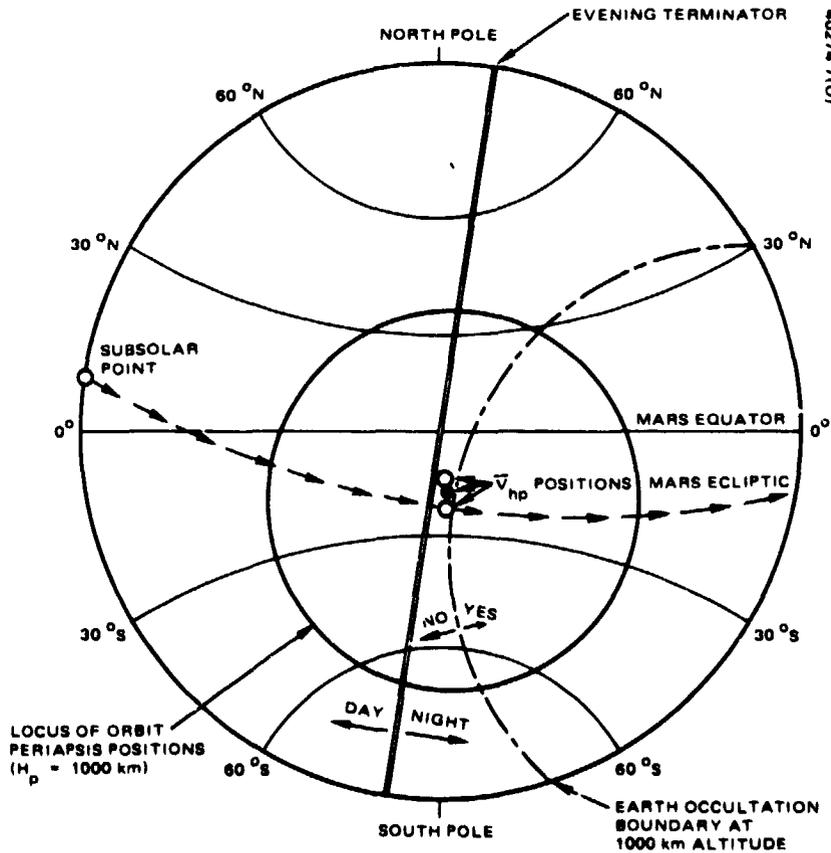
FIGURE 7. MARS AT PMO ARRIVAL (7 SEPTEMBER 1980)

2. 633 km/sec with a variation of 7 m/sec over the window. The maximum launch energy requirement (C_3) of 9. 4 (km/sec)^2 provides a payload capability of 1091 kg (including adapter) for the Atlas/Centaur/TE 364-4 launch vehicle. The interplanetary transit trajectory is biased sufficiently to give a probability of less than 10^{-4} for launch vehicle impact on Mars.

### 3. 1. 2 PMO Baseline Interplanetary Trajectory

Figure 6 depicts the relative positions of the Earth, the PMO, and Mars every 30 days after launch during the PMO interplanetary trajectory phase. The orbits of both planets are also shown. The nominal launch date is 2 November 1979, and after a 310 day transit, arrival at Mars is scheduled for 7 September 1980. The heliocentric transit angle is approximately 202°. The maximum communication distance during transit is approximately 2. 87 x 10^8 km, which is experienced at Mars arrival.

3. 1. 3 PMO Mars Arrival Conditions

Interplanetary transfer energy characteristics dictate a Mars arrival date on or near 7 September 1980 (Julian date = 2444490; see Table 3) for low energy 1979 orbiter missions. The Mars arrival conditions on this date are depicted in Figure 7. For purposes of this discussion, the Eastern hemisphere (right half of planet as seen from the Sun) is presented. The subsolar point (local noon) is on the left side of the primitive circle, 7. 9° above the Mars equator. The motion of the subsolar point along the Mars ecliptic plane with passage of time is shown as arrows within the hemisphere. It crosses the Mars equator in a southerly direction (autumnal equinox) approximately 40 days after arrival. The northern season at arrival is late summer, just before formation of the North polar hood. Recession of the south polar cap has not started yet. The evening terminator is shown as a double line in the center of the diagram. Lines of constant planetocentric latitude have also been included for completeness.

The orientation of minimum capture energy orbits is closely related to the asymptotic approach direction of the spacecraft to Mars. In particular, the exit point of the asymptotic approach velocity ($\bar{V}_{hp}$) vector on the planet is of interest. Three of these $\bar{V}_{hp}$ positions are shown near the center of the hemisphere, one for each of three launch dates. The middle (solid) dot corresponds to the approach direction for a 2 November 1979 launch date. The open dots correspond to launch dates 10 days before and after this reference date. Once a reference $\bar{V}_{hp}$ position has been established, specifying the capture periapse altitude (assuming minimum energy periapse capture) determines the locus of all possible initial orbit periapse positions. This locus of points appears as a circle around the reference $\bar{V}_{hp}$ position in Figure 7.

Note the significance of the orbit periapsis locus. All initial periapsis locations are in the vicinity of the evening terminator with a bias toward the southern hemisphere. The intersection of the planet and a polar orbit is a great circle passing through the north pole, south pole, and the $\bar{V}_{hp}$ position. Initially, periapsis is located at the northern intersection of the orbit plane and periapsis locus for the north polar orbit and the southern intersection for the south polar orbit.
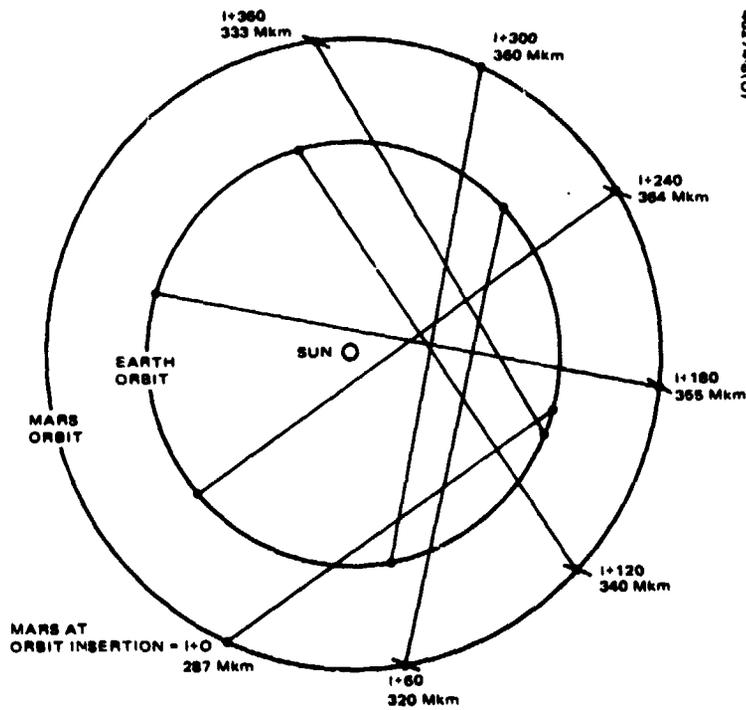
FIGURE 8. COMMUNICATION GEOMETRY 0 TO 360 DAYS
AFTER MARS ORBIT INSERTION
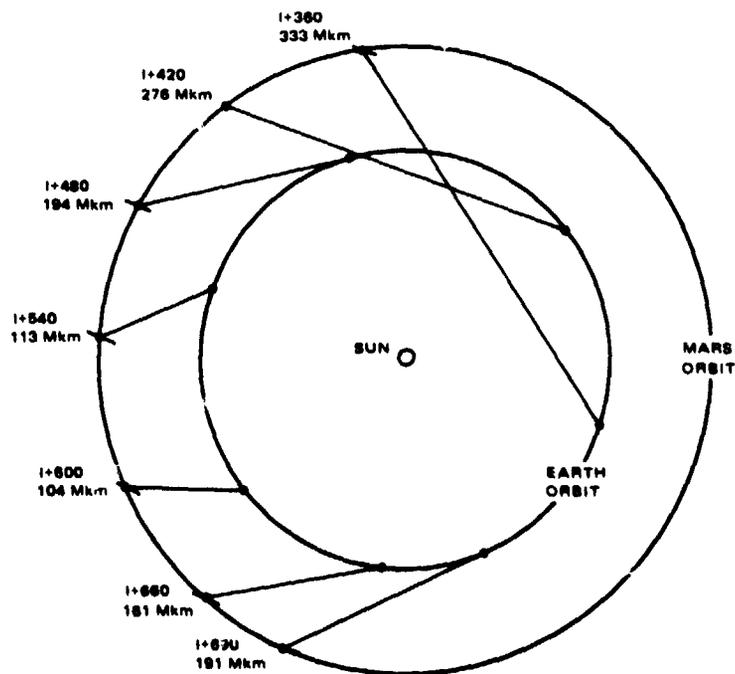
FIGURE 9. COMMUNICATION GEOMETRY 360 TO 690 DAYS
AFTER MARS ORBIT INSERTION

16

On the right-hand side of the hemisphere, a dash-dot circle has been added indicating the Earth occultation boundary for a satellite at 1000 km altitude above the Mars surface. For the elliptical Mars-synchronous orbits (period = 24.6 hours) with 1000 km periapsis, Earth occultations would not occur until 5 months after orbit capture.

3.1.4 PMO Mars Orbit Phase

The PMO Mars orbit must satisfy the following mission considerations: 1) periapsis altitude compatible with planetary quarantine, 2) orbital period which assures repeatable communications between penetrators deployed in the Martian soil and the PMO; and 3) orbital inclinations compatible with the Mars arrival conditions; i.e., between 17° and 163°.

Two baseline PMO orbits have been selected for illustration purposes: a north polar orbit and a south polar orbit. Both have a nominal period of 24.6 hours, synchronous with Mars rotation, and with periapsis altitude of 1000 km. The plane of the orbit is inclined 90 ±2° to Mars equator with a dispersion resulting from residual errors in the asymptotic approach velocity vector ($\bar{V}_{hp}$). For a north polar orbit, the initial periapsis latitude is 37°N ±6°, the uncertainty arising from launching anywhere in the 10 day launch window and the error in $\bar{V}_{hp}$ noted above. For a south polar orbit, the initial periapsis latitude is 72°S ±6°.

Perturbations of the PMO Mars orbit occur primarily due to the following sources: solar pressure, planet oblateness, and velocity and attitude control maneuvers. Solar perturbations will cause the uncorrected periapsis altitude to vary ±15 km about the nominal altitude of 1000 km. Uncorrected solar pressure will precess the orbiter spin axis by approximately 0.2°/day. The significant oblateness of Mars results in an apsidal rotation of about -0.1°/day. The attitude and velocity control system is utilized to correct the orbiter attitude and periapsis and apoapsis altitude.

The PMO/Earth communications geometry is depicted in Figures 8 and 9. Figure 8 applies for the first half of the mission; namely, zero to 360 days, and Figure 9 shows the geometry for 360 to 690 days into the mission. The communication distances are shown in millions of kilometers (Mkm). Initially, at PMO Mars orbit insertion (time I), the distance is 287 Mkm. It increases to a maximum of 364 Mkm at I + 240 days, and then drops to a minimum of approximately 95 Mkm at I + 570 days.

Two similar eclipse seasons occur during the north polar and south polar orbits. The first extends over nearly 60 days centered at about 150 days into the missions and occurs just prior to passing through periapsis on each orbital revolution. (See Figures 10 and 11.) The second season lasts for about 90 days centered at 500 days into the mission and occurs just after periapsis passage. Maximum eclipse duration in an orbital revolution is about 75 minutes for both missions.

Earth occultation periods nearly overlap the eclipse periods. (See Figures 10 and 11.) Note that a third occultation period occurs briefly at about 600 days into the south polar mission.
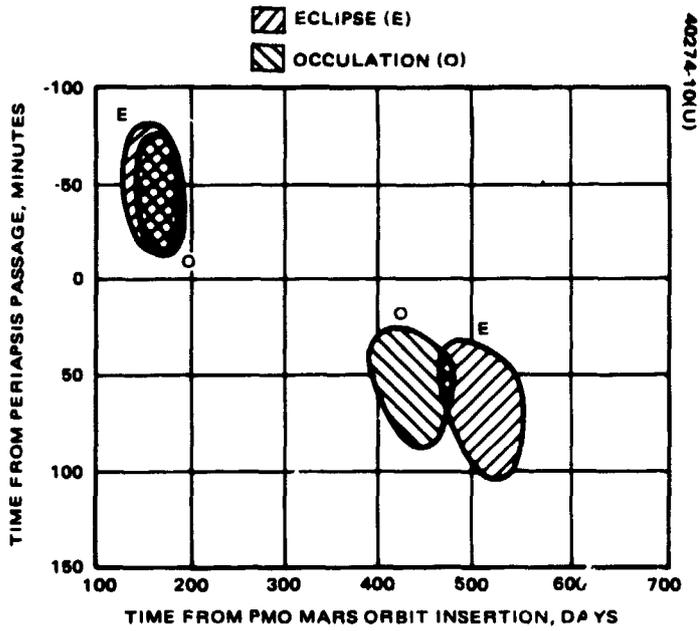
17

FIGURE 10. ECLIPSES AND OCCULTATIONS –
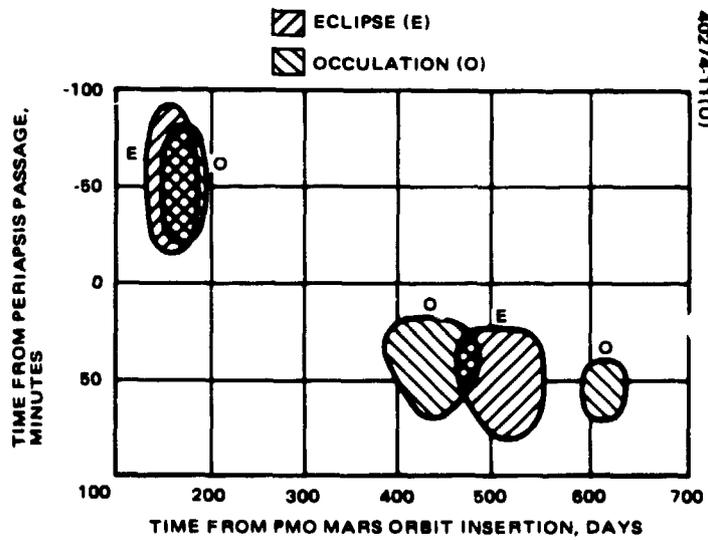NORTH POLAR ORBIT

FIGURE 11. ECLIPSES AND OCCULTATIONS –
SOUTH POLAR ORBIT

18

Superior conjunction occurs 207 days after insertion. During a 15 to 20 day period around superior conjunction, PMO/Earth communications will be interrupted. The most pertinent penetrator data can be stored onboard the PMO for transmission after the blackout period.

3.2 MISSION OPERATIONS

The launch operations for this mission are similar to those employed for the Pioneer 10 mission. The interplanetary transit phase is similar to that for the PV mission.

During the PMO Mars orbit insertion and also the penetrator deployment the PMO high gain antenna is not pointing to Earth; thus, the PMO can only receive but not transmit in these attitudes. A simple attitude reacquisition scheme which ensures mission safety has been developed.

The penetrator data transmission to Earth stations is achieved via the PMO. The large PMO data storage capability offers flexibility and easy scheduling.

Orbital eclipses and occultation have a negligible effect on the mission.

3.2.1 Launch and Interplanetary Transit

The Pioneer Mars Surface Penetrator mission will start with the Atlas/Centaur/TE 364-4 launch from Cape Kennedy. Atlas and the first burn of the Centaur will achieve injection into a low altitude parking orbit. Following a short coast of 30 minutes or less, the Centaur and TE 364-4 burns will inject the PMO into a Type II interplanetary trajectory to Mars. (The launch vehicle and the launch profile are almost identical to the Pioneer 10 launch.) Attitude determination on basis of the PMO star and sun sensors and orbit determination from the Deep Space Network (DSN) tracking will be performed throughout the mission. This data will be utilized for the PMO velocity and attitude corrections.

During the interplanetary transit, midcourse corrections are tentatively planned at:

1) 5 days after launch

2) 20 days after launch

3) 30 days prior to arrival at Mars

The first midcourse correction magnitude is 90 m/sec (3σ), and will be performed with axial thrusters. This maneuver will require reorientation of the PMO spacecraft. The following two maneuvers will be considerably smaller and will be accomplished by axial and radial thruster burns without spacecraft reorientations. The above operations are identical to the PV mission profile.

Shortly before arrival at Mars (1 day or less), the PMO will be reoriented to the Mars orbit insertion attitude. At the appropriate time, the orbit insertion will be accomplished by ground command.

During the orbit insertion motor burn and penetrator deployment maneuvers, the spacecraft spin axis will not be normal to the ecliptic, a .d the high gain antenna will not point to Earth. Because of gain limitations of the omni antenna, orbiter sensor information cannot be transmitted to the ground control, as it is for PV, although ground control center will still be able to send commands to the spacecraft. The PMO must therefore perform the entire orbit insertion operation "open loop"; i. e. , the commands (to reorient the PMO spin axis to the proper attitude, fire the orbit insertion motor, and then return to a spin axis attitude compatible with Earth acquisition of the high gain antenna) are all transmitted without receiving information from the PMO.

The following — open loop — high gain antenna reacquisition sequence is efficient even in the presence of large attitude errors. The high gain antenna despin control system (DCS) will be used to slowly spin the antenna platform relative to inertial space. After the entire spin-plane has been examined for the Earth signal, attitude jets will precess the spin axis approximately one antenna beam width and the new spin-plane will be examined. This process is continued until the high gain antenna receives the Earth signal and the DCS acquires lock. Using an antenna spin rate of 2 rpm and a beam width of 8°, this process would take at most 23 minutes.

The lack of verification of the spacecraft attitude prior to orbit insertion has no significant effect on the attainable PMO Mars orbit accuracy. The PMO heliocentric orbit determination and Mars ephemeris errors cause an estimated 300 km (3σ) error in the B-vector at Mars approach. These errors statistically dominate other error sources (retromotor impulse, spacecraft attitude, spacecraft mass, retrofire timing). A total of 40 m/sec (3σ) is required from the attitude and velocity control system to correct periapsis and apoapsis altitudes (and therefore orbit period). The 2° (3σ) dispersion in orbit inclination is not corrected.

3. 2. 2 PMO Mars Orbit Phase

After insertion into Mars orbit, the PMO attitude and orbit determination is continued. The PMO attitude is corrected as required (following each maneuver and also due to solar torque perturbations) to maintain the spin axis normal to the ecliptic plane.

The penetrator deboost from the PMO will take place near apoapsis, with the spin axis aligned normal to the radius vector. Since the penetrators are deployed at times to be selected by the science experimenters during the mission, it is most likely that an orbiter reorientation will be required prior to each deployment. The attitude reacquisition will be accomplished with the identical type of maneuver as that following orbit insertion.

3.2.3 Data Transmissions

During the Mars orbit phase, the PMO will receive the science data from the penetrators in the proximity of periapsis. Nominally, data transmission will be initiated by command from the PMO. Adequate onboard memory is available in the PMO to store the data from all penetrators. Commands to the penetrators will be transmitted either before or after penetrator data readout. Simultaneous receive and transmit operations for this link are not planned.

The PMO/Earth memory readout to a DSN station requires a maximum of 2.6 hours (with a 26 meter DSN antenna). This permits very leisurely scheduling for the PMO/Earth link.

3.2.4 Operations During Eclipses and Occultations

During the mission lifetime, the PMO will experience both solar eclipses and Earth occultations (see Figures 10 and 11). The impact of these events on mission operations is minor. For example, during eclipses, the spacecraft batteries provide power to the subsystems and spin reference is provided by the star sensor. Upon exiting from eclipse, the vehicle power is supplied by the solar panel and spin reference is returned to the sun sensor. The eclipses are considerably shorter than for the PV mission, thus the despun control system may be operated from batteries, which allows the high gain antenna to maintain an Earth pointing altitude.

The duration of the Earth occultations will be approximately the same as that of the eclipses. Due to the short time required for the PMO/Earth link operations, this effect is not significant.

3.3 ORBITER SCIENCE POTENTIAL

For the current Pioneer Mars Surface Penetrator mission, all science instrumentation is carried in the penetrator. The PMO acts only as a communications relay for transmitting the penetrator science data to Earth stations. The PMO antennas have sufficient coverage to implement, without spacecraft reorientation, the penetrator to Earth station data relay function for all deployment options throughout the mission. The PMO capability exceeds about four times the maximum planned penetrator data return, see Reference 2.

Since the PMO is a derivation from the Pioneer Venus orbiter (PVO), the feasibility of retaining the PVO science capability for the PMO was evaluated. It was concluded that the current PVO science complement would not likely yield any meaningful science data due to the PMO Mars orbit periapsis altitude of 1000 km and due to the greatly different instrument viewing angles as compared to PVO.

A limited new orbiter science potential exists. From a spacecraft standpoint, the most severe constraint is the required science instrument
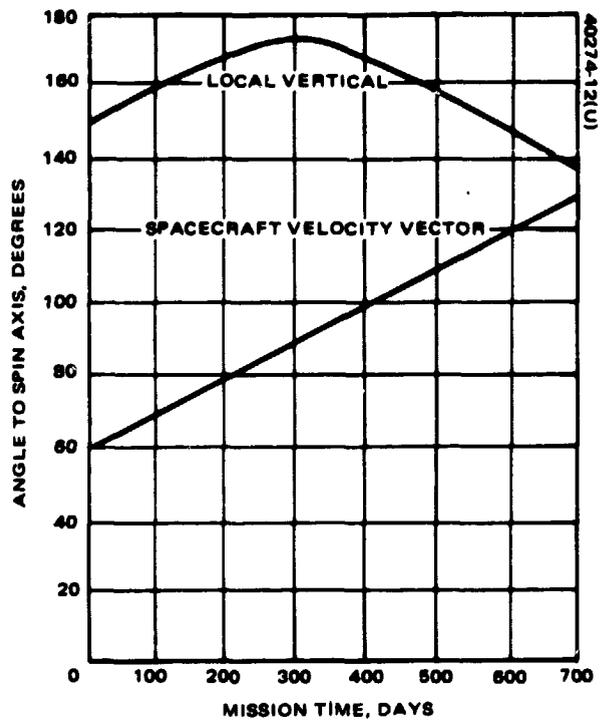
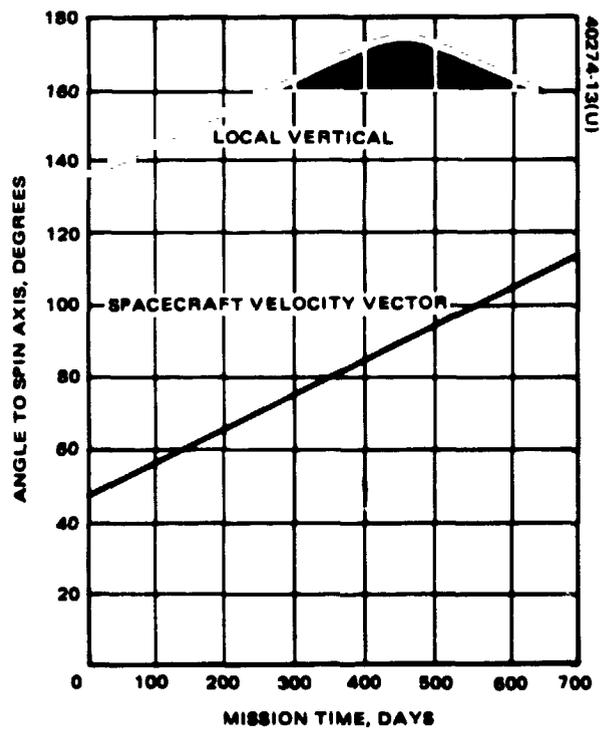FIGURE 12. PMO SPIN AXIS ORIENTATION AT
PERIAPSIS – NORTH POLAR ORBIT

FIGURE 13. PMO SPIN AXIS ORIENTATION AT
PERIAPSIS – SOUTH POLAR ORBIT

mass which would have to be charged again-t the spacecraft mass contingency of 40. 10 kg (additional mass would be available by removal of a penetrator). The available power for the instruments cannot be identified directly because in addition to the instruments, the science data return (an increase in the communications time) requirements must be accounted for. In general, however, nearly all of the spacecraft battery power (270 W-hr/per orbit) could be made available.

To provide an insight to the potential science instrument pointing directions, two examples are discussed: the bas line north polar and south polar orbits.

It is assumed that the science experiments will be performed in the vicinity of the PMO Mars orbit periapsis and that velocity sensitive experiments are arranged parallel to the spin axis, and surface pointing experiments scan normal to the spin axis. The spin axis orientation is normal to the ecliptic. Depending on the mission, the initial periapsis latitudes are about 37°N (north polar orbit) and 72°S (south polar orbit). Apsidal rotation due to oblateness of Mars causes the periapsis location to move in the orbit plane by about -0. 1°/orbital revolution.

The orientation of the periapsis position and velocity vectors relative to the spin axis indicate how effectively experiments might be performed. The sense of the spin axis is chosen to accommodate penetrator communications. The spin axis for the PMO in the north polar orbit must point toward the south celestial pole, and toward the north celestial pole for the south polar orbit.

For the above set of constraints, Figures 12 and 13 illustrate the time history of the angle at periapsis between the spin axis and the velocity vector and between the spin axis and the local vertical (position vector). Over the mission, the velocity angles deviate considerably from the desired zero degrees. Similarly, the local vertical angles are significantly offset from 90°. The local vertical curves never reach 180° because the orbit inclination relative to the ecliptic is about 5°.

3. 4 PENETRATOR DEPLOYMENT

The penetrator targeting options depend on the selection of the initial orbit about Mars, the penetrator Mars atmosphere entry angle limits, PMO orbital precession (orbital period control), and the time from PMO Mars orbit insertion. Any Mars latitude and longitude may be attained by the appropriate selection of the above parameters.

A penetrator impact within ±100 km (3σ) along the PMO orbital path and ±10 km (3σ) across the orbital path from any nominal target point can be achieved.

Accuracy in uetermining the penetrator impact point with respect to the PMO orbit is excellent. Position can be determined within ±23 meters (3σ) along the orbital path, and within ±50 meters (3σ) normal to the orbital path.

A communications link between the penetrators and the PMO can be easily maintained for polar orbits for approximately 700 days after penetrator impact. For orbital inclinations less than 63°, apsidal rotation prevents long term continuous penetrator/PMO communications.

The penetrator targeting options, attainable targeting accuracy, impact position determination, and relative geometry between the penetrators and the PMO are discussed in this subsection.

3.4.1 Deployment Options

Penetrator targeting options are constrained by selection of the initial PMO orbit about Mars, penetrator atmospheric deceleration system, design constraints on the entry angle, PMO orbital precession, and the total impulse of the penetrator deboost motor. Targeting flexibility within these constraints is achieved by in-flight selection of the PMO true anomaly at deployment, the ΔV application direction at deboost, and the choice of deployment time during the mission.

Figure 14 presents the range of possible in-plane locations of the initial penetrator impact as measured from the FMO periapsis as a function of time from the start of the mission. The curve is shown for a range of penetrator entry angles from -12.5° to -21.0°, which correspond to penetrator impact locations from -19° to -43° relative to the orbiter periapsis. Since the orbiter line-of-apsides precesses at approximately -0.1°/orbit, the inplane location of penetrator impact changes at the same rate and traverses 67.9° during the mission.
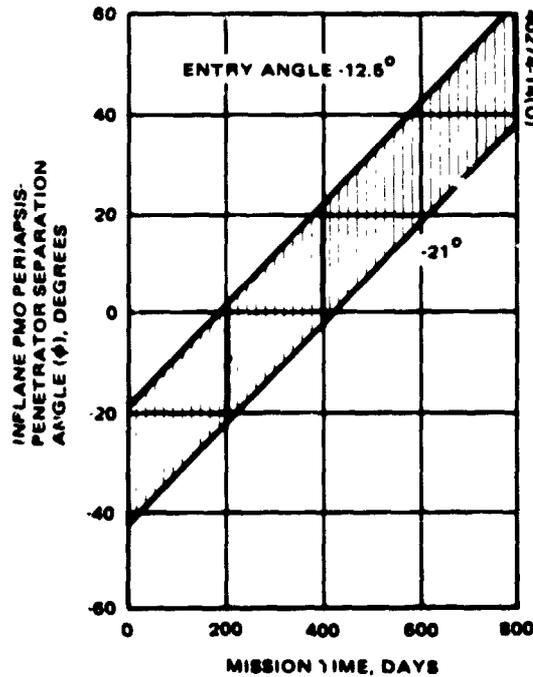
FIGURE 14. INPLANE PENETRATOR LOCATION FOR A PENETRATOR DEPLOYED ON FIRST DAY OF MISSION

24
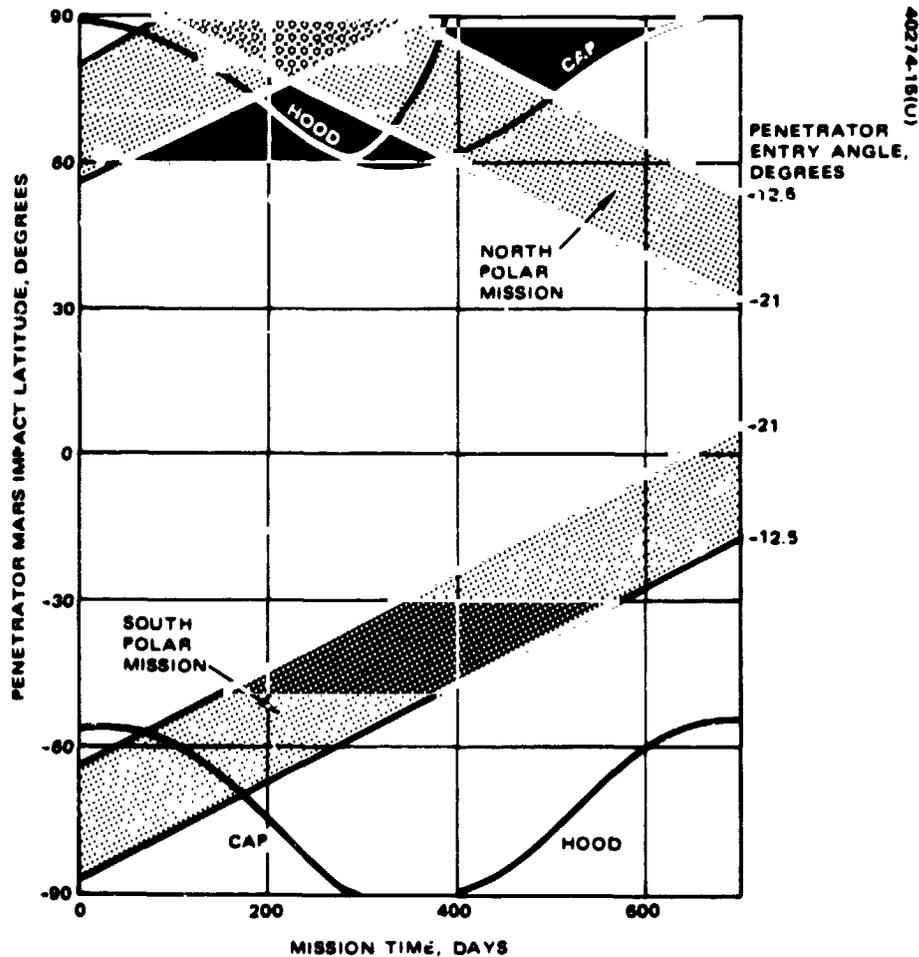
FIGURE 15. PENETRATOR DEPLOYMENT OPTIONS

Two mechanisms are available whereby penetrators may be directed to locations out of the orbit plane. By introducing an out of plane bias in the deboost orientation, impact locations 200 km out of plane may be achieved. Little flexibility exists with this method because the penetrator trajectory from deboost to impact is nearly 180° in true anomaly. Through orbit period control, any longitudinal offset can be obtained. However, the maximum out of plane distance which allows adequate communications geometry is about 1500 km.

For the nominal arrival conditions at Mars, the orbiter initially has a periapsis latitude of 72° south for the south polar orbit and 37° north for the north polar orbit. Penetrator impact latitudes between 63° and 87° south and between 56° and 80° north are achievable for the start of the south and north polar missions, respectively. The oblateness of Mars causes a steady apsidal rotation of about -0.1°/day. In a polar orbit, this precession causes only a latitude change in the permissible penetrator impact locations.

Figure 15 shows the locus of nominal impact point latitudes over the 700 day mission for the north and south polar missions. Note that the north polar mission primarily covers the north pole area and the south polar mission covers the southern hemisphere.

25

TABLE 4. PENETRATOR TARGETING ACCURACY

Impact Dispersions	Entry Angle	
	12.5°	21°
Inplane*, km	94	57
Out of plane**, km	3	9
Entry angle*, deg	0.55	0.42

*RSS of 1.5 percent ΔV and 2.0° pointing errors.
**1.2° pointing error.

3.4.2 Targeting Accuracy

Penetrator targeting dispersions for the nominal deboost ΔV have been computed. A typical 3σ error in total impulse is 1.5 percent. Pointing errors in the deboost ΔV contribute to entry angle errors inplane and out of plane impact point errors. Attitude orientation errors during penetrator deboost are 2.0° (3σ) in the orbit plane and 1.2° (3σ) normal to the orbit plane. The RSS of the targeting errors due to ΔV magnitude and deboost pointing errors are shown in Table 4.

3.4.3 Penetrator Impact Position Determination

The penetrator impact position determination will be accomplished by observing the doppler shifts during the penetrator data transmission to the PMO. The expected 3σ position determination accuracies are:

● along orbiter path ±23 meters

● across the orbiter path ±50 meters

The position determination across the orbiter path is ambiguous in the sense that positions to the left or right from the path will have identical doppler effects. Small orbital precessions will resolve the ambiguity.

3.4.4 Communications Geometry

Communications with a penetrator are constrained by elevation of the orbiter relative to the point of penetrator impact and the distance between the penetrator and the orbiter. Figure 16 illustrates the history of orbiter elevation relative to the penetrator impact point assuming the penetrator is in the orbit plane. (Rotation of Mars can be neglected in the curves because the time span is short). Curves are shown for three penetrator locations: $\phi = 0°$, and ±40° from periapsis. The time scale corresponds to minutes from passing through the penetrator zenith.

Also indicated on the figure is the minimum penetrator antenna elevation coverage. The ±45° coverage is based on a 60° half angle conical beamwidth and 15° antenna axis dispersion about the local vertical when erected on the ground. Each penetrator location gives a minimum transmission time of over 8 minutes.

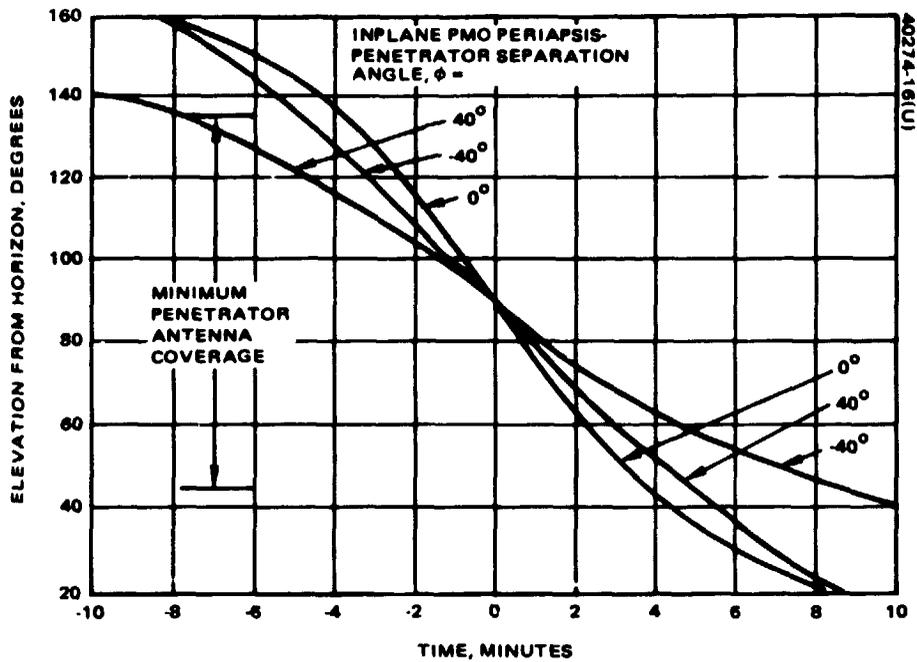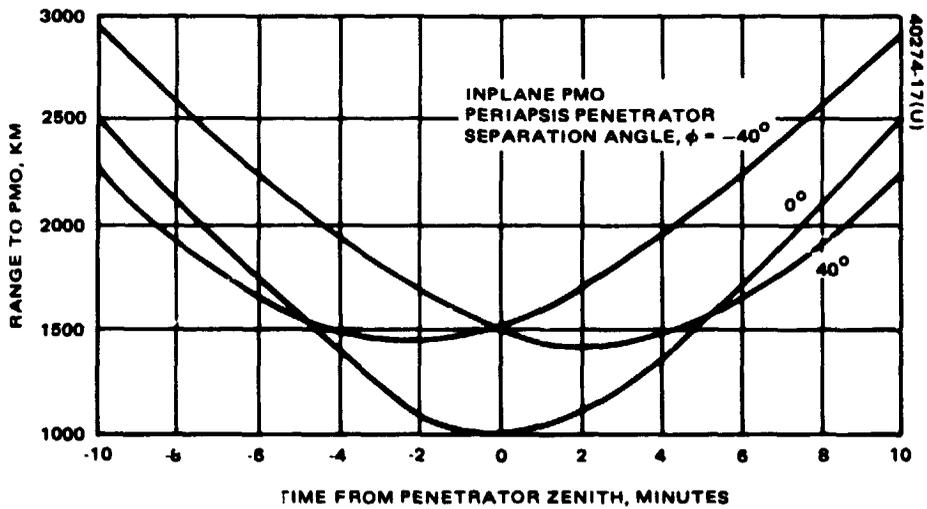FIGURE 16. PENETRATOR COMMUNICATION GEOMETRY IN ORBIT PLANE

FIGURE 17. PENETRATOR COMMUNICATION GEOMETRY IN ORBIT PLANE

Figure 17 illustrates range between the penetrator and the orbiter as a function of time before passing through the penetrator zenith. Again, curves for penetrator locations of 0° and ±40° of separation angle ϕ are shown. The ranges prior to zenith passage, as the elevation angles in

27

the previous figure, have the greatest spread because of the differences in altitude at zenith. In all cases the range for the time interval of interest is well below the 3000 km maximum. Out of plane implant of penetrators of about 1500 km can, therefore, be permitted without exceeding the maximum communication range.

3.5 COMMUNICATIONS AND DATA HANDLING

The penetrator science instrument data is relayed to the Deep Space Network (DSN) stations via the PMO. A data storage capability in the penetrator permits a continuous collection of the science data throughout the mission. The data is read out to the PMO once per orbital pass for both the north and south polar orbits. The data readout is initiated by a timer in the penetrator. The timer and the data rate for the penetrator transmission can be updated by commands from the PMO. This approach maximizes the penetrator data readout potential and the penetrator battery lifetime. The data storage (1 million bit memory) capability in the PMO is adequate to receive all the data from six penetrators on each orbital pass for at least three consecutive orbits and eliminates the need for transmitting the data to DSN stations in real time.

The above approach to the penetrator science data transmissions makes it convenient to deal with the communications in two separate phases: the penetrator/PMO and the PMO/Earth link, subsections 3.5.1 and 3.5.2, respectively.

3.5.1 Penetrator/PMO Communications Link

The penetrator/PMO communications link functions are to transmit commands to the penetrator, to receive at PMO the data transmitted by the penetrator, and to locate the penetrator positions on the surface of the planet by a doppler technique. The nominal operations are scheduled by a penetrator clock. Immediately prior to deployment, the clock is updated to match the PMO time.

After impact in the Martian soil the penetrator antenna is erected and data is transmitted to the orbiter at a preset time and rate. Signal acquisition and bit synchronization in the PMO is accomplished within about 4 seconds. The received signal strength is measured to establish an optimum data rate for penetrator transmissions on the subsequent PMO orbital passes. Furthermore, doppler frequency is measured to provide data for penetrator position estimation.

On subsequent PMO orbital passes a command capability permits the optimization of penetrator operations; namely:

1) Transmission time can be reduced to save battery life.

2) Data rates may be changed to suit most conditions. They may be increased or decreased to compensate for penetrator transponder performance.

3) Commands to experiments become feasible.

4) Clock updates become feasible.

In the absence of commands, the penetrator operations are maintained on the basis of the most recently updated schedule. The planned command link implementation includes a 10 watt transmitter in the PMO. The modulation scheme in the command link is FSK. For a nominal 4 bps command rate, the link margin is about 25 dB.

The penetrator data reception at PMO depends on the communications distances, the penetrator antenna and transmitter performance (EIRP), and the penetrator and PMO antenna patterns and pointing directions. The communications geometry has already been discussed in subsection 3.4.3. The penetrator transmitter RF power is assumed to 0.5 watt, and the antenna gain is assumed to be 1 dB. The penetrator antenna is assumed to be inclined 15° from the local vertical. According to Sandia this is a conservative assumption.

For a communications distance of 3000 km, PMO antenna gain of -10 dB (penetrator at 135° with respect to the PMO spin axis), and linearly polarized signal, a link budget has been constructed in Table 5. The above assumptions represent the worst expected geometry during the mission. The PMO receiver characteristics are summarized in Table 6.

TABLE 5 LINK BUDGET FOR PENETRATOR DATA TRANSMISSION TO PMO

Transmitter power, 0.5W	27 0 dBm
Line loss	0 5
Transmitter antenna gain	1 0
Space loss (400 MHz) 3×10^3 km	154.0
Receiver antenna gain	10 0
Receiver coaxial loss	-0 5
Total received power	137 0 dBm
Noise power density (T_S - 600°K)	-170.8 dBm/Hz
Budget minimum S/N_o	33 8 dB/Hz
Data bit rate (50 bps)	17.0 dB/Hz
Received E/N_o	16 8 dB
Required E/N_o (P_e - 10^{6})	10 5 dB
Margin	6 3 dB

TABLE 6 PMO RECEIVER CHARACTERISTICS

- Six tunable channels, 401 to 406 MHz
- Simultaneous reception of three signals
- PSK biphase modulation
- Programmed data rates 400, 200, 100, 50, 25, 12.5 bps
- Acquisition within 200 bits
- Encode AGC level (6 bits) for signal strength measurement
- Encode received signal frequency - 18 bits or doppler frequency, twice per second
- Preset frequency to minimize lockup time
- Antenna circular polarization – spacecraft orientation either vertical or horizontal

TABLE 7. ATTAINABLE TOTAL DATA PER ORBITAL PASS

Rate, bps	Communications Time, min	Total Data, bits
12.5	21.0	15,750
25	19.6	29,400
50	16.1	48,300
100	11.7	70,200
200	6.4	76,800
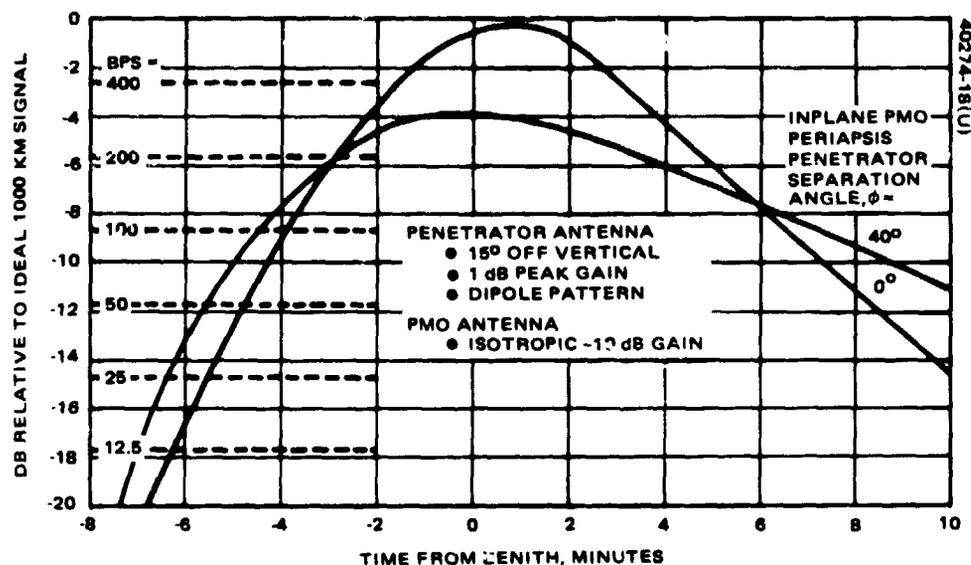
FIGURE 18. PENETRATOR SIGNAL STRENGTH AS RECEIVED AT PMO

For each penetrator there will be a time during the mission when the PMO Mars orbit periapsis will be aligned with the local vertical at the penetrator impact position. Using such a condition (optimum communications geometry) as a reference, the relative penetrator signal strength during the feasible communications periods is shown in Figure 18. The PMO zenith position, with respect to a penetrator, is used as the time reference. The signal strength may be related to the attainable data rates as shown with the dashed lines. Note that the penetrator transmitter power is held constant. Analysis of this data, as summarized in Table 7 (for $\phi = -40°$) shows that total data readout can be optimized by using the highest sustainable data rate.

3.5.2 PMO/Earth Link

The PMO/Earth link is implemented with equipment identical to the PVO. This consists of three antenna systems: 1) high gain (Earth pointing), 2) sleeve dipole, and 3) omni; a transmitter that can operate at two RF power levels, 10 and 20 watts, respectively, and a receiver. Two modes of operation, command and telemetry, are required during the mission.

30

Commands to the PMO can be received with all three antenna systems, which insures a continuous command capability regardless of the orbiter attitude. The selected command rate for the PVO is 4 bps. This rate has been retained for the PMO. During nominal operation, commands from the Earth are sent via a 26 meter DSN antenna and are received with either the high gain or sleeve dipole antenna systems. Should the PMO attitude (e.g., during penetrator deployment) necessitate reception with the omni antennas, the 64 meter DSN antenna with a 200 kW transmitter provides sufficient EIRP to command the PMO even at the maximum communications range.

Telemetry from the PMO to Earth consists of the penetrator science data and small amount of spacecraft status information. The PMO high gain antenna with the transmitter RF power level set at 10 watts will be utilized. These transmissions can be supported with the electric power available from the PMO solar panel. With the 26 meter DSN antenna, the link data rate is one-fourth of the nominal PVO rate of 128 bps, namely, 32 bps. The decrease in the data rate results from operating the transmitter at 10 watts RF power (nominal PVO RF power level is 20 watts), which halves the data rate, and from the increase in the transmission distances for the Mars to Earth link, which lowers the sustainable data rate by a factor of two (as compared to the Venus to Earth link). The link parameters for the nominal operating mode are summarized in Table 8.

TABLE 8. PMO/EARTH COMMUNICATION LINK PARAMETERS

EIRP	62.3 dBm
P_{FD}	10^{-4}
E_b/N_o	6.9 dB
Modulation	PCM/PSK/PM
Coding	Convolutional
Ground readout	DSN 26 meter dish
Performance margins	
Data	1.2 dB
Carrier	1.4 dB
Bit rate family	8×2^n
Transmitted bit rate	32 bps
Command bit rate	4 bps

The penetrator memory size is 50 kilobits, and the theoretical maximum data return in any day (from six penetrators) is 0.30 megabits. The average data return will likely be lower than this, even in the absence of penetrator failure, because the total transmission is limited by the penetrator battery capacity. Furthermore, all penetrators may not be deployed at once. The average bit rate required during a 700 day mission to transmit all the data within the battery capability for six penetrators is 0.17 megabits/PMO orbit, about half the maximum. This is a reasonable estimate of average DSN capability required. DSN transmission time is parameterized in Figure 19.

31
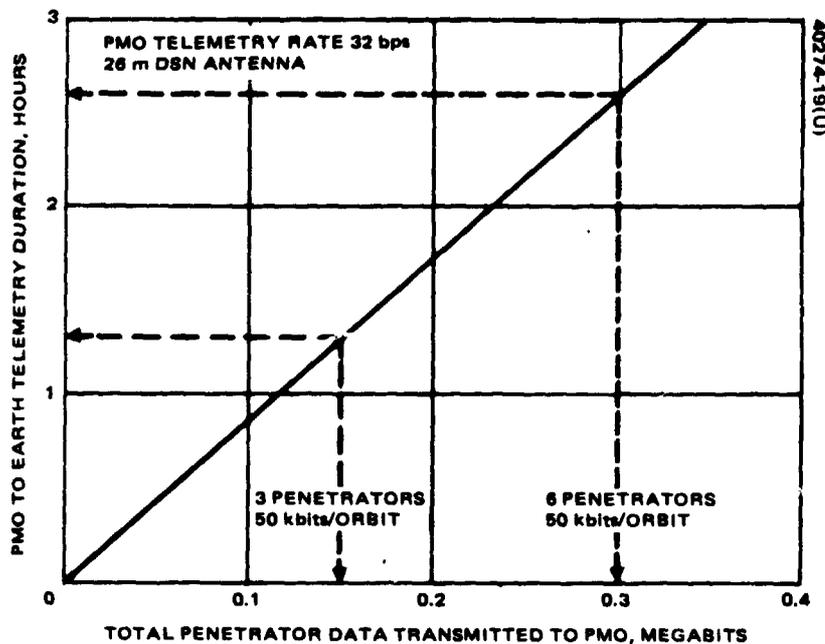
FIGURE 19. PMO TO EARTH DATA TRANSMISSION

Two options in addition to the nominal operation are possible. First, the PMO transmitter may be operated at the 20 watt RF power level (which will double the data rate) by use of battery augmentation. Up to 5 hours of operation are feasible without exceeding a safe depth of discharge for the batteries. A second option (a backup mode for the high gain despun antenna failure) is to utilize the sleeve dipole in conjunction with a 64 meter DSN antenna.
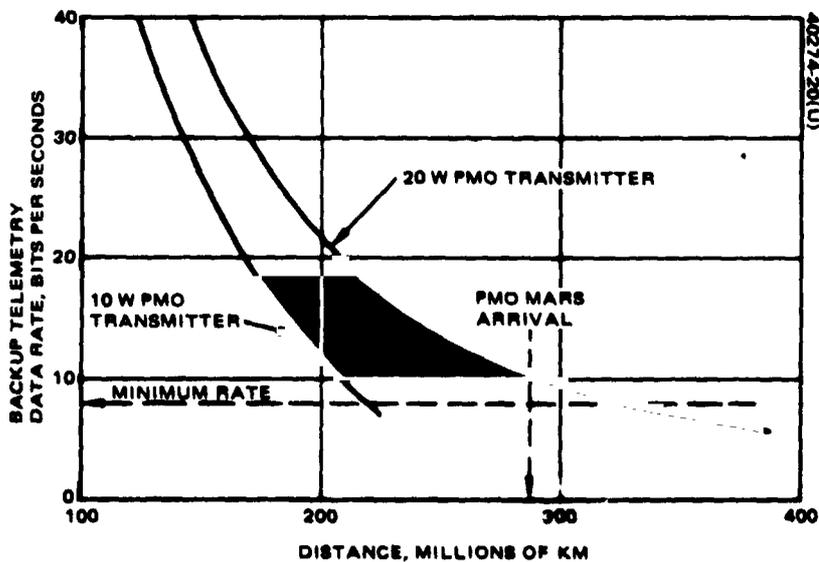
FIGURE 20. BACKUP TELEMETRY MODE

The backup mode telemetry potential is shown in Figure 20. The transmission distances vary throughout the mission as shown in Figures 6, 8 and 9. With the transmitter at the 10 watt power level, and using the sleeve dipole antenna, the link PMO telemetry can be supported during most of the interplanetary transit phase. During the PMO arrival at Mars and for about 60 days after PMO Mars orbit insertion, the 20 watt transmitter is required to support telemetry at 8 bps. From 60 to 330 days after PMO Mars orbit insertion, the attainable bit rate is less than the minimum that can be supported with the PVO equipment. After 330 days, the distance between Mars and Earth decreases to the point where the telemetry support with the sleeve dipole antenna is feasible for the remainder of the mission.

3.6 ORBITER DYNAMICS ANALYSIS

The unique feature of the Mars penetrator mission from a dynamical viewpoint is the deployment of the penetrators. The dynamical considerations associated with the penetrators are addressed in this subsection. Analyses indicate that it is feasible to carry and deploy penetrators with little change to the attitude control procedures from PV spacecraft. The principal "penetrator effects" analyzed were: 1) the steady state attitude motion of the spacecraft during the time between penetrator launches, and 2) the transients due to the penetrator deployment. For those phases of the mission which are essentially identical (dynamically) to PV orbiter, it was verified that the PV results are still applicable.

3.6.1 Steady State Dynamics

After each penetrator deployment, the mass properties of the spacecraft change significantly. Some quantities pertinent to the attitude stability are shown in Table 9. The first three columns show the location of the spacecraft center of mass (CM). In particular, $\bar{X}$ and $\bar{Y}$ are the distances between the CM and the spin axis in the two orthogonal directions transverse to the spin axis, and illustrate that there are significant offsets when an uneven number of penetrators have been deployed. Although the attitude stability is not affected by such an offset, dynamical loads on the despun antenna

TABLE 9. MASS PROPERTY SUMMARY

Condition	Center of Mass, in.			$\dfrac{I_{Spin}}{I_{Trans.}}$	$\dfrac{1}{I_{Spin} \cdot I_{Trans.}}$ (Sl. ft^2)$^{-1}$
	X	Y	Z		
Initial orbit	0	0	51.2	1.30	0.008
1 Deployed	2.8	-1.6	51.2	1.22	0.010
2 Deployed	0	0	51.2	1.15	0.013
3 Deployed	-3.4	-1.9	51.3	1.15	0.018
4 Deployed	0	0	51.3	1.11	0.028
5 Deployed	0	-4.8	51.3	1.18	0.021
6 Deployed	0	0	51.3	1.30	0.017

platform and the despin bearing assembly are higher than those for PV. This is so because the spin axis will orbit about the spacecraft CM (which is fixed in inertial space) at spin frequency, and this motion places centrifugal loads on the platform. For a 40 rpm spin speed, these loads are an order of magnitude smaller than those encountered during launch, although potentially they will be applied for longer periods of time. A study of the effects of such loading on the bearing lifetime will be necessary.

The fourth column of Table 9 is a tabulation of the ratio of spin inertia to total spacecraft transverse inertia. This dimensionless parameter must always be greater than 1.00, theoretically (and greater than 1.05 from a practical viewpoint), to ensure attitude stability for the class of satellites under consideration. The minimum of 1.11 occurs when four penetrators have been deployed. This value has sufficient margin to ensure good attitude stability. In the fifth column a tabulation of the reciprocal of the difference between the spin inertia and the transverse inertia is presented. For a given spacecraft unbalance, spin axis wobble is proportional to this quantity. A detailed discussion of wobble is contained in subsection 3.6.2.

In Figure 21, the spacecraft angular momentum as a function of spin speed is shown for two particular spacecraft configurations. Since the RCS fuel used for attitude reorientation maneuvers (such as those during orbit insertion and penetrator deployment) is proportional to the angular momentum, the spin speed should be selected as low as possible while still allowing reasonable intervals between corrections for attitude disturbances such as solar torque. For the PV orbiter, the spin speed was selected to be 15 rpm during interplanetary cruise, 30 rpm for the orbit insertion maneuver, and 5 rpm to satisfy science requirements during its orbital lifetime. Since the orbital lifetime of the PMO mission involves a number of attitude maneuvers similar to the orbit insertion maneuver, the spacecraft angular momentum was selected to be at least as high as that for the PV orbiter during its orbit insertion maneuver. During the part of the mission when all of the penetrators are still attached to the spacecraft and the spin inertia is relatively high, the spin speed would be 15 to 20 rpm. Even after the penetrators are released, this spin speed will produce an angular momentum greater than that for the operational PV orbiter.
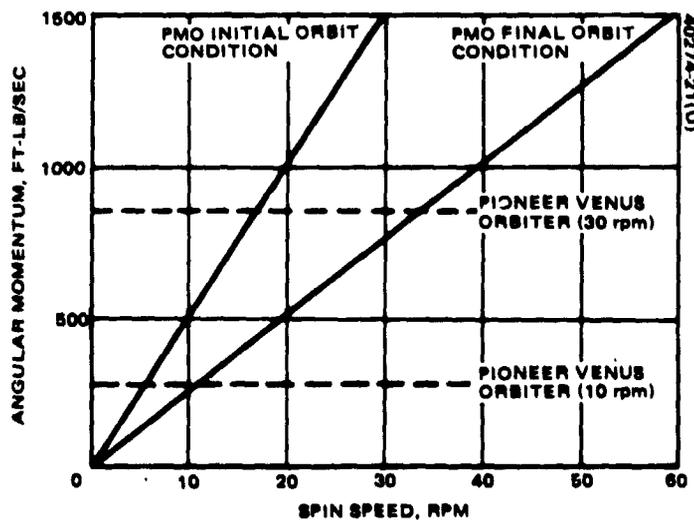

FIGURE 21. ANGULAR MOMENTUM VERSUS SPIN SPEED

3. 6. 2 Penetrator Deployment Effects

During a penetrator deboost the spacecraft will receive a net impulse of up to 6 lb-sec due to the various interaction forces between the penetrator and its launch tube. To close approximation, the direction of the impulse is parallel to the spin axis and its point of application is on the launch tube center line. This results in a net impulsive transverse torque about the spacecraft CM which induces nutation and precesses the spacecraft angular momentum vector. Immediately after the penetrator launch, the spacecraft spin axis will be nutating (coning) about the new angular momentum vector. Within a few minutes the nutation damper will virtually eliminate the coning motion, and the spacecraft will be left with a permanent attitude change equal to the precession of the angular momentum vector. Because the transverse torque is impulsive in nature, the attitude precession and the induced nutation are numerically equal.

In Figure 22, these effects are illustrated as a function of spacecraft spin speed. The upper curve shows these effects for the launch of a single penetrator which results in the impulsive force, I, as shown in the upper picture. The lower curve illustrates these effects for a dual penetrator launch, as shown in the lower picture, where the impulsive forces of the two penetrator, I_1 and I_2, differ by 20 percent. Since nutation and attitude changes on the order of 2° are introduced on other phases of the mission (such as ΔV maneuvers and attitude reorientation maneuvers), it would be reasonable to be spinning as slowly as 20 rpm for the single penetrator launch, and as slowly as 5 rpm for the dual penetrator launch without jeopardizing spacecraft attitude performance.

The steady state attitude motion acquired by the spacecraft between penetrator launches is a simple spin about the central principal axis of maximum moment of inertia. The angle between this principal axis and
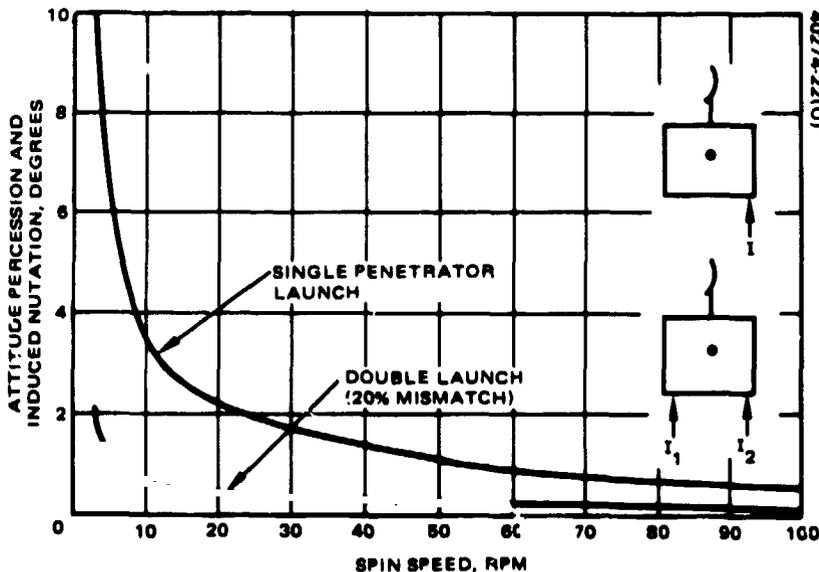

FIGURE 22. EFFECTS OF PENETRATOR LAUNCH IMPULSE

35

the nominal spin axis is called the wobble angle. The spin axis cones about the principal axis (which is fixed in inertial space) at spin speed, and this coning motion is undesirable for a number of reasons. Prior to launch, the spacecraft is carefully balanced to minimize the wobble angle. As the penetrators are released during the mission, various misalignments and offsets introduced during the penetrator mounting procedure will result in slight changes in the location of the spacecraft principal axes. Hence, a wobble angle is introduced due to various misalignments and offsets of the penetrators. This study is summarized in the next four figures. In each of the figures only one effect at a time is treated. The total spacecraft wobble would be a vectorial sum (for small wobble angles) of all wobble angle changes from all sources.

Figure 23 illustrates the effect of a misalignment between the principal axis of a penetrator about to be released and the spacecraft principal axis. With careful balancing of the bus and penetrators, this misalignment can be held to under 0.2°, which results in a 0.04° contribution to wobble.
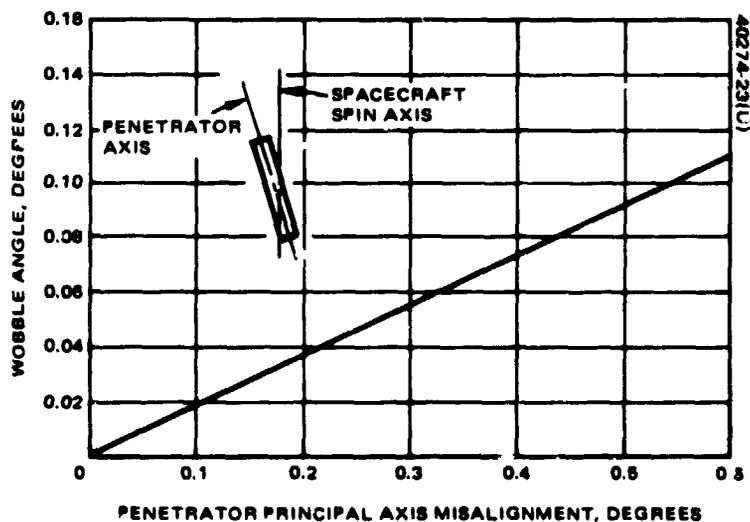
FIGURE 23. WOBBLE ANGLE VERSUS PENETRATOR PRINCIPAL AXIS MISALIGNMENT

If the penetrators are released one at a time, an important contributor to wobble (when an uneven number of penetrators is attached to the bus) is the axial offset of the penetrator CM plane relative to the space-craft CM. Figures 24 and 25 illustrate this effect. The largest uncertainty in the axial position of the spacecraft CM is due to the uncertainty in the amount of fuel used during interplanetary midcourse correction maneuvers. Figure 24 illustrates the relative axial movement of the spacecraft CM as a function of the fuel used and indicates an uncertainty on the order of 1 to 2 cm is possible. Figure 25 shows that this uncertainty could translate into wobble angles as high as 0.5° to 1.0°, and indicates that active mass balancing mechanisms may be required for single-release capability.
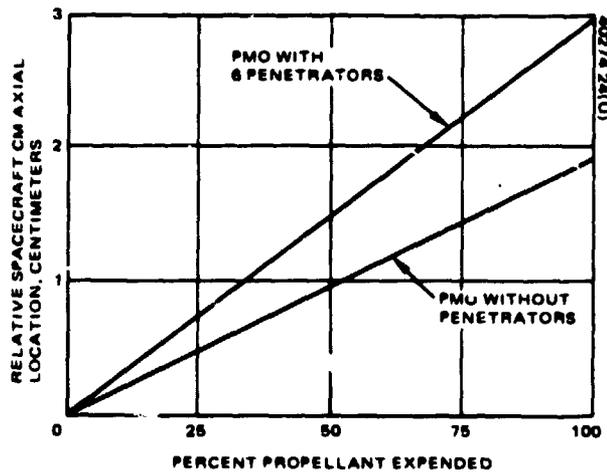
FIGURE 24. AXIAL CENTER OF MASS LOCATION
VARIATION EXPENDED PROPELLANT
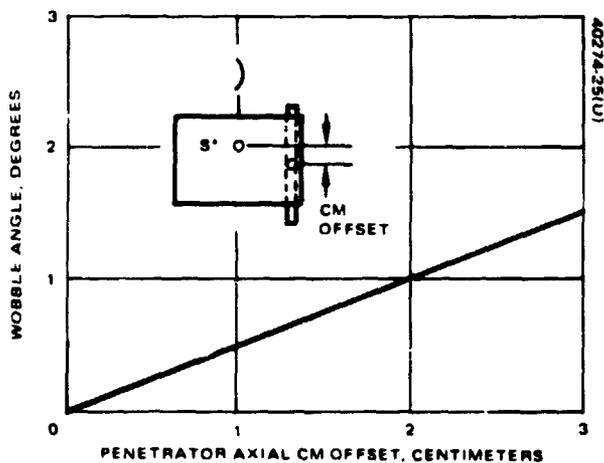
FIGURE 25. WOBBLE DUE TO PENETRATOR CENTER
OF MASS OFFSET (INDIVIDUAL LAUNCHES)
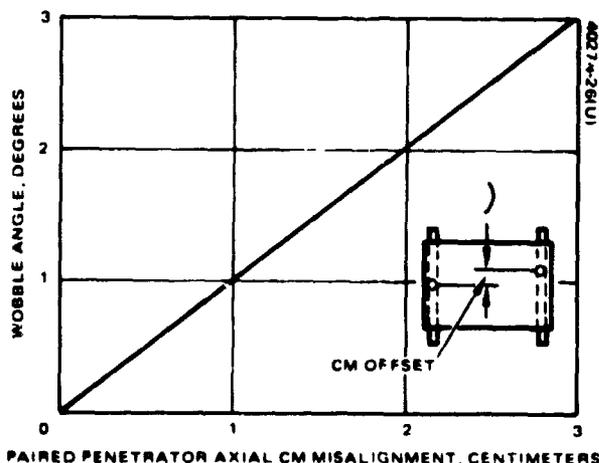
FIGURE 26. WOBBLE DUE TO PENETRATOR CENTER
OF MASS OFFSET (LAUNCHES IN PAIRS)

When two diametrically mounted penetrators are simultaneously
released, the axial misalignment of their CMs will produce a wobble angle
change. Figure 26 illustrates this effect. With careful mounting and balanc-
ing this misalignment could be held to a few millimeters, which results in
wobble angle change of a few tenths of a degree.

4. PIONEER MARS ORBITER DESIGN CONCEPT

A Pioneer Mars Orbiter (PMO) spacecraft can readily be developed from the Pioneer Venus (PV) spacecraft program. Although modifications and additions to the PV spacecraft are required, all of them are simple adaptations from various operational Hughes hardware prog--ms. Use of proven technology guarantees a low cost, reliable spacecra design.

Salient differences between the PMO and PV missions and their impact on the spacecraft design are discussed in Section 4.1. The PMO spacecraft configuration, mass properties, and power requirements are dealt with in Section 4.2.

4.1 MISSION IMPACT ON PMO DESIGN

A comparison of the PMO with the PV mission reveals the following impact on spacecraft designs:

1) Lower solar flux which:

    a) Changes the spacecraft thermal environment

    b) Lowers the solar panel output

2) Increased communication distances

3) Considerably lower science data return

4) Large added payload — penetrators

5) A requirement for penetrator deployment

6) Planetary quarantine requirements for penetrators

The thermal environment changes can be resolved by implementing a passive thermal control concept similar to that utilized for the currently operational Hughes synchronous communication satellites. This concept (discussed in Section 5.5) eliminates the need for louvers.

PRECEDING PAGE BLANK NOT FILMED.

A modest increase in the solar panel size, achieved by covering the portion of the PV substrate above the equipment shelf with solar cells, results in sufficient electric power to operate one of the two PV 10 watt transmitters from the PMO Mars orbit. The attainable data rate for the PMO/Earth link with this 10 watt transmitter and the despun antenna exceeds the maximum potential science data return from all six penetrators simultaneously. Additional communication equipment for the penetrator/PMO link can easily be derived from Hughes communication satellite hardware.

The increased PMO payload (penetrators) requires addition of a third stage (TE 364-4) to the Atlas/Centaur launch vehicle. This configuration has been flight proven on Pioneer 10 and other space missions and adds approximately $0.5 million to the Atlas/Centaur launch vehicle costs. Other consequences of the increased mass are added attitude and velocity control propellant (hydrazine), the use of the PV alternate orbit insertion motor, and structural modifications.

Penetrator deployment mechanisms are derivations from the Hughes TOW missile launcher program. Since approximately 4000 TOW launches have been performed, the feasibility of implementing such a penetrator deployment system has been adequately demonstrated.

The planetary quarantine imposes a requirement that the penetrators be sterilized, and that during the time between the sterilization and their deployment, the penetrators must not be recontaminated. To satisfy these requirements, selected penetrator launch tube deployment mechanisms and deboost motor designs can sustain the thermal cycle of sterilization and the launch tube remains hermetically sealed until the penetrator deployment.

4.2 PMO DESIGN

The spacecraft configuration is an adaptation of the PV orbiter. The PV inheritance and modifications needed to adjust the design for the Mars mission environment and for the penetrators are summarized in Table 10. An exploded view of the PMO spacecraft, Figure 27, illustrates most of the design modifications discussed in Table 10. The most obvious changes are the addition of the penetrator launch tubes shown on the left of the figure and the associated structural changes — the secondary structure and the cutouts in the equipment shelf.

4.2.1 Configuration

The added orbiter and penetrator mass requires the addition of a third stage (TE 364-4) to the launch vehicle. As a result, the PMO launch vehicle stackup, shown in Figure 28, is approximately 3 meters higher than PV.

40

WIDEBEAM OMNI ANTENNA

SLEEVE
DIPOLE
ANTENNA

UHF ANTENNA (NEW)

S BAND HIGH GAIN
ANTENNA

BAPTA

ADDED
SOLAR CELLS

BAPTA
SUPPORT

PENETRATOR
ASSEMBLY
(TOW)

SOLAR PANEL
CYLINDER

EQUIPMENT SHELF
WITH PENETRATOR
CUTOUTS

SECONDARY
STRUCTURE
(NEW)

SUPPORT STRUTS

PROPELLANT TANKS (MARISAT)

RADIAL THRUSTERS

THRUST
TUBE

AXIAL
THRUSTERS

ORBIT INSERTION
MOTOR

AFT THERMAL
BARRIER (INTELSAT IV,
TELESAT)

FIGURE 27. EXPLODED VIEW OF PMO WITH PENETRATORS

41

TABLE 10. PMO DESIGN SUMMARY

Subsystem	PMO Design Approach	
	Commonality With PV Spacecraft	Equipment Adapted from Other Hughes Programs
Communications Telecommunications Data handling Command	Identical PMO/Earth link and data handling equipment	Penetrator/PMO link transmitter and receiver
Antennas	Identical, except despun antenna positioner deleted	Two UHF antennas for penetrator/PMO link
Structure	PV structure used as PMO primary structure	PMO secondary structure
Orbit insertion motor		From Hughes GMS program compatible with PV structure
Thermal control		Passive thermal control system based on Hughes synchronous satellite designs
Electric power	Identical solar panel substrate Identical solar cells Identical battery system Bus voltage limiter deleted	Added cells on substrate Array voltage limiter from Telesat program
Velocity and attitude control	Identical control system Slightly modified RCS system	One added thruster identical with PV Hydrazine tanks from Marisat program
Penetrator deployment mechanism		Derived from Hughes TOW program

DIMENSIONS IN METERS (FEET)

0.76 (2.5)
EXTENDED FAIRINGS

STANDARD
FAIRING

5.1
(16.7)

7.8
(25.7)

3.99
(13.1)

4.75
(15.6)

TE364-4
THIRD
STAGE

CENTAUR STATION 413.61 (163.9)

PIONEER MARS ORBITER WITH PENETRATORS   PIONEER VENUS ORBITER
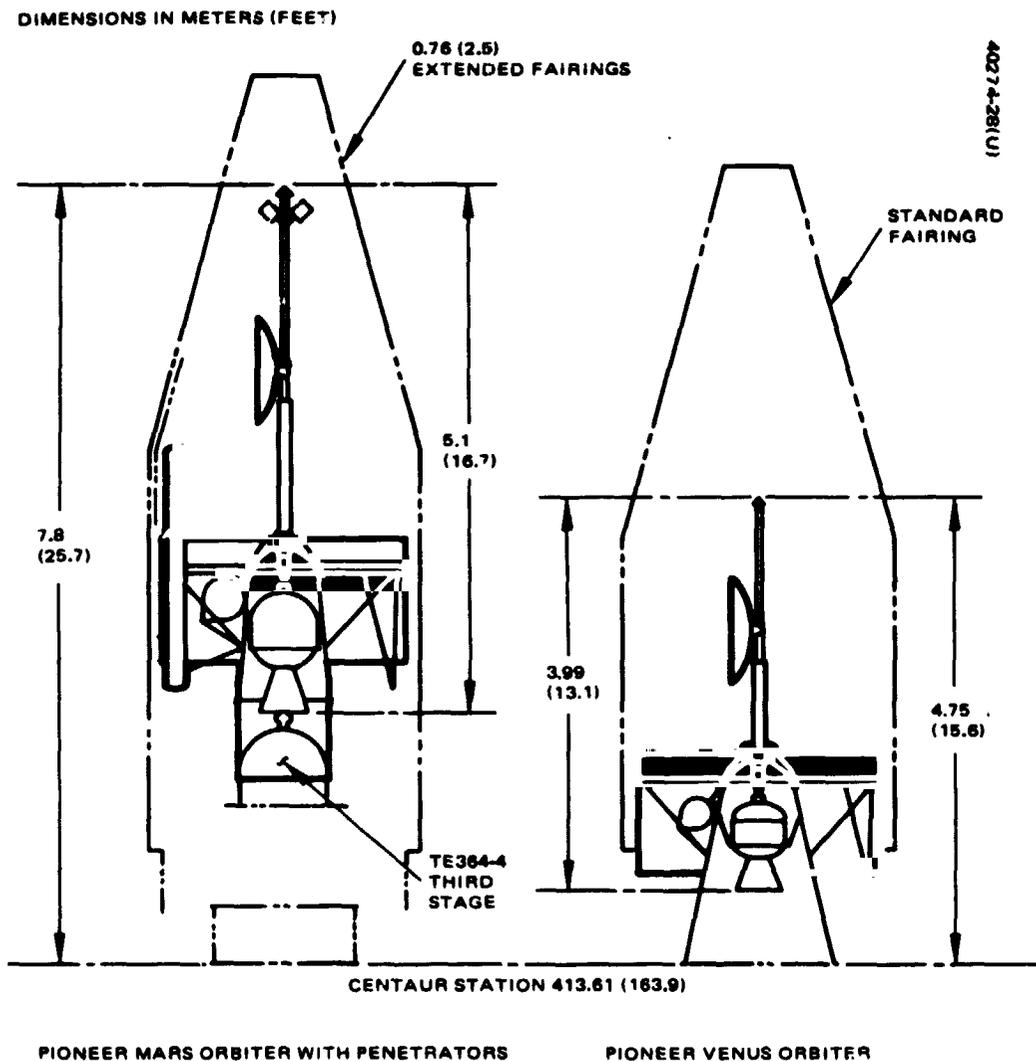
FIGURE 28. COMPARATIVE STACKUP OF PVO AND PMO WITH PENETRATORS

The standard fairing, which is more than ample for PV, would still suffice for the penetrator spacecraft except for the penetrator assembly which extends forward, well beyond the solar panel plane. The necessary fairing extension, 0.76 meter, is not a major item and does not require

43

40274-29(U)

DIMENSIONS IN CENTIMETERS (INCHES)

RADIAL THRUSTER (4)

PROPELLANT TANK (3)

PENETRATOR/EQUIPMENT SHELF SUPPORT STRUTS (12)

PENETRATOR LATERAL SUPPORT STRUT (12)

PENETRATOR SUPPORT BEAM (6)

AFT AXIAL THRUSTER (2)

333 (131)

122 (48)

254 (100) DIA SOLAR ARRAY

UHF ANTENNA (2 QUADRIFILAR HELICES)

SLEEVE DIPOLE ANTENNA

DESPUN ANTENNA SUPPORT MAST

EQUIPMENT SHELF (NOTCHED FOR PENETRATORS)

FORWARD THERMAL BARRIER

FORWARD AXIAL THRUSTER (2)

BAPTA

SEPARATION PLANE

TEM 616 ORBIT INSERTION MOTOR

TE 364-4 ADAPTER

WIDEBEAM OMNI ANTENNA

S BAND HIGH GAIN ANTENNA

THRUST CONE

PENETRATOR LAUNCH TUBE (6)

PENETRATOR

PENETRATOR EJECTION MOTOR

NARROWBEAM OMNI ANTENNA

AFT THERMAL BARRIER

FIGURE 29. PMO WITH PENETRATORS

44

fairing requalification. Despite the height increase and lengthened fairing, preliminary analysis indicates a sufficient clearance for dynamic excursions between spacecraft and fairing.

The PMO with penetrators is shown in Figure 29. The PV orbiter spacecraft load paths have been maintained but altered geometrically because of thrust cone adaption to the TE 364-4 third stage interface which is 0.94 meter in diameter instead of the 1.57 meters for PV. Although narrower conically, it has an adequate diameter to comfortably incorporate the larger TEM-616 orbit insertion motor. Support of the bearing and power transfer assembly (BAPTA) quadripod and equipment shelf by the thrust cone is identical to PV.

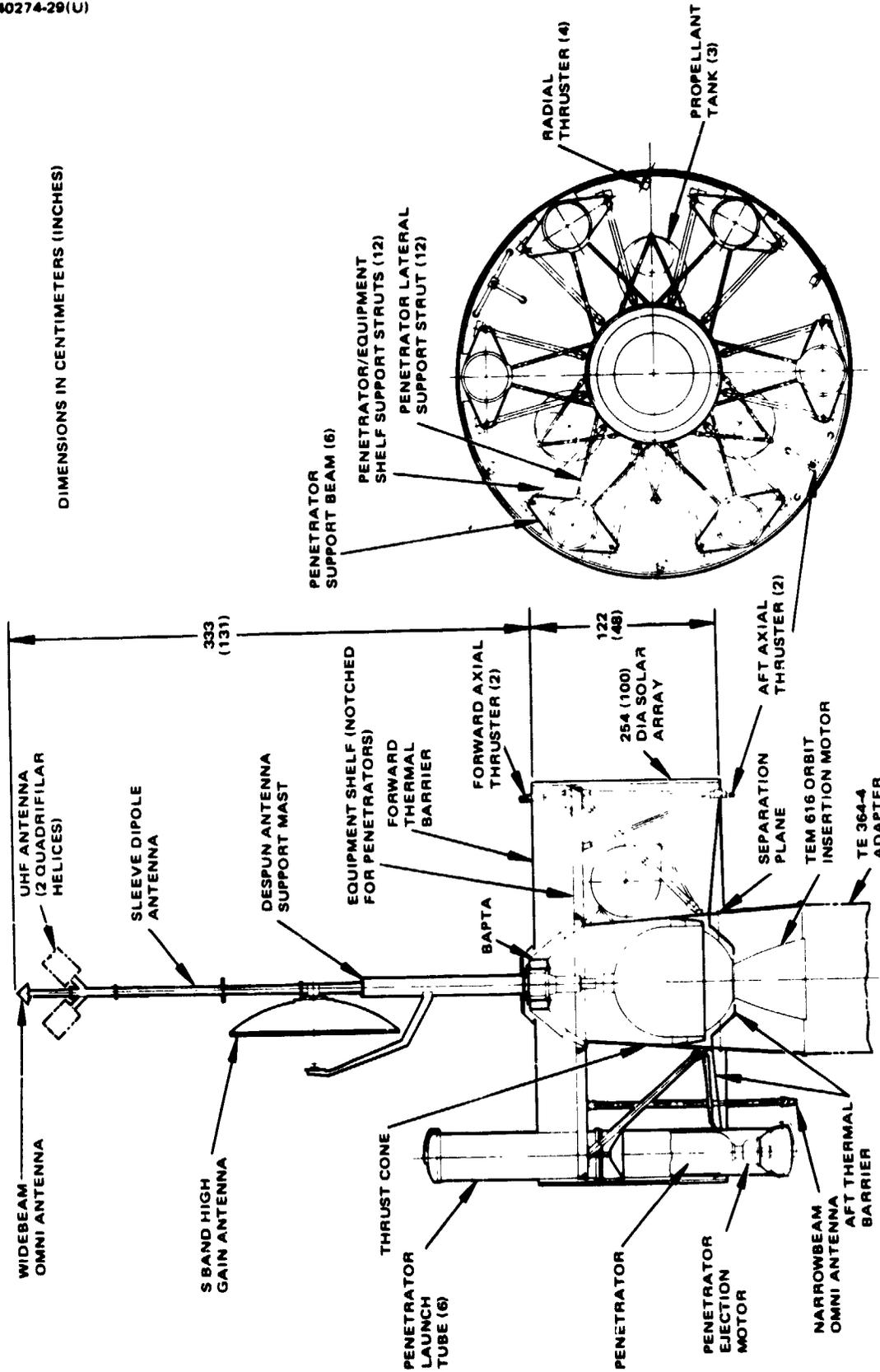The solar panel substrate is identical to PV in length (1.22 meters), and diameter (2.54 meters), but is completely covered with solar cells.

Six penetrator assemblies are housed internally but as far outboard as possible to enhance spacecraft roll inertia. Their centers of mass are placed to minimize spacecraft unbalance due to deployment. The assembly consists of a penetrator and deployment system housed in a 0.292 meter diameter launch tube 2.34 meters long (including swing away caps on both ends). A V-beam girdles the launch tube and spans between shelf support struts. A single attachment through the beam end and the strut end fitting provides axial support once the strut is attached to the shelf. A tubular bipod near the base of the launch tube provides lateral support and eliminates moment in the beam support. For thermal reasons, the launch tube makes no direct contact with the equipment shelf which is cut out locally to provide clear passage of the launch tube. To further minimize conduction, use of titanium at attach points is being considered. This support system allows for ease of assembly or removal of the penetrator launch tubes through the aft end of the spacecraft.

Additions to the spacecraft include: an aft thermal barrier for passive thermal control, two UHF antennas on the forward mast for penetrator communications, a second forward axial thruster for added maneuvering capability, a larger capacity three tank (existing) hydrazine system which neatly interdigitates with the six penetrators, and a small complement of communication equipment on the shelf to implement the penetrator/PMO link.

The antenna system of the PV is maintained except for the high gain antenna positioner, presently not required.

Although the despun antenna mast is lengthened 0.74 meter, the bearing assembly is still within load specification and needs no modification.

There is no orbiter science or louvers on the equipment shelf, so that loss of area due to penetrator cutouts does not hinder placement of equipment which can now be on the top or bottom of the shelf.

45

4.2.2 Mass Properties

The total mass of the PMO spacecraft is 1091 kg, including the penetrators and the booster adapter. The penetrators are a significant percentage of the total spacecraft mass comprising, along with the launch mechanisms, 44.5 percent of the dry spacecraft mass. Detailed mass listings, Table 11, are included to show the modifications required for the Mars mission and to apportion mass contingencies. The spacecraft modifications required to adapt the PV orbiter for the Mars mission can be implemented with hardware similar to that used on many Hughes and other spacecraft programs. Thus, a high level of confidence exists for achieving flight hardware within the present mass allocation.

The most significant subsystem change occurs in the structure and harness subsystem where the net increase is 93.5 kg. Of this increase, 67.6 kg is allocated for the six penetrator launch tubes and support structure. The launch tube development will be based on the existing Hughes TOW launcher technology. The support system is a standard tube structure. The remaining mass increase of 25.8 kg represents the changes in the thermal control system, the propellant tank support structure, the use of the PV optional orbit insertion motor, and minor increases in antenna support structure mass.

The summary mass statement shown in Table 12 compares the PMO and PV orbiter, and includes spacecraft contingency and expendables. The Hughes designed launch fitting is smaller in diameter, shorter, and has less mass than the PV launch fitting.

The penetrator and launch mechanism mass is shown as part of the dry spacecraft mass. The penetrator mass is representative of hermetically sealed, sterilizable units with external adaption to the launch mechanism. The penetrator mass estimates are assumed to include their own contingency and do not have an allocation included in the spacecraft contingency budget.

The penetrator deployment sequence used to generate the sequenced mass properties is shown in Figure 30. The selected deployment sequence minimizes spacecraft static and dynamic imbalance. The sequenced mass properties are shown in Table 13.

The spin-to-transverse moments of inertia ratios are between 1.11 to 1.30. The spacecraft experiences a lateral center of mass displacement due to imbalance caused by an uneven number of penetrators remaining on board the spacecraft. Products of inertia are minimized by placement of the penetrator centers of mass at nearly the midrange of the spacecraft vertical center of mass travel during the 700 day Mars orbit phase.

Stringent mass and center of mass requirements must be imposed during the penetrator development to preclude a problem in this area.

46

TABLE 11. PIONEER SPACECRAFT DETAILED MASS COMPARISON

Item/Subsystem	Venus Orbiter		Mars Orbiter	
	kg	lb	kg	lb
Communication Subsystem	17.91	39.5	21.09	46.5
Transponder (2)	3.99	8.8	3.99	8.8
4-way divider	0.09	0.2	0.09	0.2
2-way summer	0.05	0.1	0.04	0.1
Filter — TX BP (2)	0.82	1.8	0.82	1.8
Filter — harmonic (2)	0.09	0.2	0.09	0.2
Circulator — isolator (2)	0.23	0.5	0.23	0.5
SPDT switch (1)	0.45	1.0	0.45	1.0
Transfer switch (3)	0.95	2.1	0.95	2.1
Power amplifier (4)	3.45	7.6	3.45	7.6
Transmitter, X band occultation	1.72	3.8	0	0
Rotary joint	0.82	1.8	1.27	2.8
Coaxial cable	1.13	2.5	2.27	5.0
High gain antenna	2.77	6.1	2.77	6.1
Sleeve dipole antenna	0.91	2.0	0.91	2.0
Omni (wide beam)	0.18	0.4	0.18	0.4
Omni (narrow beam)	0.27	0.6	0.27	0.6
Penetrator antenna	0	0	0.59	1.3
Switch (3)	0	0	0.27	0.6
Preamplifier, 400 MHz (2)	0	0	0.09	0.2
Receiver/decoder (6)	0	0	0.54	1.2
Doppler set (2)	0	0	0.41	0.9
Transmitter/modulator	0	0	0.50	1.1
Diplexer	0	0	0.23	0.5
Synthesizer (2)	0	0	0.45	1.0
Shelf heaters	0	0	0.23	0.5
Data Handling System	16.96	37.4	16.24	35.8
Dual data input modules (4) (2)	1.45	3.2	0.73	1.6
Telemetry processors (2)	3.36	7.4	3.36	7.4
PCM encoders (2)	3.08	6.8	3.08	6.8
Data storage unit (2)	9.07	20.0	9.07	20.0
Command Subsystem	10.43	23.0	11.93	26.3
Command demodulator (2)	2.54	5.6	2.54	5.6
Command processor (2)	4.72	10.4	4.72	10.4
Command output module (6)	1.90	4.2	1.90	4.2
Pyro control unit	1.27	2.8	1.27	2.8
Command unit	0	0	0.91	2.0
Penetrator wire harness (6)	0	0	0.59	1.3
Controls Subsystem	29.57	65.2	19.55	43.1
Sun sensor assembly (2)	0.32	0.7	0.32	0.7
Star sensor	2.27	5.0	2.27	5.0

Table 11 (continued)

Item/Subsystem	Venus Orbiter		Mars Orbiter	
	kg	lb	kg	lb
Controls Subsystem (continued)				
Attitude data processor (2)	3.54	7.8	3.54	7.8
Solenoid driver	1.04	2.3	1.04	2.3
Nutation damper (2)	1.63	3.6	1.63	3.6
Louver (12)	3.54	7.8	0	0
Despin control electronics	4.17	9.2	4.17	9.2
BAPTA	6.58	14.5	6.58	14.5
Magnetometer deployment mechanism	3.90	8.6	0	0
High gain antenna positioner mechanism	2.04	4.5	0	0
Positioner electronic unit	0.54	1.2	0	0
Structure and Harness Subsystem	106.62	235.1	200.04	441.1
Equipment shelf	21.09	46.5	19.55	43.1
Shelf support struts	1.95	4.3	2.22	4.9
Strut fittings	2.04	4.5	2.31	5.1
Thrust tube	16.73	36.9	20.41	45.0
BAPTA support	2.22	4.9	2.22	4.9
Forward omni mast	0.27	0.6	0.41	0.9
Aft omni support structure	0.36	0.8	0.59	1.3
High gain antenna mast	2.13	4.7	2.81	6.2
Brackets, shelf to substrate	1.81	4.0	1.81	4.0
Solar panel substrate	17.28	38.1	17.28	38.1
OIM support cone	2.63	5.8	0	0
Propellant tank support	1.00	2.2	9.07	20.0
Thruster support (7) (8)	2.95	6.5	4.54	10.0
Balance weight	2.72	6.0	4.54	10.0
Miscellaneous hardware	1.81	4.0	3.63	8.0
Thermal blankets	10.52	23.2	12.83	28.3
Shelf doublers	2.27	5.0	2.27	5.0
Thermal coatings	0.91	2.0	0.91	2.0
Temperature sensors (21)	0.14	0.3	0.14	0.3
Thruster insulation (7) (8)	0.54	1.2	0.68	1.5
RF altimeter support	0.68	1.5	0	0
Magnetometer deployment support	0.86	1.9	0	0
Orbit insertion motor (OIM) support cone	0	0	3.63	8.0
Adj. mount-neutral mass spectrometer	0.36	0.8	0	0
Adj. mount-ion mass spectrometer	0.18	0.4	0	0
Separation switch (2)	0.45	1.0	0.45	1.0
Wire hareness	12.70	28.0	12.70	28.0
Aft thermal barrier	0	0	7.48	16.5

Table 11 (continued)

Item/Subsystem	Venus Orbiter		Mars Orbiter	
	kg	lb	kg	lb
Structure and Harness Subsystem (continued)				
Penetrator launch tubes (6)	0	0	44.90	99.0
Structural modifications for penetrators	0	0	22.67	50.0
Power Subsystem	<u>39.09</u>	<u>86.2</u>	<u>40.32</u>	<u>88.9</u>
Battery (2)	17.41	38.4	17.41	38.4
Undervoltage/overload control switch	0.68	1.5	0.68	1.5
Charge/discharge controllers (2)	2.72	6.0	2.72	6.0
Bus limiter (6) (2)	3.76	8.3	1.81	4.0
Solar array (excludes substrate)	12.43	27.4	15.60	34.4
Power interface unit	1.59	3.5	1.59	3.5
Current sensors (3)	0.50	1.1	0.50	1.1
Propulsion Subsystem (dry)	<u>8.89</u>	<u>19.6</u>	<u>13.92</u>	<u>30.7</u>
Propellant tanks (2) (3)	3.13	6.9	7.53	16.6
Thrusters (7) (8)	1.27	2.8	1.45	3.2
Propellant valve (7) (8)	1.59	3.5	1.81	4.0
Fill valve	0.14	0.3	0.14	0.3
Filter	0.54	1.2	0.54	1.2
Pressure transducer	0.23	0.5	0.23	0.5
Tubing	0.45	1.0	0.54	1.2
Fittings	0.45	1.0	0.45	1.0
Thruster valve heaters (7) (8)	0.02	0.05	0.05	0.1
Temperature sensors (9)	0.09	0.2	0.09	0.2
Propellant plenums	0.14	0.3	0.14	0.3
Propellant tank heaters (2) (3)	0.27	0.6	0.41	0.9
Latch valve (2)	0.54	1.2	0.54	1.2
Orbit Insertion Motor Case	<u>21.14</u>	<u>46.6</u>	<u>26.40</u>	<u>58.2</u>
Motor case (burned out)	21.09	46.5	26.35	58.1
Nozzle heater	0.05	0.1	0.05	0.1
Temperature sensors (2)	0.00	0.0	0.00	0.0
Scientific Instruments	<u>45.35</u>	<u>100.0</u>	<u>0</u>	<u>0</u>
Neutral mass spectrometer	6.26	13.8	0	0
Ion mass spectrometer	1.68	3.7	0	0
Electron temperature probe	1.59	3.5	0	0
UV spectrometer	6.26	13.8	0	0
Magnetometer	2.68	5.9	0	0
Solar wind analyzer	5.76	12.7	0	0
IR radiometer	6.26	13.8	0	0
Radar altimeter	10.43	23.0	0	0
Miscellaneous	<u>4.44</u>	<u>9.8</u>	<u>0</u>	<u>0</u>
Subsystem totals	295.96	652.6	349.49	770.6

TABLE 12. PIONEER SPACECRAFT SUMMARY MASS COMPARISON

| Item/Subsystem	PV Orbiter, kg	PMO With Surface Penetrators, kg
Subsystem and Science Total	295.96	349.49
Contingency	21.77	40.10
Dry Spacecraft Total	317.73	389.59
Penetrators (6)	0	270.00
Launch mechanism (6)	0	42.18
Dry Spacecraft (with penetrators)		701.77
Liquid Propellant	18.50	71.02
Pressurant	0.05	0.23
OIM expendables	151.75	296.00
Wet Spacecraft Total	488.03	1069.02
Spacecraft attach fitting	34.97	22.40
Launch Vehicle Payload	523.00	1091.42
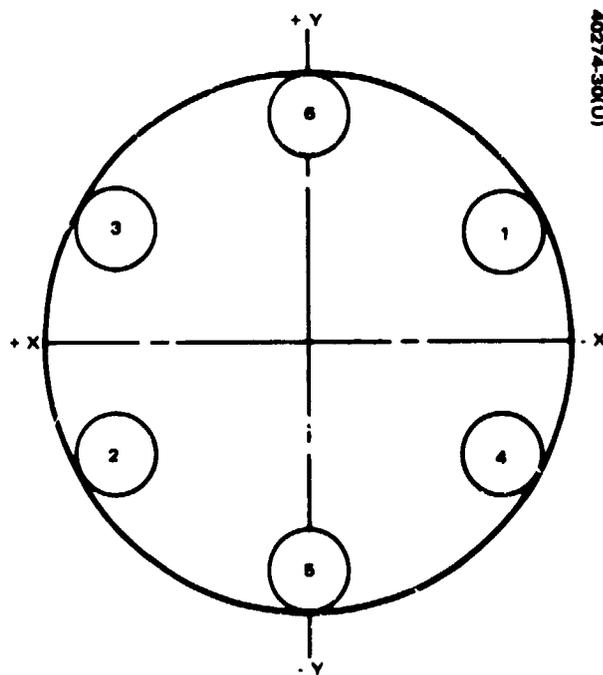
FIGURE 30. PENETRATOR DEPLOYMENT SEQUENCE

TABLE 13. SEQUENCED MASS PROPERTIES

Condition	Mass	Z m	X m	Y m	I_{zz} kg-m2	I_{xx} kg-m2	I_{yy} kg-m2	I_s/I_t
					Moments of Inertia			
Launch mass	1091.42	1.12	0	0	896.17	787.90	787.90	1.14
Separated spacecraft	1068.61	1.14	0	0	891.97	768.65	768.65	1.16
Initial Mars orbit	734.33	1.28	0	0	726.37	559.68	559.55	1.30
One penetrator deployed	680.63	1.28	0.07	-0.04	659.56	525.94	492.87	1.22
Two penetrators deployed	626.94	1.28	0	0	602.10	494.50	433.11	1.15
Three penetrators deployed	573.24	1.28	-0.09	-0.05	534.34	460.62	365.76	1.15
Four penetrators deployed	519.55	1.28	0	0	477.70	429.45	306.81	1.11
Five penetrators deployed	465.85	1.28	0	-0.12	408.58	344.08	289.60	1.18
Six penetrators deployed	412.15	1.28	0	0	353.29	272.39	272.39	1.30
Dry spacecraft	389.16	1.29	0	0	344.08	362.15	362.15	1.29

As shown in Table 14, the mass contingency for the orbiter spacecraft is 10.2 percent of the dry spacecraft (less penetrator) mass. After allocation for the existing and modified equipment, a contingency of 18.3 percent is available for the new equipment for the PMO spacecraft.

Contingency classifications chosen for the analysis are identical to those used for PV. These are: 1) existing items are allocated 3 percent contingency, 2) modified existing items are allocated 7 percent contingency, and 3) new items are allocated a minimum of 15 percent contingency, which has been shown to be the approximate contingency required for new hardware development.

TABLE 14. MASS CONTINGENCY ALLOCATION

Mass Classification	Equipment Mass, kg	Contingency, %	Contingency Mass, kg
PV Orbiter			
Existing hardware	54.98	3.0	1.63
Modified hardware	141.38	7.0	9.89
New hardware	54.29	18.9	10.25
Spacecraft contingency	21.77	—	—
Dry spacecraft less instruments	272.42	8.0	21.77
PMO With Surface Penetrators			
Existing hardware	59.23	3.0	1.77
Modified hardware	197.69	7.0	13.84
New hardware	134.33	18.3	24.49
Spacecraft contingency	40.10	—	—
Dry spacecraft less penetrators	431.35	10.2	40.10

51

The dry spacecraft (less penetrators) contingency of 10. 2 percent is considered an adequate design margin since use of existing and modified equipment (with their smaller mass contingency requirements) permits 18. 3 percent mass contingency to be allocated to the new equipment items.

4. 2. 3 Electric Power Summary

The PMO electric power is derived from the solar panel and batteries. The solar panel power output varies with the distance from the sun. Near Earth, the panel power output is approximately 280 watts, whereas at Mars it is 140 watts. The batteries can provide up to 270 W-hr without exceeding a 70 percent depth of discharge and may be used to augment the solar panel power output.

An evaluation of the spacecraft power requirements for individual mission phases indicates that available solar panel and battery power capabilities will satisfy all mission requirements, including a 10 percent contingency. The mission phases that may require battery augmentation of the solar panel are:

1) Interplanetary transit midcourse corrections

2) Attitude maneuvers before and after Mars orbit insertion

3) Attitude maneuvers before and after penetrator deployment

All of these maneuvers require 1 to 15 minutes.

TABLE 15. PMO DC POWER BUDGET

	Power Consumption, W		
Subsystem	Battery Charging	Data Transmission	Eclipse
Telecommunications	12.5	52.1	12.5
Data handling	11.7	11.7	11.7
Command	6.9	6.9	6.9
Attitude control	13.0	13.0	5.0
Propulsion	0.3	0.3	0.3
Thermal	48.3	36.7	15.8
Electric power	34.6	6.6	5.0
Subtotal	127.3	127.3	57.2
10% contingency	12.7	12.7	5.7
Total	140.0	140.0	62.9

The spacecraft power utilization during the PMO Mars orbit phase is summarized in Table 15. The expected maximum data transmission will require about 1.25 hours per orbit which allows ample time for battery charging. During battery charging, the communication system is powered down (Table 15), and the spacecraft heaters turn on automatically to maintain temperature on the shelves. A large part of the thermal load provides heat into the hydrazine tanks, lines, and jets and thus supplements thermal control of the spacecraft.

5. SUBSYSTEM DESCRIPTIONS

5.1 TELECOMMUNICATIONS

Figure 31 is a block diagram of the telecommunication equipment. As shown, the equipment comprising the telecommunication area consists entirely of Pioneer Venus (PV) spacecraft components with the exception of the equipment required to communicate between the Pioneer Mars orbiter (PMO) and the Mars penetrators. There is an interface shown with each of the three other spacecraft subsystems, i.e., the communication, command, and data handling subsystems. Figure 32 is a conception of the unique spacecraft equipment required for communication with the penetrators. The UHF antenna interfaces with the existing PV equipment through a rotary joint provided by deleting the existing X band occultation equipment.
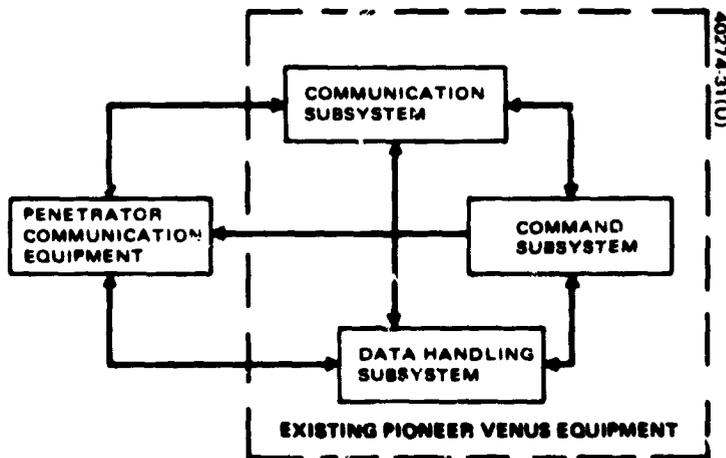
FIGURE 31. TELECOMMUNICATIONS BLOCK DIAGRAM
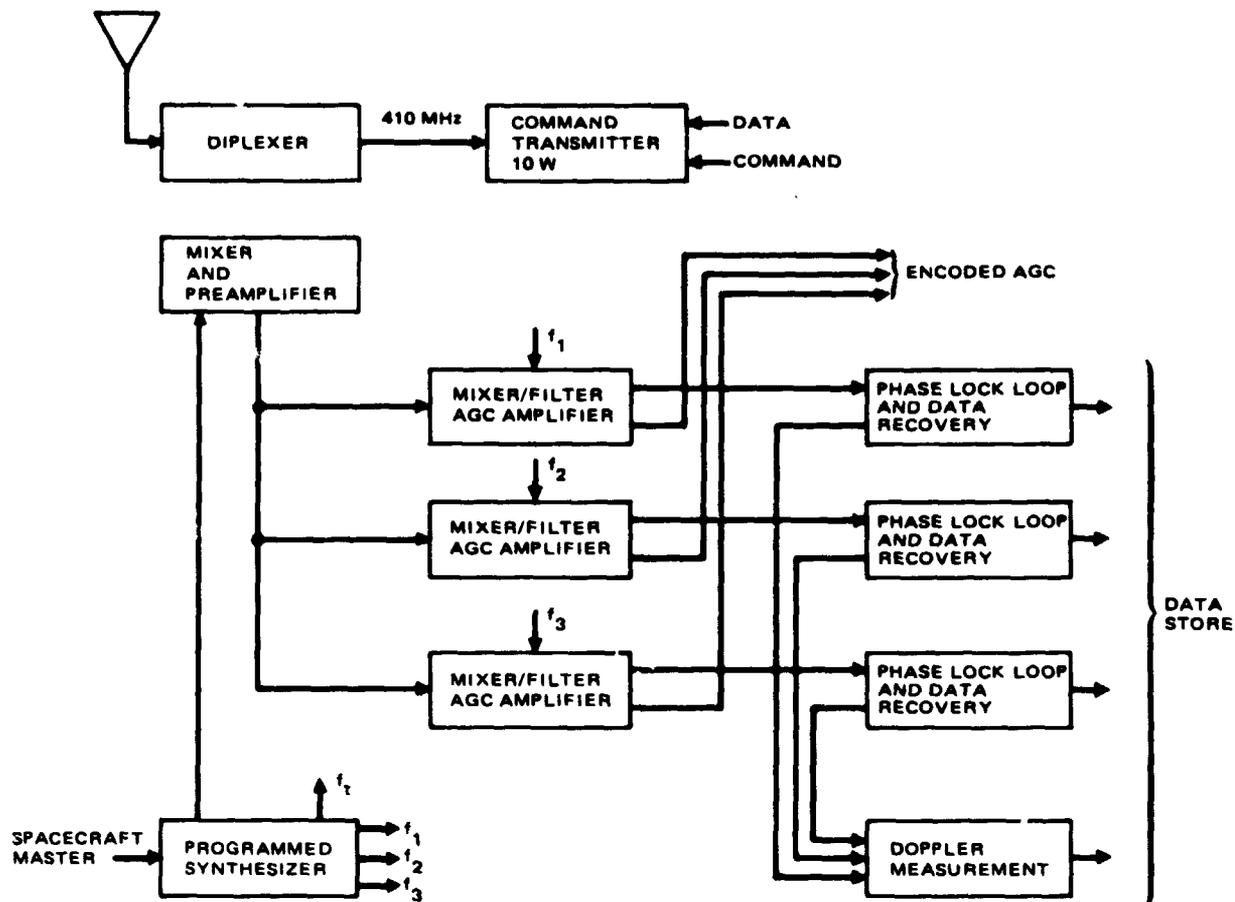
FIGURE 32. PENETRATOR/PMO LINK EQUIPMENT BLOCK DIAGRAM

5.1.1 Communications

The Pioneer Mars spacecraft communication equipment is identical to the PV spacecraft equipment although the power subsystem in a nominal operating mode supports only one of the two 10 watt RF power amplifier modules.

The PMO/penetrator communication equipment consists of a transmitter, receiver, and an antenna system. The solid state transmitter, which provides 10 watts output power, is a derivative of existing Hughes communication satellite equipment.

The receiver has enough capacity to receive three penetrator signals simultaneously. It consists of a broadband (relatively) mixer and postamplifier with a power divider to three second conversion local oscillators, which

are controlled in frequency by the synthesizer on command. A narrowband automatic gain controlled amplifier will filter out the desired signal which will then be decoded with a Costas or second harmonic carrier phase locked loop. The AGC voltage will be encoded in the data handling subsystem and will be used as a data present indicator. The AGC voltage will be obtained from a coherent detector in the phase lock loop. This receiver is similar to the Viking Lander transponder receiver.

Out of the phase locked carrier oscillator (1 MHz) in the decoding stages, a signal is provided to a counter chain to yield a time interval gate of about 0.5 second. This gates a frequency of 30 MHz from the master oscillator. The 18 least significant digits are retained as a measure of the doppler frequency.

Variation of the count from nominal of $15 * 10^6$ is $\pm 15 * f_d$. These data are transmitted to the memory for subsequent transmission to Earth.

Accuracy of the doppler frequency measurement is a function of the signal-to-noise ratio, the quality of the spacecraft oscillator, and the penetrator transmitter oscillator quality. From the standpoint of the doppler measurement, a short term stability of better than a part in 10^9 is desired.

For normal system performance, the signal-to-noise ratio will be adequate for acquisition in a reasonable bandwidth on the tracking loop. With a bandwidth of 100 Hz, a sweep rate of 10 kHz per second is an approximate upper bound. Then acquisition will require 4 seconds maximum. If the signal-to-noise ratio is very low because of anomalous behavior of the penetrator transmitter, other strategies must be employed.

5. 1. 2 Data Handling

Data handling equipment aboard the Pioneer Mars spacecraft is identical to the PV equipment. It is anticipated that since the PV spacecraft makes maximum use of extremely flexible OSO data handling hardware, the only changes required to accommodate the Pioneer Mars mission are minimal wiring/ routing/software changes. These changes are necessary only in order to accommodate the deletion of PV science experiments and the substitution of penetrator peculiar receiver/transmitter equipment. Physical characteristics of the subsystem are listed in Table 16.

5. 1. 3 Command

The Pioneer Mars command subsystem is identical in all respects to the PV command subsystem. In eliminating the PV science complement and substituting the penetrator peculiar equipment, there will be 75 commands available for the penetrator communication subsystem with no changes in existing PV equipment. Functional characteristics of the Pioneer Mars command subsystem are given in Table 17.

TABLE 16. DATA HANDLING SUBSYSTEM FUNCTIONAL CHARACTERISTICS SUMMARY

Parameter	Characteristic
Telemetry modes	Real time or stored
Word size	8 bits
Number of data inputs	256
Analog-to-digital conversion accuracy	±0.4% (8 bits)
Data bit rates	11 to 2816 bps
Data formats	16
Major frame length	64 words
Subcommutation length	64 words
Number of subcommutators	4
Error code	Convolutional, length 32, rate 1/2
Modulation type	PCM/PSK
Subcarrier frequency	33,792 Hz
Data storage capacity	1,048,576 bits

TABLE 17. COMMAND SUBSYSTEM FUNCTIONAL CHARACTERISTICS SUMMARY

Parameter	Characteristic
Command modes	Real time and stored
Command types	Discrete and quantitative
Command initiation	Ground command or stored command memory
Command format	45 bits (13 Barker code bits, 25 data bits, 7 polynominal code bits)
Bit rate	4 bps
Modulation	PSK
Probability of executing false command	Less than 1×10^{-9}
Probability of missing command	Less than 5×10^{-4}
Number of discrete command outputs	384 (192 redundant pairs)
Number of quantitative command outputs	24 (12 redundant pairs)
Word size of quantitative commands	16 bits
Command storage word length	24 bits
Command storage capacity	2064 bits (86 words maximum)
Resolution of command executions	±250 ms (stored mode)
Stored command processing initiation	Real time ground command, spacecraft 4096 sec clock transition, or separation switch
Redundant pairs of pyrotechnic drivers	3 pairs
Number of pyrotechnic initiators (firing capability)	18

5.2 ANTENNAS

Figure 33 illustrates a general layout of the placement and coverage of the PV spacecraft antennas. Two omnidirectional antennas, one at the top end of the spacecraft and one at the aft end, are provided to give full 4 pi sr coverage at a net gain of -6 dBi. The widebeam antenna is a slotted cone dipole antenna similar to the Surveyor antenna, whereas the narrow beam onmidirectional antenna is conical log spiral derived from a Hughes military space program.

The high gain antenna is a mechanically despun dish antenna with a 109 cm diameter that is used for primary telemetry data return to the DSN. Its gain is 25.3 dBi. A backup antenna with 8 dBi gain to the primary despun dish is a collinear sleeve dipole antenna similar to the antenna used on the Hughes/Comsat Early Bird satellite. These antennas are retained for the PMO.
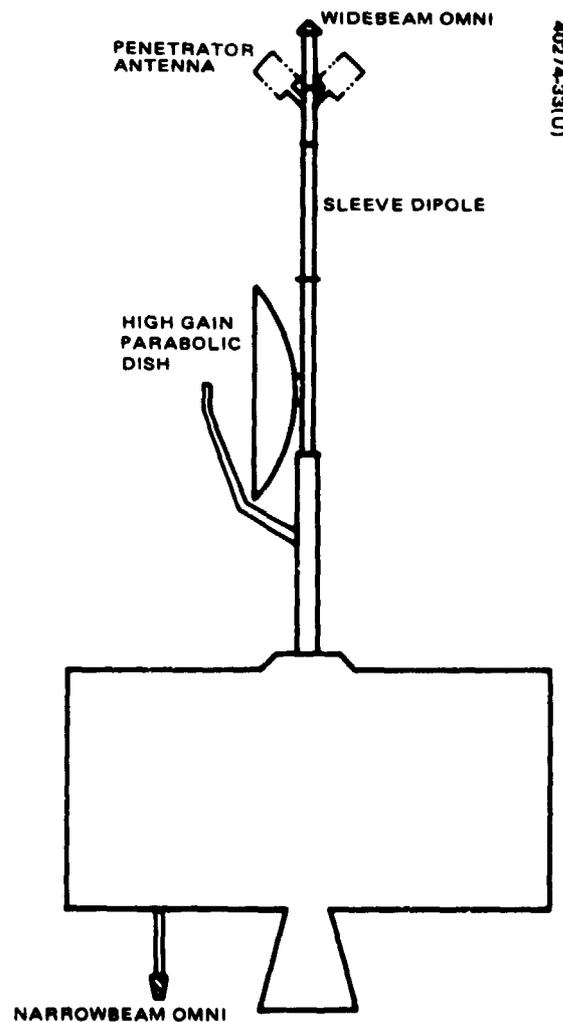
FIGURE 33. ANTENNA PLACEMENT

59

To implement the penetrator PMO link, two UHF antennas are added. These are placed on the antenna mast between the sleeve dipole and widebeam antennas. The requirement for the antenna is that it be simple and have a cardioid pattern for the reception of a linear polarized signal in any orientation. The communication geometry is such that reception will be possible from 0° to 135° off the mast axis. A tradeoff study of four candidate antenna configurations has been performed. The selected baseline for this application is a pair of quadrifilar helices, Figure 34, set coplanar at an angle of about 50° to the mast. The estimated performance is given in Table 18. The rotating joint in the BAPTA will have to be modified to substitute the 400 MHz feed lire for the PV X band occultation experiment feed line.

TABLE 18. PERFORMANCE OF PENETRATOR LINK PMO ANTENNA

$\theta,°$	Gain, dB	Axial Ratio, dB	Minimum Gain for Linear Polarization, dB
0	1	3 – 4	-7
± 90	1	3 – 4	-7
±135	-2	3 – 4	-10
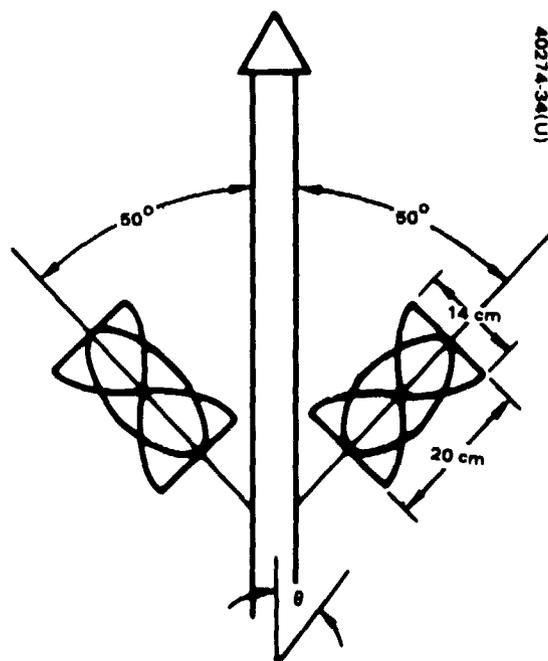
FIGURE 34. PMO ANTENNA FOR PENETRATOR LINK

5.3 STRUCTURE

The PMO structure is developed by use of a primary and a secondary structure. The primary structure is an adaptation of the PV; the secondary structure, required for the added payloads (penetrators), is a new development. The prime consideration in low cost spacecraft design is the attainment of a high degree of commonality.

The PV spacecraft structure includes sufficient design margins to be directly applicable as the primary structure of the PMO. Thus the emphasis in the PMO development is on the secondary structure and its integration with the primary structure.

Structural design criteria for the PMO are summarized in Table 19. Ultimate loads and accelerations are presented. The load factors result from both quasi-static and vibration environment.

TABLE 19. QUASI-STATIC ULTIMATE LOAD FACTORS (g)

Axis	Load Condition					
	1	2	3	4	5	6
Thrust (Z)	−4.35	+1.5	−4.35	+1.5	−25	−6.0
Lateral (X, Y)	+ 4.5	+4.5	As shown in Figure 35		+1.5	0.5*

*Added to this lateral load factor is 0.15R g, radically directed spin loading for each component. R radial distance, in inches, to component cg.
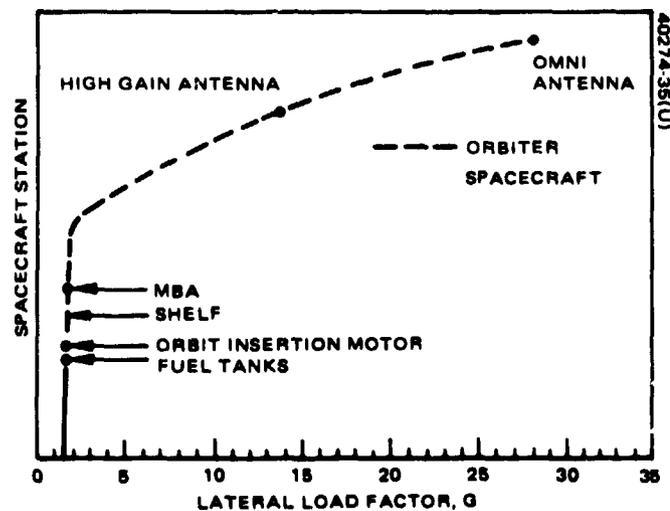

FIGURE 35. NONUNIFORM LATERAL LOAD CURVE

61

- Conditions 1 and 2 represent the liftoff compression and tension loading conditions.

- Conditions 3 and 4 are derived from quasi-static nonuniform lateral loading conditions at liftoff. The nonuniform type loading is characterized by relatively high lateral loads at the top of the spacecraft with much lower loads in the region of the adapter. Loads vary as the fundamental spacecraft lateral modes. Axial loads used in conjunction with the nonuniform load curve (shown in Figure 35) are as for conditions 1 and 2.

- Condition 5 represents the loads during the maximum steady state acceleration events. These loads encompass the load levels that recommended for the MECO loading event.

- Condition 6 represents PMO spacecraft loads during orbit insertion.

A design concept compatible with the critical load conditions given in Table 19 as well as the internal loads that result from thermal gradients in the spacecraft has been developed. Sufficient structural stiffness to meet natural frequency requirements and to maintain the alignment of critical components after application of limit design loads is also implemented. Figure 36 shows the primary structural elements, identifies the material of each, and lists the factors which influenced the design selection.

Components stresses have been analyzed for the corresponding critical load conditions. The ultimate margins of safety and corresponding modes of failure are presented in Table 20. Another criterion is that stresses based on the application of limit loads will not exceed the allowable yield stress at any point.

Portions of the structure and some components are designed to stiffness or alignment requirements, rather than strength. Natural frequency of the antenna mast and boresight pointing accuracy for the reflector feed are considered in the design of the mast, bearing assembly, and feed support areas. Analysis will be performed to ensure that critical antenna alignments will be maintained in orbit in the most severe thermal environment after application of boost and orbit insertion motor loads. The relatively high accelerations of the PMO spacecraft high gain antenna can probably be reduced by further analysis and small changes in the structural design.

Thermally induced stresses are combined with stresses resulting from design loads in the calculation of margins of safety. The margins of safety as shown in Table 20 are defined as:

$$\text{(MS) ultimate} = \frac{\text{ultimate allowable stress}}{1.25 \times \text{limit design stress}} - 1$$

62

ANTENNA MAST
(A, 1, 2, 7, 8)

EQUIPMENT SHELF
(HA, 2, 6, 7, 8)

SOLAR PANEL
(HF, 2, 6, 7, 8)

THRUST TUBE
(A, 7, 8)

SPACECRAFT
ATTACH FITTING
(M, 6, 7, 8)
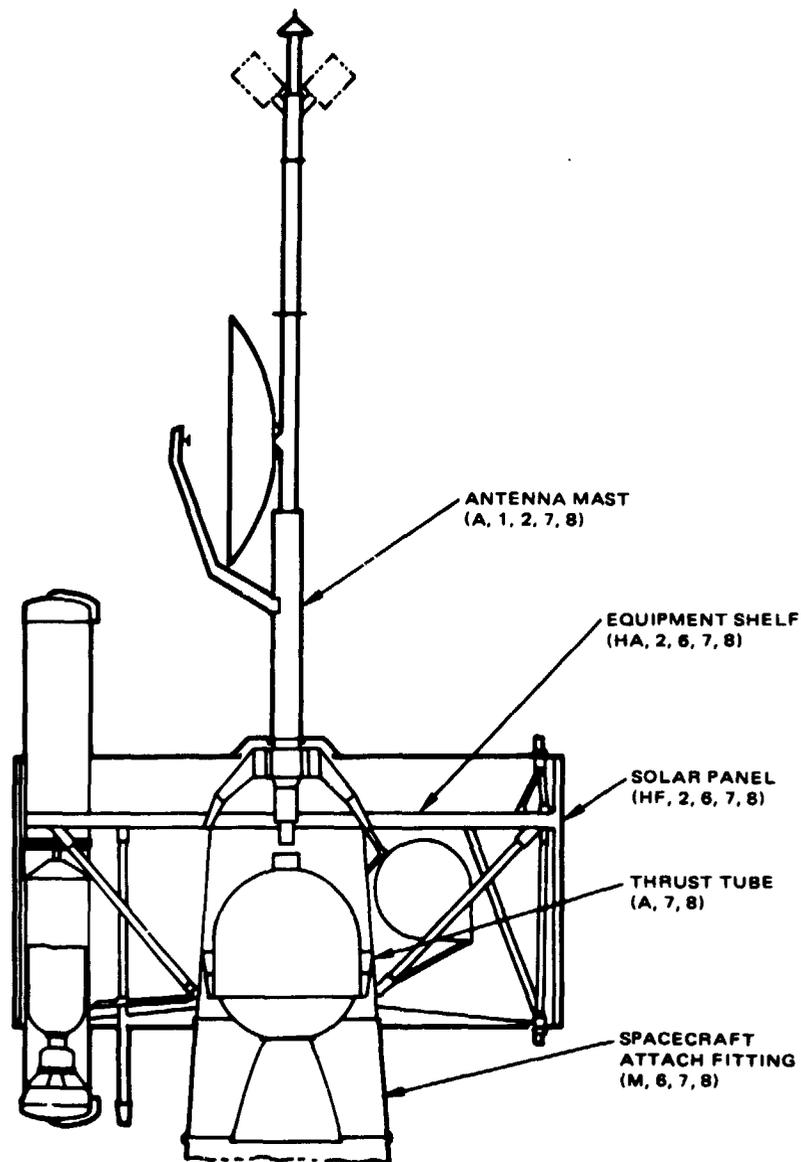
MATERIAL CODE

A — ALUMINUM
B — BERYLIUM
HA — HONEYCOMB CORE/ ALUMINUM FACING
HF - HONEYCOMB CORE/FIBERFLASS FACING
M — MAGNESIUM

SELECTION FACTORS

1 — STRENGTH
2 — STIFFNESS
3 — THERMAL ENVIRONMENT
4 -- ARRANGEMENT & ACCESSIBILITY
5 — GROUND HANDLING
6 — MASS
7 — MANUFACTURING COST
8 — PIONEER VENUS STRUCTURE

FIGURE 36. PMO WITH PENETRATORS

TABLE 20. SUMMARY OF MINIMUM MARGINS OF SAFETY

Part Name	Material	Critical Design Load Condition	Mode of Failure	Ultimate Margins of Safety
Despun Section				
Antenna mast	2024-T3 Al	4.35 g condition 3	Bending	Large
Bearing shaft	6AL-4V Tl	4.35 g condition 3	Bend shear	0.12
Spin section				
Spacecraft attach-ment fitting	AZ31B-H24 Mg	4.35 g condition 3	Buckling	0.30
Thrust tube	2024-T3Al AZ31B Mg	4.35 g condition 3	Buckling	0.30
Shelf support strut	2024-T3Al	Vibration qualification	Column buckling	0.30
Shelf	Aluminum honeycomb and face sheets	Vibration qualification	Crippling	>0.50
Penetrator fitting	2024-T4Al	25 g condition 5	Bending	0.58
Solar panel	Aluminum honeycomb core and fiberglass face sheets	Handling	Sheet tension	>1.00

5.4 ORBIT INSERTION MOTOR

The Thiokol TEM-616 motor, shown in Figure 37, was selected for the orbit insertion. This motor was developed for the Canadian Technology Satellite and was the candidate motor for the PV type I trajectory mission. This motor will also be used in the Geostationary Meteorological Satellite (GMS) presently under design at Hughes.

The required propellant loading for the Mars penetrator mission is 296 kg. This falls well within the GMSS loading specification, 285 to 315 kg, which avoids any requalification requirements.
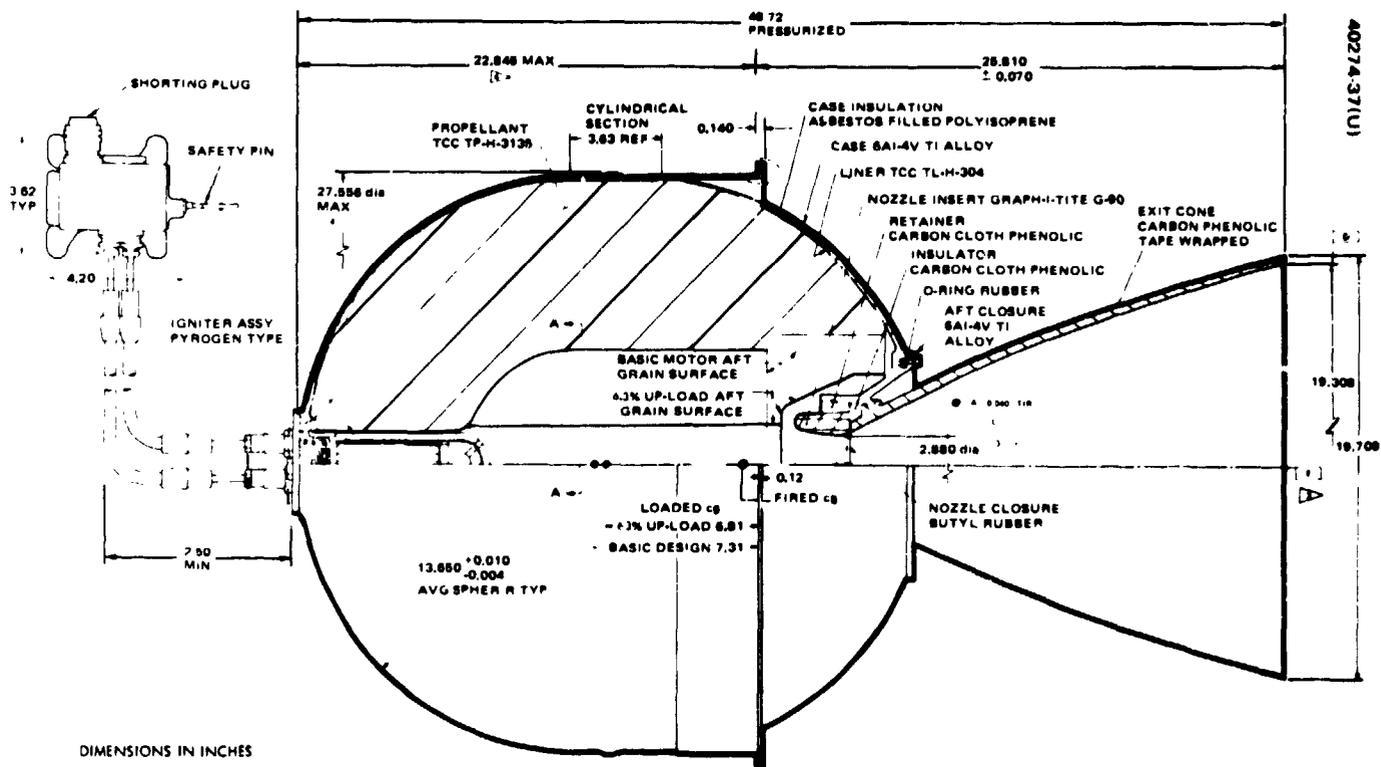
64

FIGURE 37. ORBIT INSERTION MOTOR (TEM-616)

5.5 THERMAL CONTROL

The thermal control design goals are to maintain key spacecraft elements within desired temperature ranges, as indicated in Table 21, with a passive thermal control system augmented by heaters.

TABLE 21. THERMAL CONTROL CONCEPT

Design Goals	
Equipment shelf	$4°$ to $32°C$
Reaction control subsystem	$4°$ to $49°C$
Propellant (OIM)	$4°$ to $32°C$
Constraints	
Passive system	
Nonlouvered if possible	
Resources	
Sun orientation fixed	
Excess power expended in array	
Heater power as required	

65

The spacecraft spin axis attitude - normal to the ecliptic plane - simplifies the thermal control design since direct solar radiation on the primary thermal control surface (forward barrier) will be experienced only during penetrator deployment maneuvers.

The thermal control concept, shown in Figure 38, utilizes an insulated main body design (passive design) and augments the RCS and the orbit insertion motor (OIM) with heaters. The spacecraft equipment shelf is insulated from the aft section of the spacecraft with a multilayer insulation equipment shelf blanket. A shelf heater provides a margin for uncertainties in the insulation blanket thermal properties.

The large variation in solar intensity experienced in transit from Earth to Mars can best be resolved by isolating the main body of the spacecraft from the solar panels. The solar panels which would normally provide a stabilizing sink temperature for this configuration operating near Earth, undergoes a temperature decrease of about 65°C in going to Mars from Earth. Expected solar panel temperature variations are shown in Figure 39.

The forward thermal barrier is the primary thermal control surface (radiator). Bulk equipment shelf sensitivity to the effective radiation coefficient ($\epsilon A \sim m^2$) of the radiator led to the selection of a design point of 0.24 square meter.
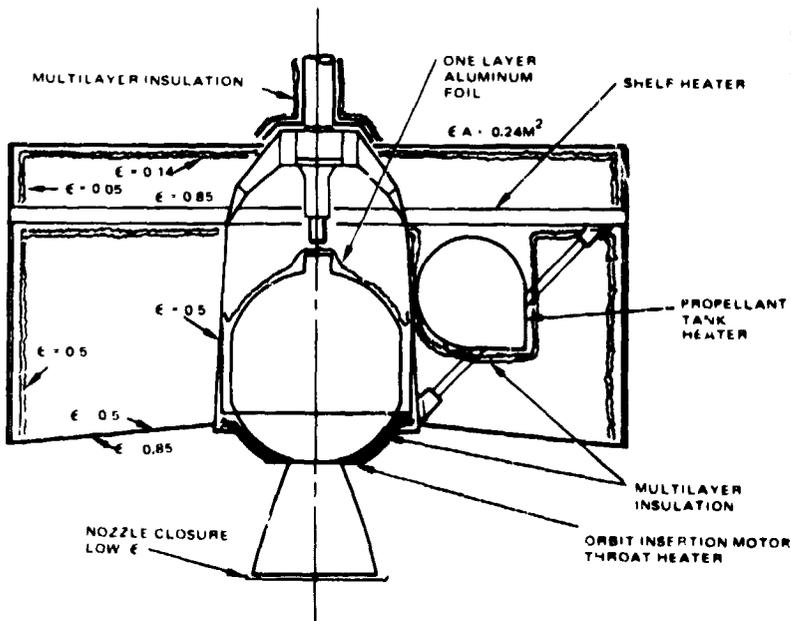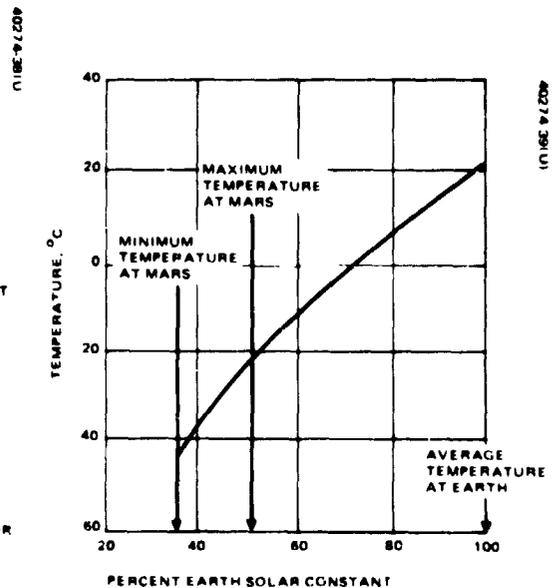

FIGURE 38. THERMAL CONTROL CONCEPT

FIGURE 39 SOLAR PANEL TEMPERATURE VERSUS PERCENT OF EARTH SOLAR CONSTANT

Nominal thermal dissipations are 109 watts near Earth and 127. 5 watts near Mars (with a 10 watt transmitter operating). The noneclipse minimum shelf temperature occurs near Mars during battery charging. The shelf temperatures are shown in Figure 40.

Typical spacecraft temperature distributions near Mars are illustrated in Figure 41. The bulk equipment shelf temperature (27°C) is maintained within the desired 4° to 32°C design range.

Illustrated in Figure 42 is the spacecraft solar panel eclipse temperature response. The solar panel temperature decay rate is very similar to that of the PV orbiter spacecraft.

The eclipse transient responses of the spacecraft equipment shelf and the propellant tanks are very similar to that expected for PV. A combination of 45 watts thermal dissipation on the equipment shelf and 5 watts per propellant tank provides eclipse transients well within the desired temperature ranges for the shelf and the propellant tanks as shown in Figure 43.

A passive thermal control approach with provisions for a shelf heater seems feasible. Active heating will be required for the RCS thrusters, for propellant tanks and for the OIM prior to orbit insertion. The effectiveness of the thermal control will be sensitive to material and manufacturing deviations, particularly in the thermal blankets. Thermal testing is recommended.
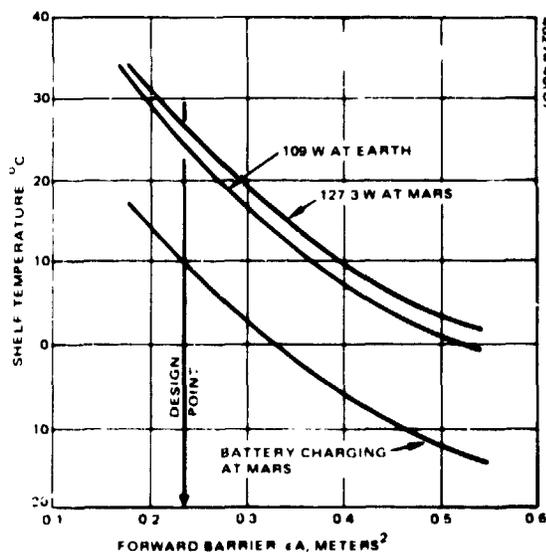

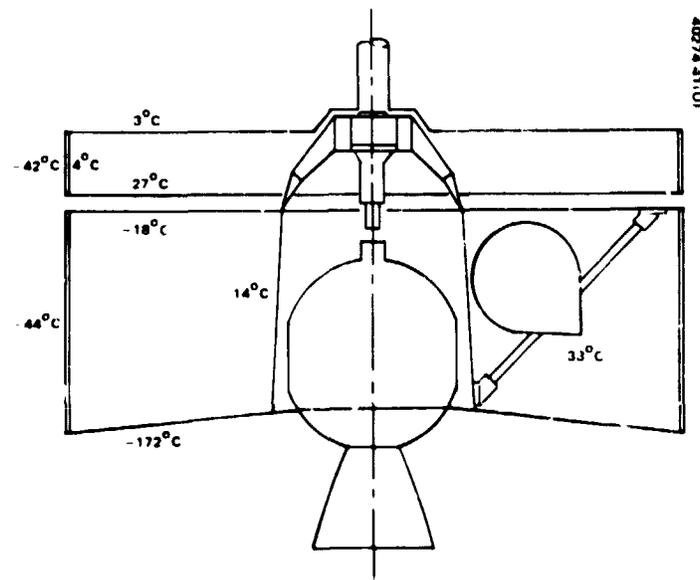FIGURE 40 EQUIPMENT SHELF TEMPERATURES (SIDE SUN)

FIGURE 41. TYPICAL TEMPERATURE DISTRIBUTION (SIDE SUN A = 0.242 M^2. PLATFORM HEAT = 127 5 W)
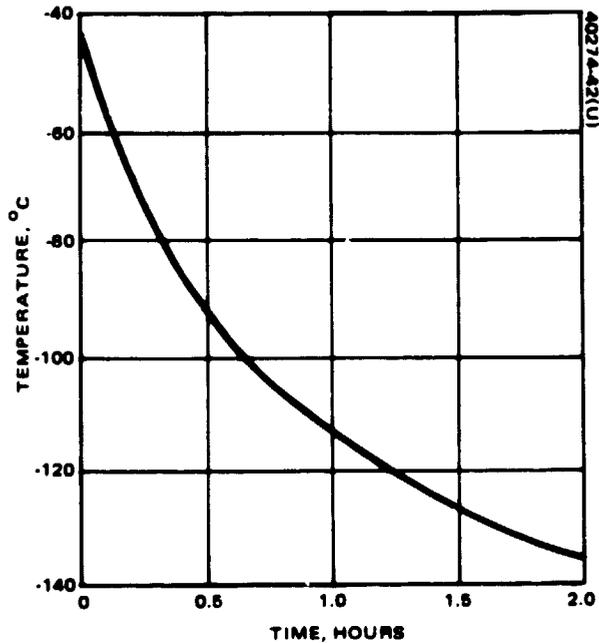
FIGURE 42. SOLAR PANEL ECLIPSE RESPONSE
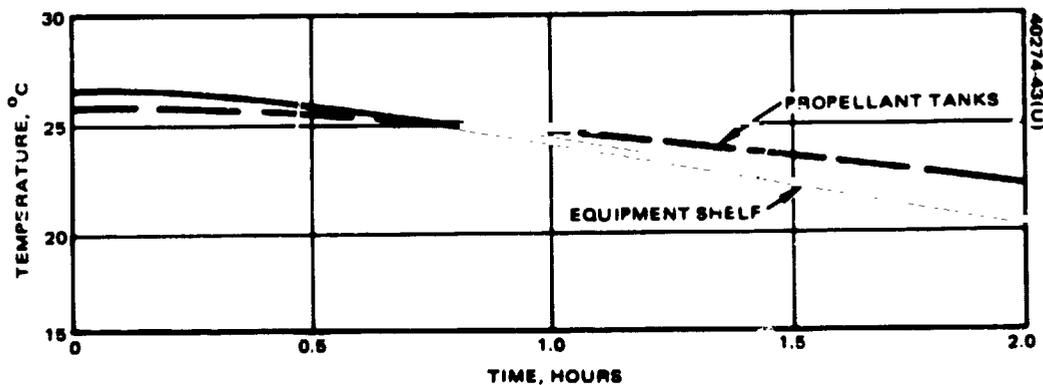

FIGURE 43. ECLIPSE TRANSIENT FORWARD BARRIER (A = 0.242 M²)

An RTG heater is packaged with each penetrator to provide heater power for the penetrator payload after penetration of the Martian surface. Since RTGs are activated prior to launch, provisions have to be made to reject the power generated by these units for the time period from activation to ejection from the spacecraft in Mars orbit.

The thermal design objective was to maintain penetrator-ejector interface temperatures at approximately -12 °C prior to release in Mars orbit. A combination of temperature difference, ΔT, from the control point to the radiator and effective radiator temperature sets the temperature at the control point.
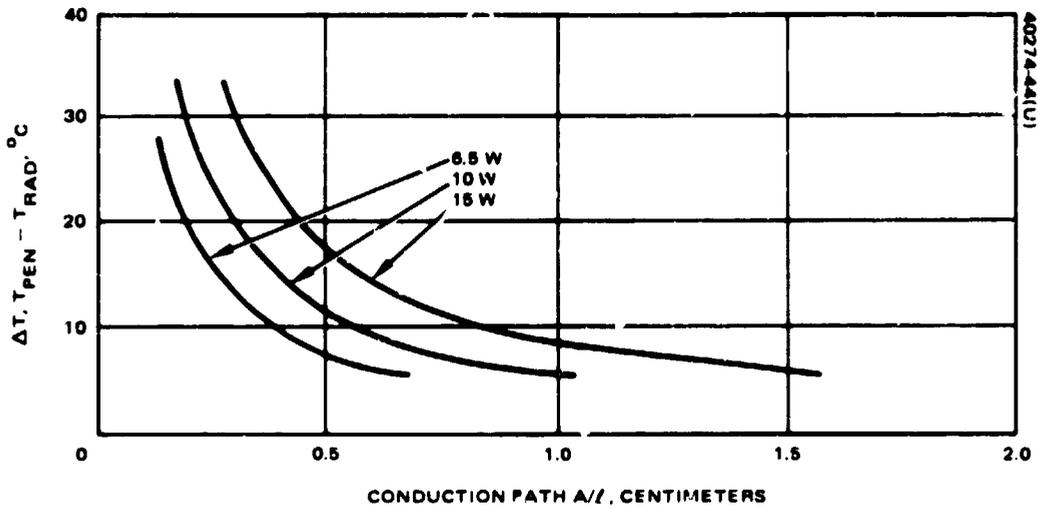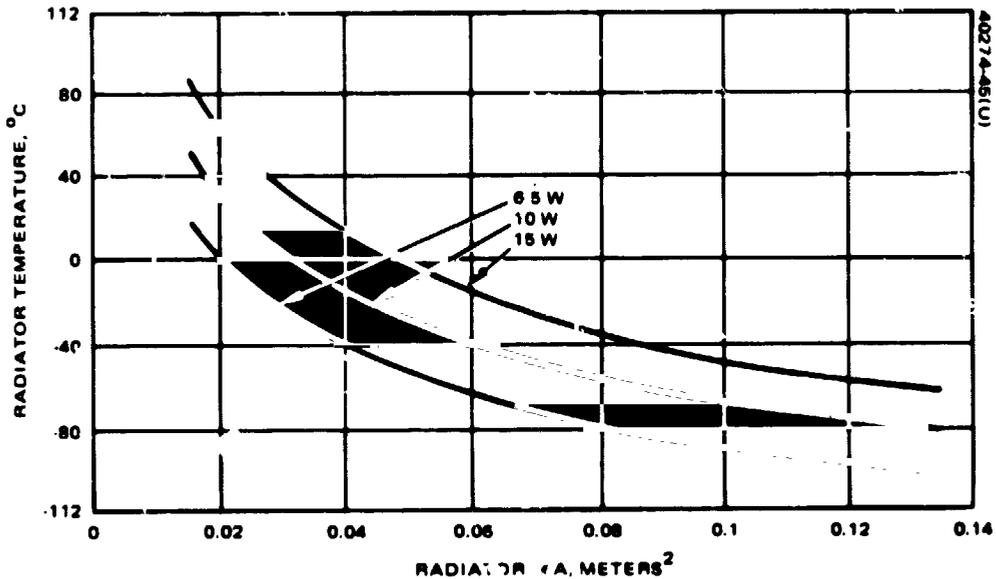
68

FIGURE 44. CONDUCTION FROM PENETRATOR TO RADIATOR

FIGURE 45. PENETRATOR RADIATOR

The sensitivity of the control point to radiator ΔT, to the effective conduction path, A/ℓ, for power levels of 6. 5, 10, and 15 watts is illustrated in Figure 44. The baseline design conduction path is $A/\ell = 0.4$ cm. The effective ΔT from control path to radiator is 30°C for the baseline 20 watt dissipation. The sensitivity of radiator temperature to the effective radiation coefficient (ϵA, m^2) is illustrated in Figure 45 for power dissipations of 6. 5, 10, and 15 watts. The baseline effective radiation coefficient is sized for the desired radiator temperature. An effective radiator coefficient of $\epsilon A = 0.12$ m^2 was selected to yield a radiator temperature of -42°C with 20 watts dissipation. The current design point is a radiator with an area of 0.141 m^2 and a high emissivity ($\epsilon = 0.85$) thermal finish. The radiating area is the aft portion of the penetrator tube and the aft tube cover.

69

5.6 ELECTRICAL POWER

The PV power subsystem design was modified only as necessary to
ɪɪ ᴄᴄ the requirements of this mission. The power requirements summarized
in Section 4.2.3 were used as design criteria. Modifications (Figure 46)
are restricted to the design of the solar cell array and voltage limiters; all
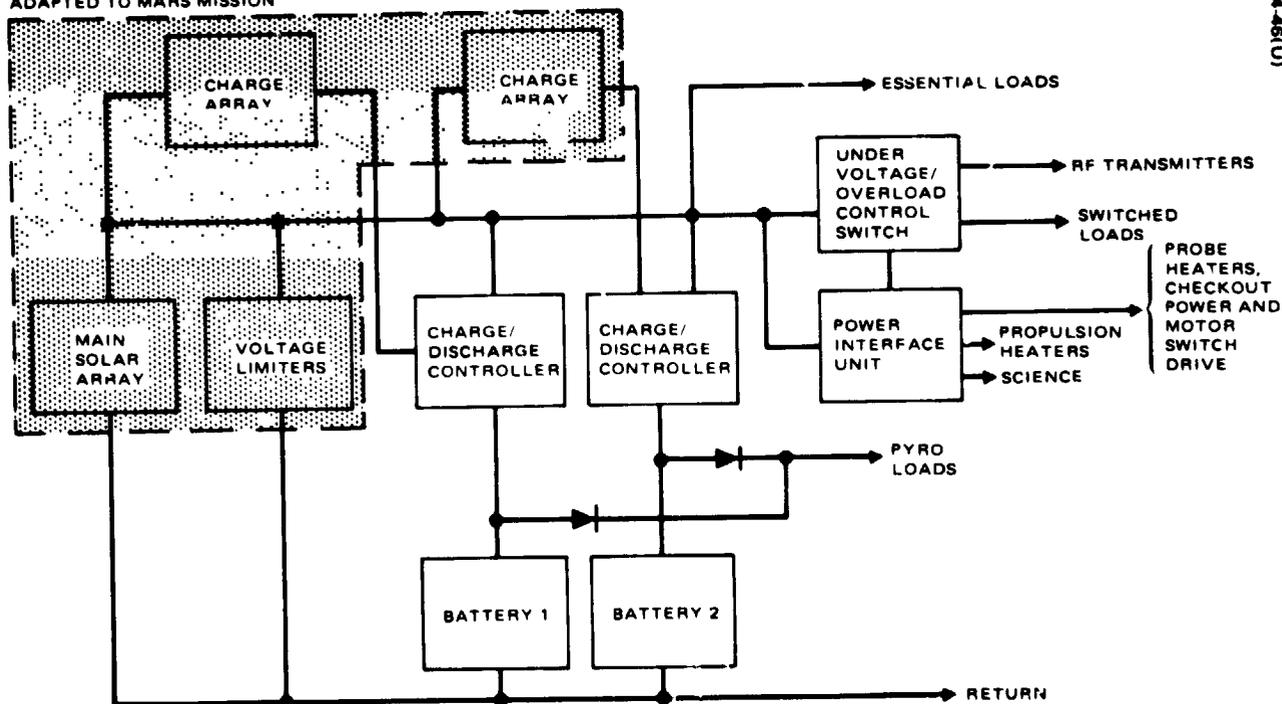other equipment is identical.

The solar panel size is increased by adding cells to a portion of
substrate that was left uncovered for PV experiment viewin� ports. The
resulting change in the solar panel configuration is indicated in Table 22.

The cell characteristics are identical to those used in the PV pro-
gram. The solar array voltage must be controlled in Mars orbit, but requires
little or no control during the interplanetary phase of the mission. To

TABLE 22. SOLAR PANEL CONFIGURATION

Main array	6776 cells 52 series x 63 parallel (on shelf end) 50 series x 70 parallel (on aft end)
Charge array (each of two)	595 cells 17 series x 35 parallel
Panel height (solar cells)	122 cm

FIGURE 46. PMO POWER SUBSYSTEM SIMPLIFIED BLOCK DIAGRAM

70

simplify the spacecraft thermal design, the bus voltage limiters are replaced with space proven solar array tap limiters which dissipate much less heat than the bus limiters would. The solar array tap limiters are identical to those on Anik and Westar satellites and their mass is somewhat less than the bus voltage limiters used on PV.

The power system will provide 26.5 to 30.8 volts dc electrical output during operation in Mars orbit. The solar array voltage to the loads will be limited to 30.8 volts dc by solar array tap voltage regulators. There are two 24-cell nickel-cadmium batteries which will provide the required secondary power. The output voltage of these batteries is regulated to 27.8 ± 0.1 volts dc and will drop to 26.5 volts dc in the unlikely case of 70 percent depth of discharge, end of life, with a shorted battery cell. Since the voltage of the fully charged batteries exceeds the maximum allowable bus level, dissipative battery discharge regulators are utilized. The regulated battery output voltage is maintained by these regulators until the battery terminal voltage decays to approximately 29.05 volts dc. The regulator saturates at this level and its output starts to track the battery terminal voltage (less saturation drop).

The discharge regulators are designed to share the load current to within ±5 percent. The regulators also provide battery isolation from the bus during solar panel operation.

During all operational modes, there is a relatively long period of time available for battery charging. Most of the time, the batteries will be trickle charged at a rate between C/30 and C/60. This charge rate is sufficient to keep the batteries in charged state during interplanetary transit and during short duration eclipses of 24 minutes or less. A higher charge rate of C/15 is required after relatively longer duration eclipses. A battery charge system is used for that purpose. Small boost charge strings of solar cells boost the output voltage of the main solar array. Trickle charge capability is provided by switching a resistor in series with the charge string. A thermal switch will terminate battery charging when temperature reaches 36° ± 2.8°C. This technique is a reliable, safe method of charging and has been proven successful on many Hughes satellites.

The power interface unit (PIU) provides power switching for the propulsion heaters, checkout, buses, and motor driven main power switches. Circuit fusing is also provided in the PIU.

Power is distributed on four separate buses. Under overload or undervoltage conditions on the bus, the nonessential loads must be removed to protect the spacecraft from possible catastrophic failure. The overload/undervoltage switch provides a trip signal if the total load current exceeds 125 percent of nominal or if the main bus voltage drops to 26.5 volts. On the trip signal, the switched loads are turned off sequentially until the minimum essential bus loads remain. The essential bus loads include the transponders and command subsystem vital to the spacecraft and the heaters for the axial and radial jets. These jets must be kept at constant temperatures and, having little thermal mass, cannot tolerate temporary loss of heater power.

71

TABLE 23. POWER SUBSYSTEM EQUIPMENT SUMMARY

Unit	Quantity/ Spacecraft	Unit Power Dissipation, W	Unit Size L x W x H, cm	Design Derivation
Charge/discharge controllers	2	0.5 standby	25.4 x 16.5 x 7.62	PV
Bus limiters	2	0.24	14.5 x 24.0 x 3.8	Same as Telesat and Westar
Undervoltage/ overload control switch	1	0.75	10.2 x 11.4 x 5.1	PV
Current sensors	3	0.37	6.4 x 6.1 x 5.3	PV
Power interface unit	1	0	20.3 x 12.7 x 6.4	PV
Battery (Ni-Cd)	2	0	21.8 x 10.2 x 10.9	PV
Solar array less substrate	1	0	254 cm diameter; 122 cm height	Similar to Telesat
Total	12			

Two 7.5 A-hr batteries with two redundant charge/discharge controllers are implemented. All of the current mission requirements can be accomplished with one battery with minimum change to the operating schedule of the spacecraft systems.

Table 23 summarizes the electric power subsystem equipment.

As a future design option, higher performance solar cells are available. Such cells with considerably higher power output were recently flight qualified by Hughes and are incorporated into spacecraft now in production. These new K4 and K6 solar cells can provide up to 22 percent more power than the 2 ohm-cm base resistivity cells selected for PV. Thus, for the same power output, a smaller size array could be provided or the solar array power output could be increased if desired.

5.7 VELOCITY AND ATTITUDE CONTROL

The PMO penetrator mission requires the control of the spacecraft attitude, spin speed, and adjustments of the spacecraft velocity vector. It is proposed to perform these functions with a liquid monopropellant hydrazine subsystem employing 4.45 N (1 lbf) thrusters with Shell 405 ABSG catalyst beds.

The proposed propulsion subsystem is similar to the propulsion subsystem being employed on the PV orbiter spacecraft, differing only in the size and number of propellant tanks and the inclusion of one additional axial thruster. Figure 47 is a schematic of the propulsion subsystem. The subsystem is a reliable, simple design employing a pressure blowdown mode of operation. The propellant and pressurant are stored together in three tanks
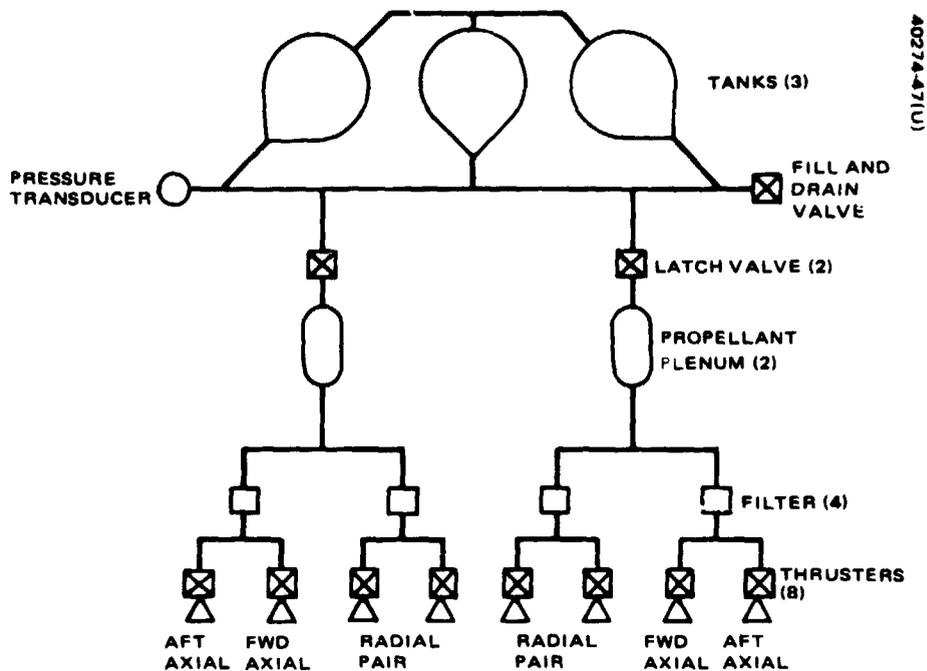
FIGURE 47. PROPULSION SUBSYSTEM

located 120° ⌐ ᵣ about the spacecraft spin axis. The propellant/pressurant interface in eacʜ tank is established by the centrifugal force associated with spacecraft rotation during the mission. The tanks are conispherical in shape with the propellant outlet at the apex of the conical section. This outlet is placed in an outboard location relative tc the spacecraft spin axis to provide complete propellant utilization. Interconnecting manifolds equalize the pressure between tanks and distribute the propellant, through filters, to the thrusters.

Due to the increased propellant required for the PMO penetrator mission as listed in Table 24 as opposed to the PV mission, it was r ᵣessary to increase the size of the propellant tanks. By incorporating three ᵢpellant

TABLE 24. RCS PROPELLANT REQUIREMENTS

Maneuver	Propellant, kg
Midcourse (ΔV = 96 m/sec and reorientations)	49
Orbit insertion errors (40 m/sec velocity and pointing)	15
Solar torque	2
Reorientations	5
Total	71

tanks, it is possible to carry the required 71 kg of propellant in the already developed and qualified HS-356, Marisat, 37,690 cubic centimeter tanks. In addition, the use of three of these tanks allows for a possible 39 percent growth in propellant loading while maintaining the policy of using flight proven components.

As an alternate approach to the recommended HS-356 propellant tanks (which are fully qualified and will contain the required 71 kg of propellant at a 2. 6:1 blowdown ratio), it is deemed possible to increase the blowdown ratio to as high as 6:1, thus allowing a growth in propellant load to 97. 5 kg.

One additional thruster has been added at the forward axial position to increase the spacecraft maneuverability as required for tnis mission. Addition of this thr ͺter does not affect the number of other components required in the subsystem and, in fact, makes the two thruster legs schematically identical.

6. PENETRATOR DEPLOYMENT MECHANISM

The major requirements of the deployment mechanism are as follows:

1. Support penetrator in spacecraft

2. Eject penetrator with a desired velocity

3. Provide initial penetrator trajectory control (minimize tipoff)

4. Provide launch motor blast protection to spacecraft

5. Provide holdback restraint to penetrator system (ensure buildup of pressure before release)

6. Provide electrical umbilical provisions to launch motor and penetrator

7. Provide a   or for RTG within penetrator system

8. Maintain and la   a sterilized penetrator and launcher parts

9. Provide a velocity increment of 80 m/sec to a 45 kg penetrator system

A system design concept that meets the above requirements has been developed on the basis of the Hughes tube-launched, optically tracked, wire-guided (TOW) missile program experience which has operationally demonstrated a very high reliability.

The system design and the pertinent system performance aspects are discussed in the following sections.

6.1 DEPLOYMENT SYSTEM DESIGN

The penetrator deployment system consists of a launch container, deployment mechanisms, and a deployment motor. The selected hardware is an extrapolation from the TOW missile program which has had some 4000 operational firings.

6.1.1 Penetrator Launch Container

The launch container, shown in Figure 48a, houses the penetrator, holdback restraint mechanism, electrical umbilicals, and the deboost rocket motor assembly.

The launch container consists of a glass fiber-wrapped aluminum alloy tube. Construction is similar to the TOW missile container with the exception of an aluminum liner to aid sealing. The container is hermetically sealed to ensure that any sterile deployment mechanisms which enter the Mars atmosphere will remain sterile. Aluminum end covers are welded in a tungsten inert gas (TIG) process to the aluminum tube to ensure a hermetically sealed container. The hermetic seal is broken only when the end covers are opened immediately prior to penetrator deboost. The end covers are attached to the container by spring loaded hinges. During the predeployment procedure, the covers are cut off from the container by flexible linear-shaped charges, allowing the covers to swing open. Figure 48b shows the penetrator at deployment partially protruding from the launch container. Burnout of the rocket motor occurs before exit of the motor from the container.
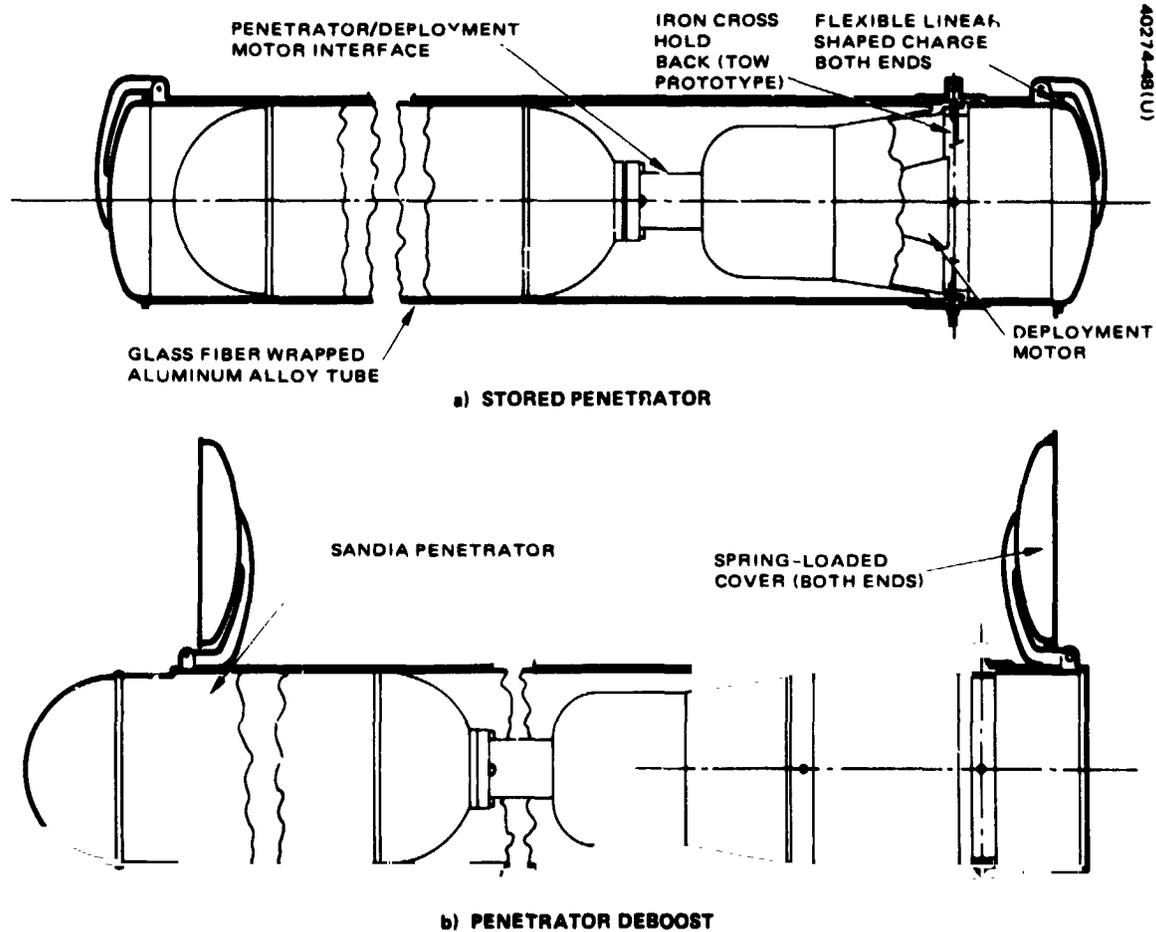

a) STORED PENETRATOR

b) PENETRATOR DEBOOST

FIGURE 48. PENETRATOR LAUNCH CONTAINER

76

6. 1. 2 Penetrator Deployment Mechanism

The penetrator deployment mechanism shown in Figure 49 combines the functions of mounting, restraining, and deploying a sterile penetrator. The holdback restraint retains the penetrator/motor assembly during earth launch and during maneuvers required for Mars orbit insertion. The holdback restraint is an "iron cross" type used on TOW missile prototypes. Advantages of this restraint are simplicity, low cost, and high reliability. The restraint is accomplished by four pins (one per quadrant) that lock the deployment motor support housing to the launch container. At motor ignition, the impact of the igniter and the exhaust gases against the iron cross removes the four restraint pins, thereby releasing t'e penetrator/deployment motor assembly. An extremely high reliability of this device was demonstrated during early TOW development tests.

Two electrical umbilicals are required — one for the deboost motor igniter and one for penetrator test and telemetry functions. Both electrical umbilicals wi.1 automatically separate during penetrator deployment.

The motor is connected to the penetrator through an aluminum alloy mounting plate. The plate is mounted so that a sufficiently large force will cause the plate to shear between the penetrator and the motor mounting locations. The plate retains the penetrator to the restrained motor during launch and spacecraft maneuvers, but shears during penetrator deboost. After deboost motor burnout, the separation spring separates the motor from the penetrator.

As was shown in Figure 48, the container is hermetically sealed by TIG welding aluminum end covers onto the container's ends. The covers shown in Figure 50 are removed by cutting with a flexible linear-shaped charge, which burns circumferentially and radially. The shaped charge can
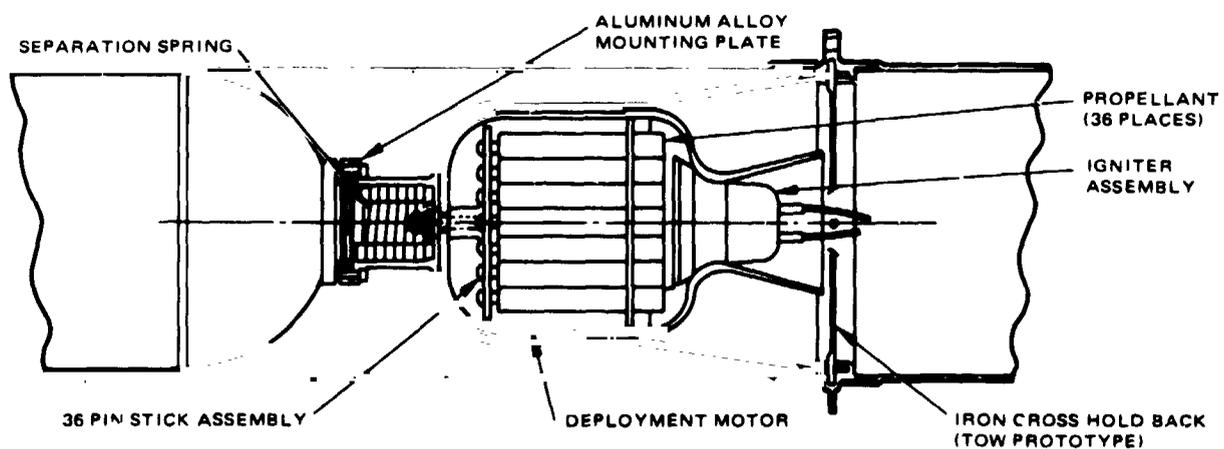

FIGURE 49. PENETRATOR DEPLOYMENT MECHANISM

ALUMINUM ALLOY COVER

TIG WELD 2 PLACES

FLEXIBLE LINEAR SHAPED CHARGE

GLASS FIBER WRAPPED (TOW CONTAINER TYPE)

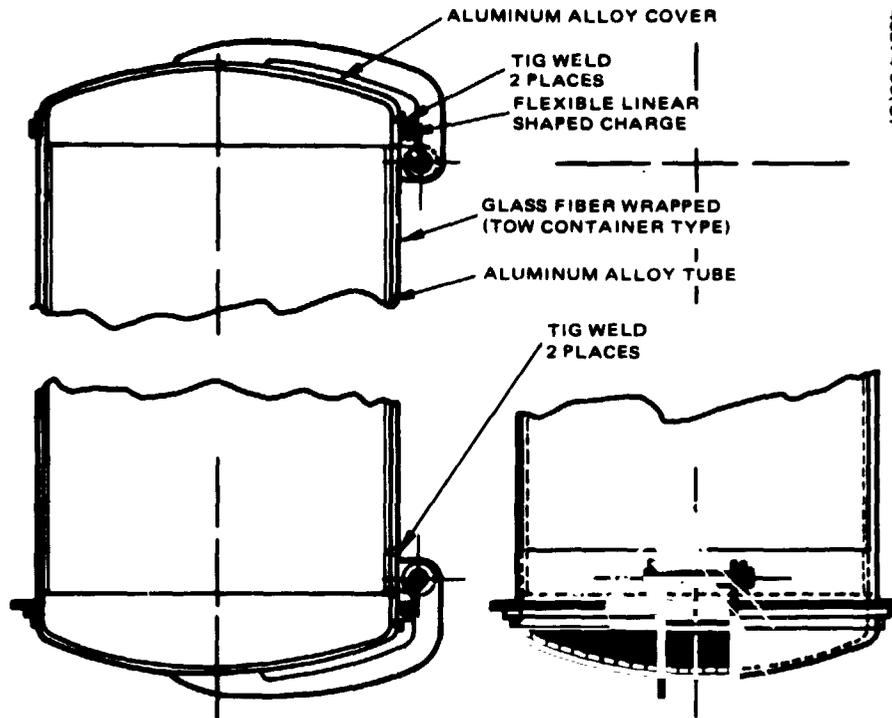**ALUMINUM ALLOY TUBE**

TIG WELD 2 PLACES

40274-50(U)

FIGURE 50. PENETRATOR CONTAINER COVERS

be designed to burn radially inward or outward to separate the cover from the container; however, radially outward is preferred to prevent debris from being expelled with the deployment mechanism. After cover separation occurs, the covers swing out of the way on spring loaded hinges also attached to the container.

6. 1. 3 Explosive Cord

Explosive cord is the pyrotechnic used to cut the metal container so that the covers will be hinged open by the spring for deployment of the penetrator. Candidate detonating materials are listed in Table 25. The most likely detonating material to be used for the penetrator application is RDX or HNS. RDX is supplied to NASA by the Army, and HNS is supplied by the Navy.

TABLE 25. EXPLOSIVE CORD TO OPEN END COVERS

● Detonating material
RDX
HNS
PETN
DIPAM
● 6100 m/sec
● Unaffected by electromagnetically induced current

78

Use of the detonating material to perform the cutting operation provides essentially instantaneous operation upon initiation, as evidenced by its fast detonating rate. The material is highly reliable, safe to handle, possesses long term storage capability, and is unaffected by electromagnetically induced current.

To ensure high quality of assemblies and maximum reliability of the detonating cord to perform its cutting function, the material is readily examined for discontinuities by X-ray or neutron radiography (N-ray) techniques.

6.1.4 Deployment Motor

The deboost motor is similar to the TOW missile launch motor in construction and propellant grain configuration. The size of the motor and propellant mass has been increased to accommodate the penetrator deboost requirements. Motor burnout is designed to occur before the penetrator completely disengages from the launch tube. This ensures that the motor force vector during burn is sufficiently aligned with the desired penetrator deorbit velocity vector and results in meeting the required deorbit parameters. Figure 51 is a cutaway view of the Hughes TOW missile launch motor.

The launch motor for the TOW missile is approximately 5.1 cm in diameter and 43.2 cm long. It contains four tubular propellant sticks to achieve a short burning time and is capable of producing a launch velocity of over 68 m/sec, with burnout occurring within the launch tube. The propellant configuration is consistent with stringent safety requirements arising from operation of the launch motor in proximity to the gunner. Noise, blast, and temperature effects have been demonstrated to be tolerable to manned firings in over several thousand missile launchings.

The operating range of this motor is -31° to +53°C; therefore, the -23°C operating temperature planned for penetrator deployment offers no motor performance difficulties.

Design concepts developed for the TOW motor, such as propellant stick retention, case design, and igniter assembly configuration will be used for the penetrator deployment motor design shown in Figure 52.

The motor configuration is similar to the TOW launch motor in construction and propellant grain configuration. The motor case length has been reduced to accommodate easier cm location of the deployment system, while the case diameter is increased to allow for the increase in propellant mass.

The propellant grain configuration is a hollow rod with a 19 mm outside diameter and a 9.5 mm inside diameter. These are held into place within the motor case by a support plate and push pins which extend through the plate and into one end of the grain. The other end is supported by an elastometric O-ring which is installed around the bundle of propellant sticks.
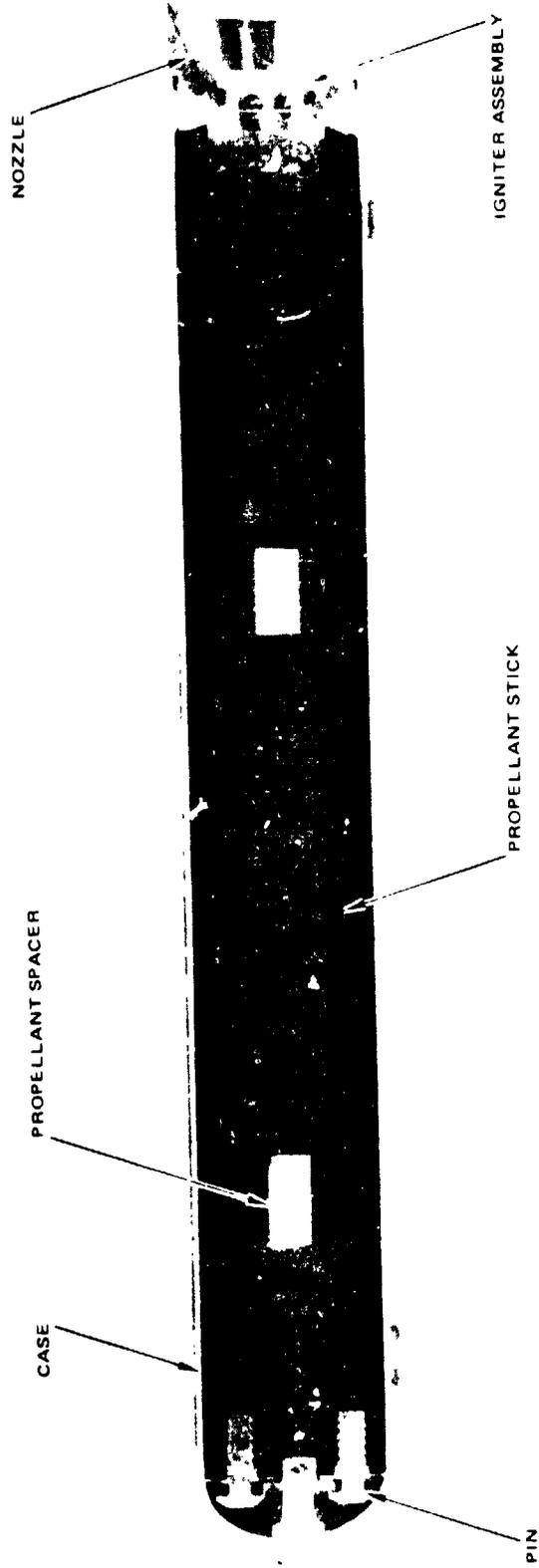
NOZZLE

IGNITER ASSEMBLY

PROPELLANT STICK

PROPELLANT SPACER

CASE

PIN

FIGURE 51. TOW LAUNCH MOTOR

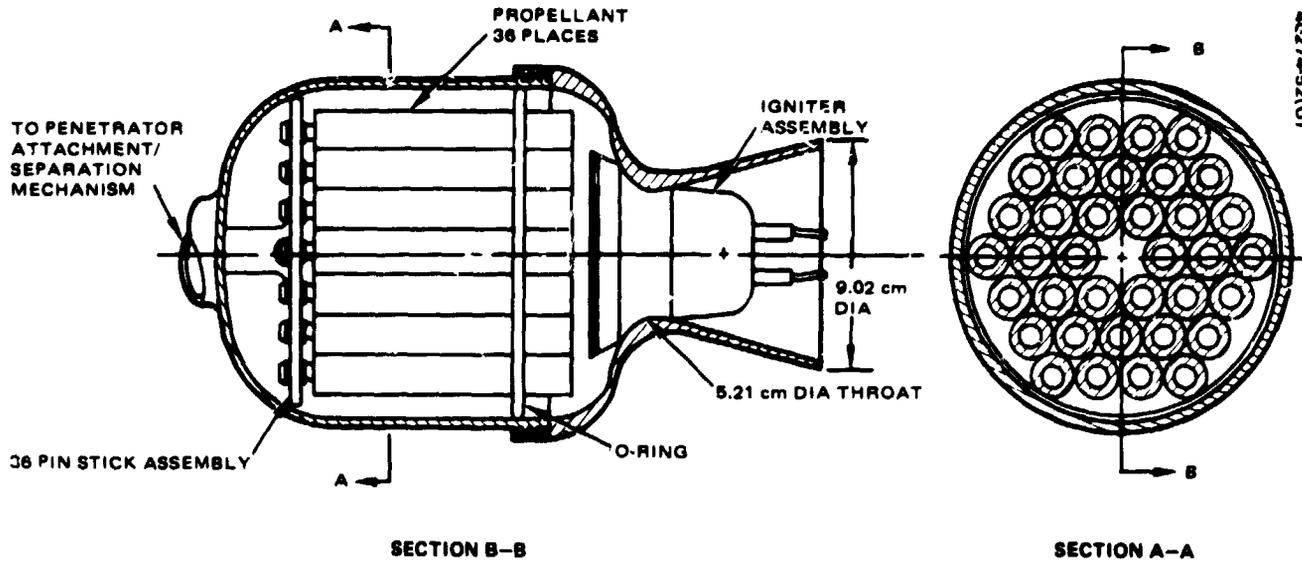SECTION B-B   SECTION A-A

FIGURE 52. PENETRATOR DEPLOYMENT MOTOR

The O-ring between the propellant bundle and motor case also helps to isolate the propellant from shock and vibration. The nozzle is attached to the case by threads which permit easy installation and removal of the nozzle without affecting any other motor components.

The case is made from maraging steel and stressed for firing at -23°C to minimize mass.

6.1.5 Launch Motor Igniter

Figure 53 shows the electric squib used in the existing TOW launch motor igniter. Two squibs are used in the igniter assembly to ensure high reliability. The squibs are adhesive bonded into the igniter assembly. The
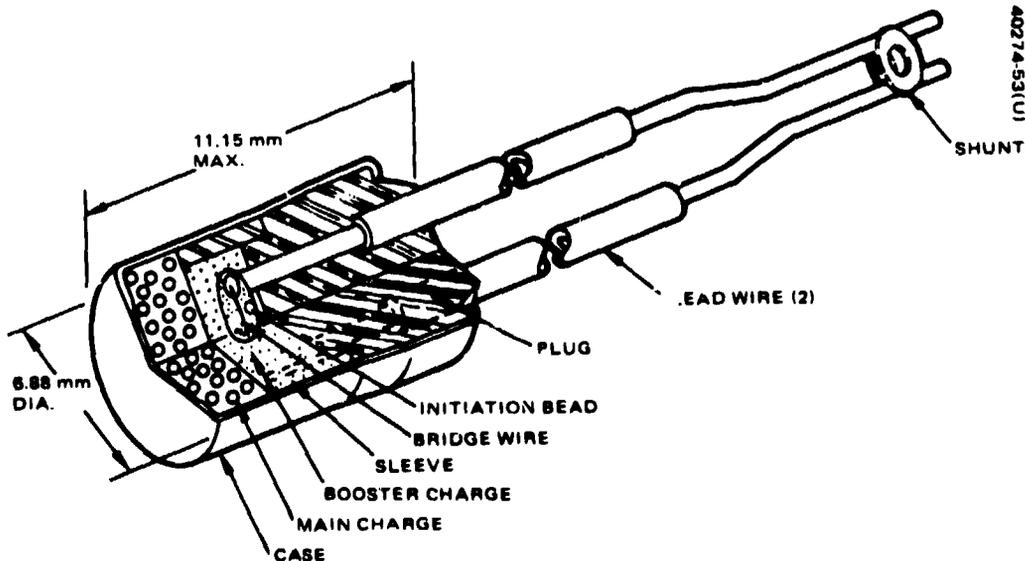

FIGURE 53. LAUNCH MOTOR IGNITER

81

TABLE 26. BASIC 207 SQUIB DESIGN PHYSICAL CHARACTERISTICS

Case material	Aluminum. Wall thickness 0.203 mm Bottom thickness 0.0635 mm
Lead wires	Type 22 gage solid, 24 gage stranded, or 26 gage stranded copper Length as desired, up to a maximum of 3.05 m Insulation nylon or Teflon
Seal	Molded phenolic plug
Length	11.15 mm maximum
Outside diameter	6.88 mm Maximum 7.21 mm

squib ignites a propellant charge. Average functioning time of this squib is a function of current. For example, at 21°C the functioning time is 0.8 ms at 10 amperes and 13 ms at 2 amperes.

The squib design characteristics are given in Table 26. Other characteristics are listed in Table 30 along with the characteristics of squibs, which have a higher autoignition temperature.

6.1.6 Deployment Mechanism Estimated Mass

The mass estimated in Table 27 was based on a design utilizing construction and materials that provide high strength to mass ratios. The container is aluminum with a glass fiber wrapping. Also, to minimize mass, the motor is steel and stressed for firing at -23°C with 1.91 kg of propellant.

TABLE 27. DEPLOYMENT MECHANISM ESTIMATED MASS

Component	Mass, kg
● Container	7 48
● Motor	5.18
● Motor support housing	1.34
● Separation spring	0.33
● Fasteners/attach hardware to motor and penetrator	0.25
● Holdback mechanism	0.05

6.2 DEPLOYMENT SYSTEM PERFORMANCE

The parametri performance relationships that were used in developing the baseline concept, nominal performance parameters, and a method for off-loading the baseline motor have been summarized in this section.

6.2.1 Performance Tradeoffs

The parameters shown in Figure 54 are for a 45 kg penetrator and a Δvelocity of 80 m/sec. The curves reflect ideal conditions and neglect the effects of friction.

The selected design point is 40 ms burn time which is compatible with the penetrator and launch tube length and reflects the use of the existing propellant grain shape used in the TOW missile launch motor.

The performance parameters previously indicated for the 40 ms burn time dictate the remaining motor characteristics which are given in Table 28.

TABLE 28. PENETRATOR DEBOOST MOTOR
(PARAMETERS AT -23°C)

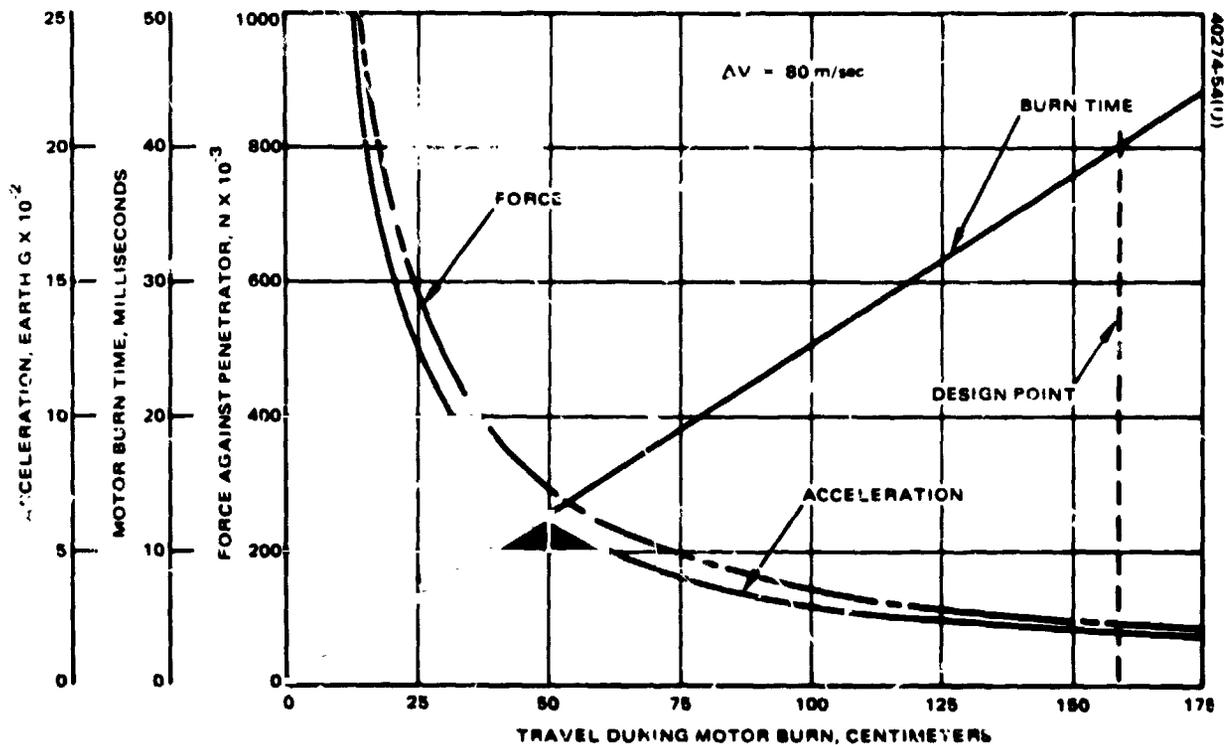| Parameter	Metric Units	U.S. Equivalent Units
Total mass	5.18 kg	(11.24 lb)
Propellant mass	1.91 kg	(4.22 lb)
Total impulse	3981 N/sec	(895 lb/sec)
Thrust (essentially constant)	99,250 N	(22,374 lb)
Acceleration (average)	203 g	
Chamber pressure (average)	3102 N/cm^2	(4500 psi)
Burnout length	160 cm	(62.9 in.)

FIGURE 54. PENETRATOR DEBOOST MOTOR PERFORMANCE PARAMETERS

83

6.2.2 Downloading Method

The penetrator launch motor can be downloaded readily from the baseline design total impulse (100 percent) to lower values of total impulse as shown in Figure 55. Total propellant mass is decreased by shortening or removing propellant sticks to obtain the desired total impulse. The nozzle throat diameter is also changed consistent with the desired total impulse. Changing propellant mass and throat diameter together results in keeping the motor performance parameters of pressure and burn time constant at the baseline design condition.
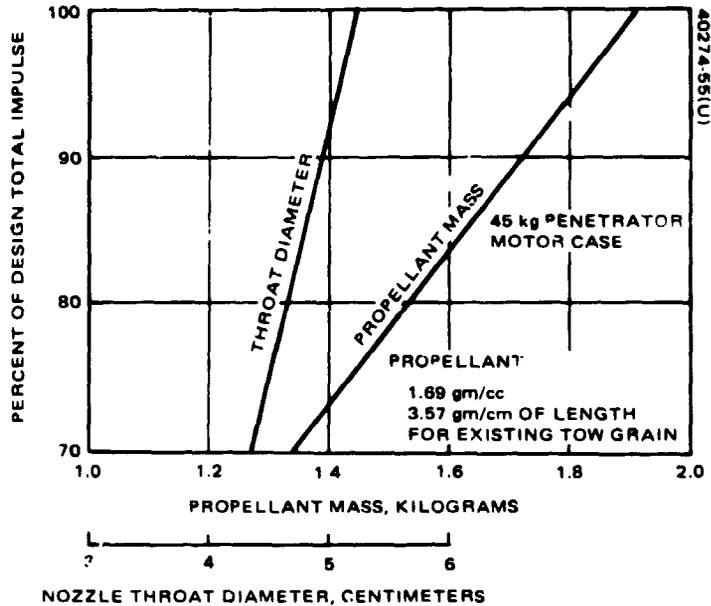

FIGURE 55. DEBOOST MOTOR OFF LOADING

The relationship between the penetrator mass and Δvelocity acceleration and travel are shown in Figure 56. The baseline motor is designed for an impulse of 3981 N-sec. Since the motor has the capability of being downloaded, curves are shown down to 70 percent of design impulse. The curves show, as penetrator mass decreases, the velocity may be kept constant if desired, or with a constant mass the velocity may be varied by motor loading.

6.2.3 Typical Launcher Reaction Versus Launch Temperature

Figure 57 is a plot of total impulse versus motor temperature for a typical tube launched system. The significant contributing forces to launch impulse are hot gas impingement on the tube wall, tube flare (nozzle) thrust, gas separation, friction between moving parts and tube, and forces associated with the holdback restraint and electrical umbilical release. A typical summation of these impulses results in the plot shown in Figure 55. These impulses are extremely low, being 12 N-sec (2.7 lb-sec) at -23°C. Bringing the total impulse to a low magnitude is accomplished by designing the aft nozzle to counteract the summation of the other impulses. For the PMO, the deployment mechanism impulses will be designed to pass through zero at approximately -23°C to minimize the reaction to the spacecraft attach points.
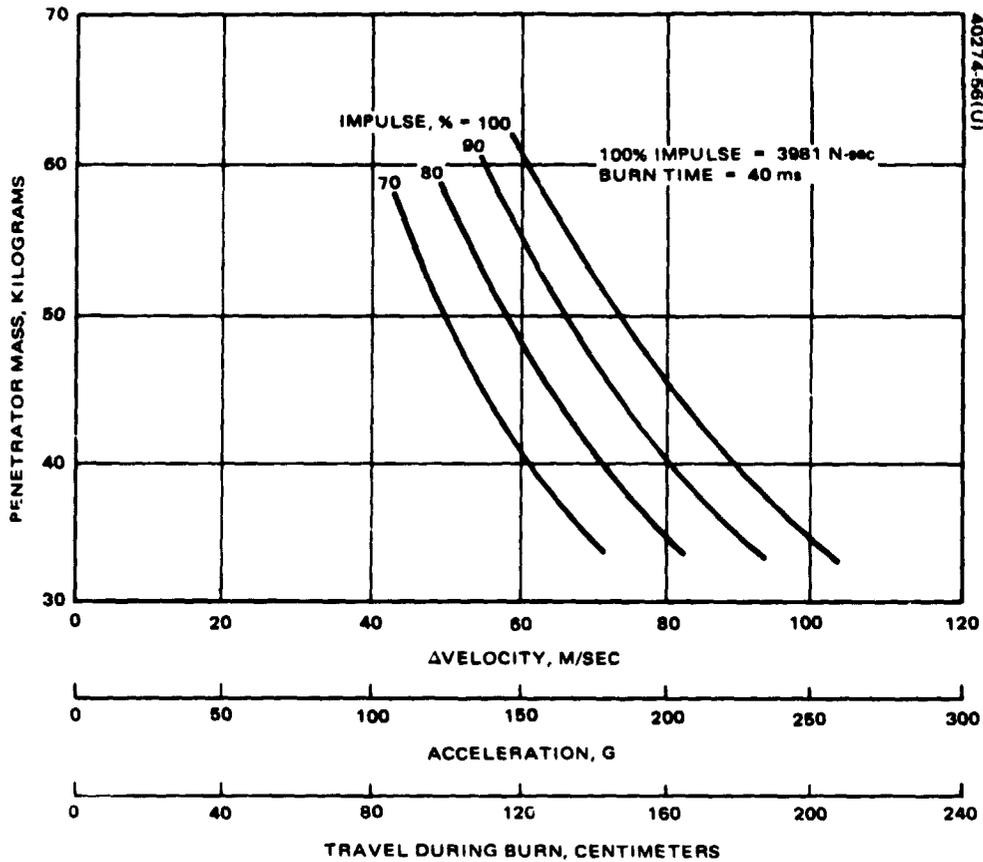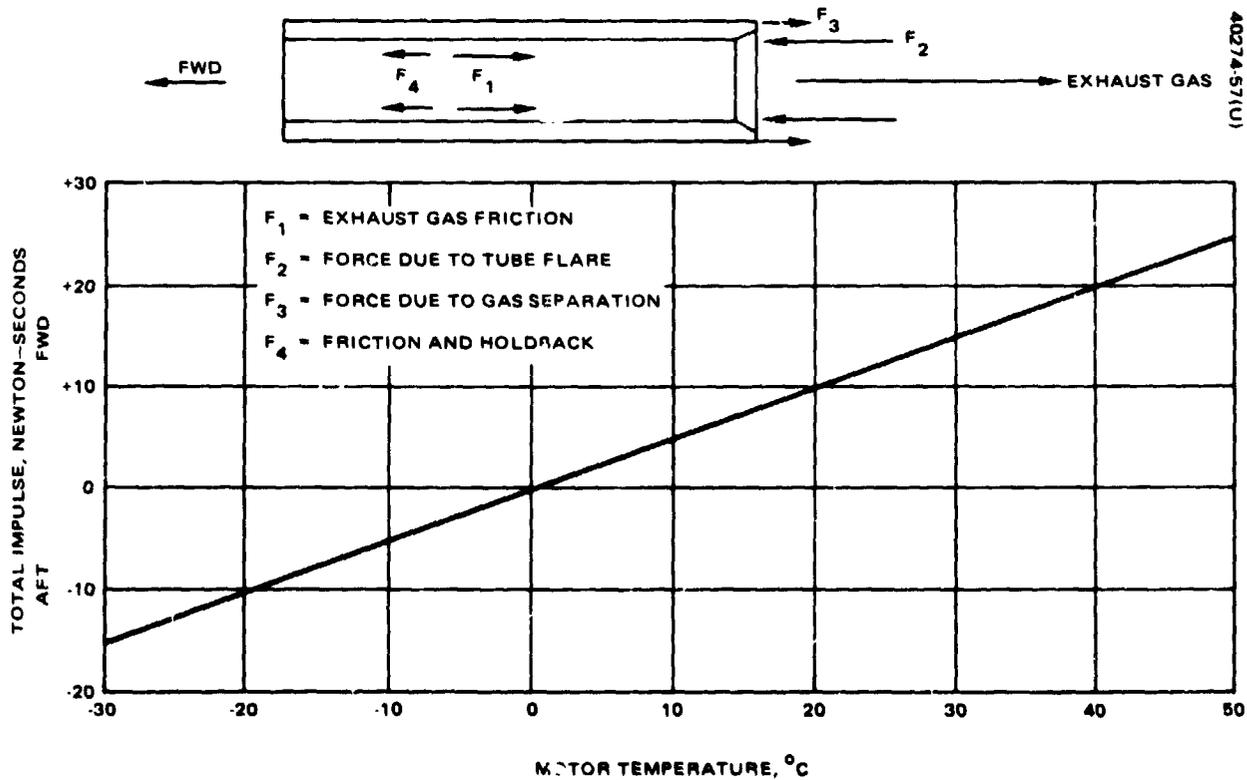
FIGURE 56. DEBOOST MOTOR OFF LOADED PERFORMANCE

F_1 = EXHAUST GAS FRICTION

F_2 = FORCE DUE TO TUBE FLARE

F_3 = FORCE DUE TO GAS SEPARATION

F_4 = FRICTION AND HOLDBACK

FIGURE 57. TEMPERATURE EFFECTS ON DEBOOST MOTOR PERFORMANCE

85

6.2.4 Total Impulse Dispersions

Table 29 shows a reasonable design objective of total impulse variation for the penetrator deployment mechanism.

The TOW launch motor qualification test results indicate that the total impulse variation is 1.5 percent (3σ) for tests at constant temperature. A reasonable design objective for the penetrator motor is ±1 percent (3σ), achievable by accurately controlling factors such as propellant composition, using a single propellant batch during loading, controlling nozzle dimensions to low tolerances, and controlling motor mass precisely.

Other factors that affect penetrator deboost velocity are expected to be controlled within a ±0.5 percent (3σ), by accurately controlling penetrator mass, the moving mechanism mass, and forces to release the holdback restraint and electrical umbilical. In addition, surface finish of rubbing parts will be closely controlled to minimize friction. Deployment of the penetrator will also be accomplished at a defined temperature to minimize impulse dispersion. As a result of accurately controlling the factors specified in Table 29, a total impulse variation of 1.5 percent (3σ) appears to be a reasonable objective for deployment of the penetrator.

TABLE 29. 3σ TOTAL IMPULSE DISPERSIONS

Typical TOW Motor Performance at Constant Temperature	±1.5%
Reasonable Design Objective	
Penetrator motor	±1.0%
Propellant composition	
Single batch loading	
Nozzle tolerances	
Motor mass	
Additional impulse dispersion factors	±0.5%
Penetrator mass	
Mechanism mass	
Shear umbilicals impulse	
Friction	
Launch temperature	
Total Impulse Variation Objective	±1.5%

6.3 STERILIZATION COMPATIBILITY

Table 30 indicates the autoignition temperature of the propellant used in the existing TOW launch motor. The autoignition temperature of 120°C makes the propellant incompatible with a 125°C sterilization temperature requirement. Two sterilizable alternate propellant candidates for the PMO application are both composite propellants and designated HES-8028 and Hi-Temp, both manufactured by Hercules Incorporated. The HES-8028 propellant has the highest autoignition temperature (177°C), resulting in the greatest temperature margin during sterilization. In addition, the propellant has good physical and thermodynamic properties; the heat resistance, clean burning, noncorrosive exhaust, high density, and high specific impulse make it suitable for the penetrator application.

The explosive cord for cutting the end covers open presents no problem during the sterilization procedure.

High autoignition temperature (>232°C) squibs are available for the launch motor igniter as shown in Table 30 if greater temperature margin is desired during sterilization.

TABLE 30. STERILIZATION COMPATIBILITY

Component	Parts in Current Hughes Usage	High Temperature Options	
Launch motor Main charge	Double Base* M7 Picatinny Arsenal	Composite HES-8028 Hercules	Composite Hi-Temp Hercules
Autoignition temperature	120°C (after five hours)	177°C	149°C
Igniter Designation	207A Flare Northern	105-4 Flare Northern	105-7 Flare Northern
Autoignition temperature	140°C	232°C	232°C
Explosive cord RDX. Greater than 177°C autoignition temperature			

*Existing TOW launch motor propellant.

6.4 POWER REQUIREMENTS

Electrical power is required for the penetrator deployment mechanism to ignite the launch motor and to initiate the explosive cord for opening the container end covers. Electrical characteristics of the existing TOW launch motor igniter are listed in Table 31 along with the characteristics of squibs having a high temperature range. Although the existing TOW igniter is suitable for the PMO application, a squib having a higher autoignition temperature would result in greater temperature margin during sterilization procedures.

The firing current for igniting the explosive cord to open the container end covers is also given in Table 31.

TABLE 31. POWER REQUIREMENTS

TOW Igniter	Higher temperature range igniters
Launch motor igniter (2 squibs of following characteristics required)	
No-fire: Maximum current for nonignition 1.0 A dc from 24 V source	1 A, 1 W
Firing current: 2 A dc from 24 V source for 100% functioning	3.4 A for 5 ms
Operating temperature: -54° to +110°C	-62° to +177°C
Explosive Cord	
Firing current – 2.0 A/end cover	

6.5 SYSTEM RELIABILITY DATA

As indicated in Table 32, the TOW weapon system launch motor and launch container during advanced development proved to be highly reliable, exceeding or equaling design predictions. Reliability of these items during the production phase has continued to be excellent as established during several thousand firings (3860 production missile firings through January 1973). Since it is planned to utilize many of the proven design concepts of the TOW program for the PMO, the penetrator deployment mechanism is expected to be equally as reliable as experienced in the TOW missile system.

TABLE 32. TOW WEAPON SYSTEM RELIABILITY DATA

Component	Experimental Firings	Prototype Firings	Design Prediction
Launch motor	1,000 (32/32)	1.000 (65/65)	0.9990
Launch container		1.000 (34/34)	1.0000

6.6 LAUNCH SEQUENCE

The launch sequence electronics design precludes penetrator deployment without completion of specified prelaunch activities. These activities are to open the front cover and verify that it is open and then open the rear cover and verify that it is open. When these functions occur, a signal is generated to indicate that motor ignition may occur at any time thereafter.

A simplified launch sequence diagram and a time sequence chart are shown in Figure 58 for the major functions that occur during deployment.
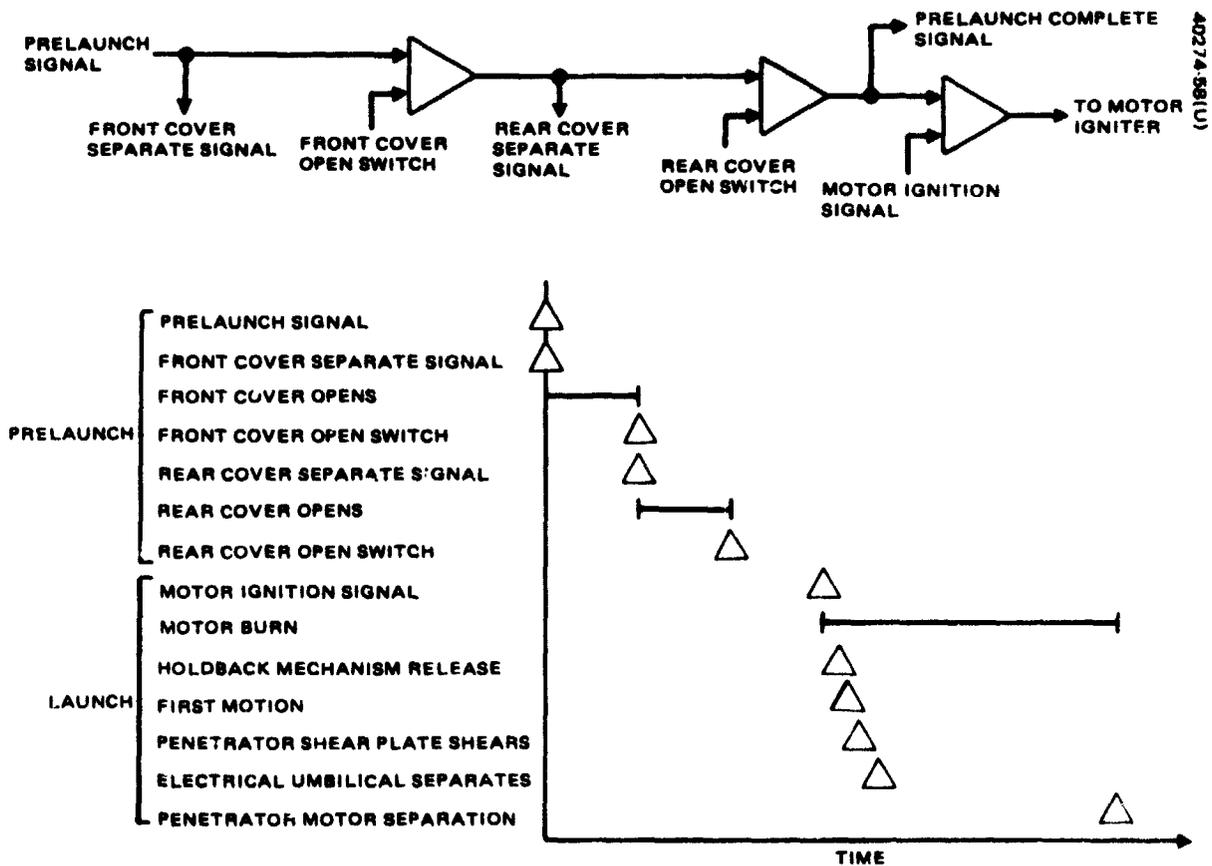

FIGURE 58. PENETRATOR DEBOOST SEQUENCE DIAGRAM

REFERENCES

1. "Proposal For The Design and Development of The Pioneer Venus Spacecraft System," Vol. 1, Technical Proposal, SCG 30243P, Hughes Aircraft Company, August 1973

2. "Mars Science Missions in The Post Viking Era: Possible Contributions of Pioneer Type Missions," NASA/Ames Research Center, August 1974

3. "Mars Penetrator: Subsurface Science Missions," SAND-74-0130, Sandia Laboratories, August 1974

4. "Pioneer Mars 1979 Mission Options," Report SAI 120-M1, Science Applications Inc., January 29, 1974

PRECEDING PAGE BLANK NOT FILMED